CHALMERS
UNIVERSITY OF TECHNOLOGY

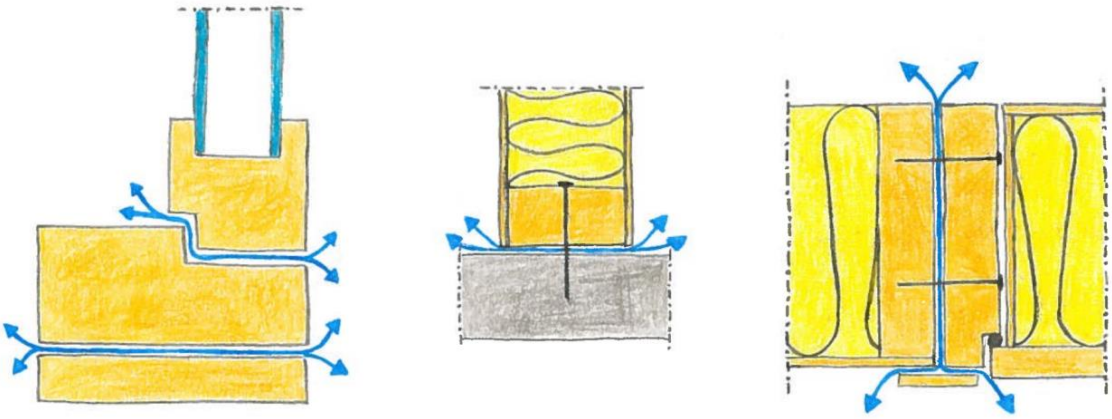

Yearly Variations in Airtightness of Detached Wooden Houses

Simulations and Laboratory Measurements to Investigate Causes and Consequences

Master of Science Thesis in the Master's Program Structural Engineering and Building Technology

FREDRIK DOMHAGEN

Department of Civil and Environmental Engineering
Division of Building Technology
CHALMERS UNIVERSITY OF TECHNOLOGY
Master's Thesis BOMX02-16-76
Gothenburg, Sweden 2016

MASTERS'S THESIS BOMX02-16-76

Yearly Variations in Airtightness of Detached Wooden Houses

Simulations and Laboratory Measurements to Investigate Causes and Consequences

Master of Science Thesis in the Master's Program Structural Engineering and Building Technology

FREDRIK DOMHAGEN

Department of Civil and Environmental Engineering
Division of Building Technology
Building Physics Group
CHALMERS UNIVERSITY OF TECHNOLOGY
Göteborg, Sweden 2016

Yearly Variations in Airtightness of Detached Wooden Houses
Simulations and Laboratory Measurements to Investigate Causes and Consequences

Master's Thesis in the Master's Program Structural Engineering and Building Technology

FREDRIK DOMHAGEN

Examensarbete BOMX02-16-76 / Institutionen för Bygg- och Miljöteknik
Chalmers Tekniska Högskola 2016

Department of Civil and Environmental Engineering
Division of Building Technology
Building Physics Group
Chalmers University of Technology
SE-412 96 Göteborg
SWEDEN
Telephone: +46(0)31-772 1000

Cover: Illustration by Fredrik Domhagen

Department of Civil and Environmental Engineering. Göteborg, Sweden, 2016

Yearly Variations in Airtightness of Detached Wooden Houses
Simulations and Laboratory Measurements to Investigate Causes and Consequences

Master's Thesis in the Master's Program Structural Engineering and Building Technology

FREDRIK DOMHAGEN
Department of Civil and Environmental Engineering
Division of Building Technology
Building Physics Group
Chalmers University of Technology

ABSTRACT

It is well known that leaky buildings have higher risks of acquiring moisture problems, are more draughty and are harder to make energy efficient compared to more airtight buildings. Previous research has shown that the airtightness varies over the year and that buildings can be less airtight during winter months. The aim of this thesis is therefore to investigate possible consequences and causes of variations in airtightness of detached wooden houses. Investigations are performed both with laboratory measurements as well as with computer calculations. The thesis starts with describing the theory relevant for the calculations and analysis performed. Following chapters describe methods and results from performed investigations.

For a chosen number of common construction details the change of leakage through the detail as a function of relative humidity is calculated. Results show that for the ideal cases, the leakage changes drastically when relativity humidity changes. One such example is the floor-wall connection where the airflow increases from 2.4 l/sm to 6.7 l/sm when the relative humidity inside the building drops from 55 % to 23 %.

Laboratory measurements are conducted on a wooden guest house. The relative humidity inside the guest house is increased to 90 % during an 8-day period and then decreased to 25 % during a 7-day period. The airtightness is measured several times during these two periods with the use of blower door equipment. Results show that the airtightness changed from 0.74 l/sm^2 when the indoor air was more humid to 1.21 l/sm^2 when the indoor air was more dry.

A computer model is set-up to resemble a typical wooden detached house. Airflows and pressure profiles are then calculated for different values of airtightness. Results show, for instance, that for every percentage point of decrease in airtightness the total exfiltration may increase with 1.9 %. Results from the simulations also show that a decrease in airtightness increases the flow of indoor air up to the attic if an attic hatch is present.

Conclusions should not be interpreted as generic but rather as indications of likely outcomes. In order to more fully understand the impact that varying airtightness has on building performance more in-depth research is needed.

Key words: airtightness, varying airtightness, air leakage, radon, cold attic, attic hatch, blower door, contam, infiltration, exfiltration

Yearly Variations in Airtightness of Detached Wooden Houses
Simulations and Laboratory Measurements to Investigate Causes and Consequences

Examensarbete inom masterprogrammet Konstruktionsteknik och Byggnadsteknologi

FREDRIK DOMHAGEN
Institutionen för Bygg- och Miljöteknik
Avdelningen för Byggnadsteknologi
Byggnadsfysik
Chalmers Tekniska Högskola

SAMMANFATTNING

Det är väl känt att byggnader med låg lufttäthet löper större risk att drabbas av fuktrelaterade problem, är mer dragiga och är svårare att göra energieffektiva jämfört med tätare byggnader. Tidigare forskning har visat att lufttätheten varierar över året och att byggnader ofta är mindre täta under vintern. Syftet med den här uppsatsen är därför att undersöka möjliga konsekvenser och orsaker till varierande lufttäthet i enfamiljshus av trä. Undersökningarna görs med laboratoriemätningar och datorsimuleringar. Uppsatsen börjar med att beskriva teorin bakom de beräkningar samt analyser som görs i uppsatsen. Efterföljande kapitel behandlar metoder och resultat från genomförda undersökningar.

Ett antal vanligt förekommande konstruktionsdelar undersöks med avseende på förändring i täthet som funktion av relativ fuktighet. Resultaten visar att läckaget ändras drastiskt när den relativa fuktigheten ändras. Ett exempel på detta är anslutningen mellan golv och vägg där läckaget ökar från 2.4 l/sm till 6.7 l/sm när den relativa fuktigheten sjunker från 55 % till 23 %.

Laboratoriemätningar utförs på en friggebod av trä. Den relativa fuktigheten inne i friggeboden höjs till 90 % under 8 dagar och sänks därefter till 25 % under 7 dagar. Lufttätheten mäts vid flera tillfällen under båda perioder med hjälp blower door -utrustning. Mätningarna visar att lufttätheten ändras från 0.74 l/sm^2 under perioden med högre luftfuktighet till 1.21 l/sm^2 under perioden med lägre luftfuktighet.

En datormodell tas fram för att efterlikna ett typiskt enfamiljshus av trä där luftflöden och tryckprofiler beräknas för olika värden på lufttäthet. Resultaten visar, bland annat, att om lufttätheten minskar med en procent så kan exfiltrationen öka med 1.9 %. Resultaten visar även att minskad lufttäthet ökar luftflödet upp till vinden om det finns en vindslucka i huset.

Slutsaterna bör inte tolkas som generella utan snarare som indikationer på troliga utfall. För att bättre förstå hur varierande lufttäthet påverkar byggnaders funktion krävs mer djupgående forskning.

Nyckelord: lufttäthet, varierande lufttäthet, luftläckage, radon, kallvind, vindslucka, blower door, contam, infiltration, exfiltration

Contents

Preface

This thesis was inspired by previous research within the field of air movements carried out at the division of Building Technology, Chalmers University of Technology and sought to increase the understanding of problems related to varying airtightness.

The work has been carried out at the division of Building Technology under the supervision of associate professor Paula Wahlgren.

I would like to thank everyone who has been sharing their knowledge and experience. Special thanks to Paula Wahlgren for her great support and encouragement. Thanks to Axel Berge for sharing his knowledge and experience with CONTAM and Tommie Månsson for helpful advices on COMSOL-simulations. Thanks to Marek Machowski for providing and demonstrating laboratory equipment and thanks to Peter Lindblom who made it possible to conduct laboratory measurements on the guest house.

Göteborg June 2016

Fredrik Domhagen

Notations

Roman upper case letters

C_p	Wind pressure coefficient	[-]
G	Moisture rate	[kg/s]
M_a	Mass flow rate	[kg/s]
R_a	Airflow rate	[m^3/s]
RH	Relative Humidity	[%]
S	Airflow resistance	[Pa·m^3/s]
U	Wind speed	[m/s]

Roman lower case letters

k	Permeability	[m^2]
m	Mass	[kg]
m_{od}	Oven-dry mass of timber	[kg]
u	Moisture content in timber	[-]

Greek upper case letters

ΔP	Pressure difference	[Pa]

Greek lower case letters

α_f	Shrinkage factor for types of wood	[-]
δ_v	Vapour permeability	[m^2/s]
λ	Decay rate	[s^{-1}]
μ	Dynamic viscocity of air	[Ns/m^2]
ρ_{air}	Density of air	[kg/m^3]
$\tau_{1/2}$	Half-life of radon	[s]
υ	Humidity by volume of air	[kg/m^3]
υ_s	Humidity by volume of air at saturation	[kg/m^3]

1 Introduction

In a recent study by Wahlgren et al. (2015) it was shown that the airtightness of a building is not steady throughout the year and can vary with as much as 10 % considering the total airflow through leakages at a pressure difference of 50 Pa. The study also indicates that timber constructions are more prone to having larger variations than concrete constructions. The reason to the variations is thought to be caused by fluctuations in relative humidity and possibly also fluctuations in temperature. However, variations in airtightness caused by relative humidity seem to have the greatest effect resulting in lower airtightness during winter and higher airtightness during summer. There are also less recent studies showing similar results such as Persily (1982), showing that the airtightness can vary with as much as 25 % throughout the year.

A varying airtightness raises a number of questions. For example, how is the moisture safety affected if air is allowed to move from the inside towards the outside of the thermal envelope and possibly condensate inside the construction? Normally this is inhibited by adjusting the ventilation in a way that ensures negative internal pressure and thus forcing the air to move from the outside towards the inside. However, if the airtightness decreases the negative pressure caused by the ventilation system might also be reduced.

Another topic which has been in focus lately is moisture condensation and mould growth in cold attics (Hagentoft and Sasic Kalagasidis, 2014). It has been indicated that the problem is related to air that leaks from the interior of the building up to the attic. It is likely that the infiltration of air to the attic changes with changes in airtightness, but to what extent?

How is the energy performance of the building affected by changes in airtightness? It is well known that energy losses increases with decreased airtightness. But to what extent and how is the required heat power affected? This might also be affected by the location of the leakages. For example if the majority of the leakages that varies are situated in both lower and higher parts of the building, the airflow might increase more than if leakages are situated at a height closer to the neutral pressure plane.

Comfort is another issue. If leakages, for example around windows, increases during the winter, cold air will blow into the building and cause problems with comfort.

In order to meet the demands of different certification standards, such as Miljöbyggnad, Bream or regulations regarding radon levels it is important that measurements are performed correctly. However, if the airtightness changes during the year such measurements might not be valid if measured during for instance a more leaky period. It might therefore be important to understand how variations in airtightness work in order to get more correct measurements and to fulfil the requirements.

1.1 Purpose

The purpose of this thesis is to investigate the correlation between varying airtightness and indoor relative humidity as well as possible consequences of varying airtightness. Focus will be on airflow through leakages and indoor air quality with respect to radon where findings will be coupled to common airtightness-related issues such as moisture, energy and comfort.

1.2 Method

The study is initiated with a literature study to learn more about typical problems related to airtightness as well as the mechanisms influencing airflow in leakages and how the geometry of leakages is affected by swelling and shrinkage. Next step is to define common leakages and use these to set up a reference model which can work as a starting-point when running simulations for different scenarios. A selection of leakages is studied more in-depth, using COMSOL, a software for performing calculations using *Finite Element Method*, the purpose is to relate relative humidity with leakage tightness. The reference model is then tested for a number of scenarios including variations in wind, temperature and airtightness where results are collected regarding airflows, pressure differences and radon concentrations. Calculations are performed in the software CONTAM which calculates airflow between zones through predefined leakage paths. Results are then used to exemplify what consequences can be expected in terms of mould growth in a cold attic, energy demand, radon and comfort.

The study also includes airtightness measurements on a guesthouse which is subjected to changes in indoor relative humidity. Blower door measurements are conducted repeatedly during two phases; a moistening phase when the relative humidity is increased and a drying phase when the relative humidity is decreased. The purpose is to relate changes in relative humidity to the airtightness of the building.

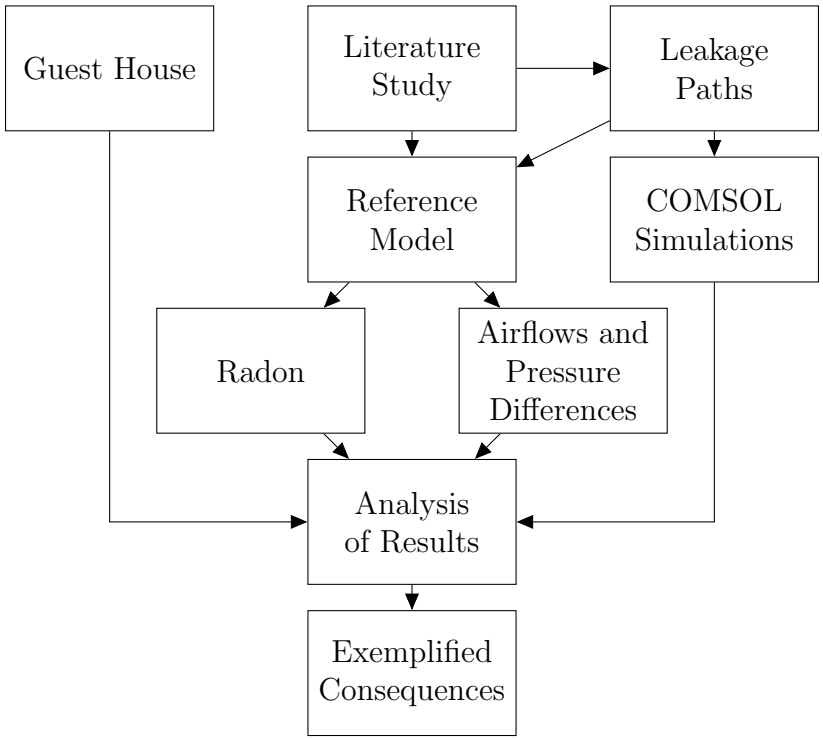

Figure 1: Flowchart showing the principle workflow for the thesis.

2 Theoretical Background

In this chapter the theory behind simulations and calculations used in the study is described.

2.1 Aerodynamics of air leaks

Infiltration and exfiltration of air through the thermal envelope is the unintentional movement of air through cracks and gaps, where *Infiltration* is air going from the exterior to the interior and *Exfiltration* is air going from the interior to the exterior. The driving force for the airflow is the pressure difference over the thermal envelope caused by ventilation, stack effect and wind. The size and geometry of the gap determines the magnitude of the airflow for a specific pressure difference where the sum of all leakages in the thermal envelope gives the total air leakage of the building.

There are a number of different models for approximating the airflow for air gaps with known geometries and pressure differences where the *Quadratic model* and the *Power law model* is two of the most common.

Quadratic model

The relationship between pressure and airflow can be described in two ways depending on whether the flow is turbulent or laminar. As for an air gap the laminar flow typically occurs in between the orifices whereas turbulent flow occurs at the orifices. This can be described with the following two equations:

$$Q = K_1 \cdot \Delta P \tag{1}$$

$$Q = K_2 \cdot \sqrt{\Delta P} \tag{2}$$

where Equation 1 describes laminar flow and Equation 2 describes turbulent flow (Walker et al., 1998). The constants K_1 and K_2 takes the geometries of the gaps into account. These equations are then combined to describe the relationship between pressure loss and airflow through the entire air gap.

$$\Delta P = A \cdot Q + B \cdot Q^2 \tag{3}$$

Here A is a coefficient describing pressure losses regarding laminar flow in the gap and B is a coefficient describing pressure losses regarding turbulent flow occurring at the

orifices. The coefficients A and B can according to Baker et al. (1987) for an air gap with rectangular cross section (see Figure 2) be described as:

$$A = \frac{12\mu L}{b^2 A} \tag{4}$$

$$B = \frac{2A^2}{C\rho_a} \tag{5}$$

where C is a loss constant dependent on the geometries of the air gap (Hopkins and Hansford, 1974). However, for an air gap with rectangular cross section penetrating an air tight building envelope, the value $C = 1.8$ can be used (Hagentoft, 2001). Similarly, the *Quadratic model* is also described in Hagentoft (2001) but with a somewhat different formulation.

In order for Equation 4 to be valid laminar flow must exist. The criterion for laminar flow to exist can be expressed with Reynolds number using the following equation:

$$Re = \frac{u_m \cdot 2 \cdot b}{\mu/\rho_a} < 2000 \tag{6}$$

where

u_m is the average air speed [m/s]
b is the gap height [m] (see Figure 2)
μ is the dynamic viscosity of air [Ns/m^2]
ρ_a is the density of air [kg/m^3]

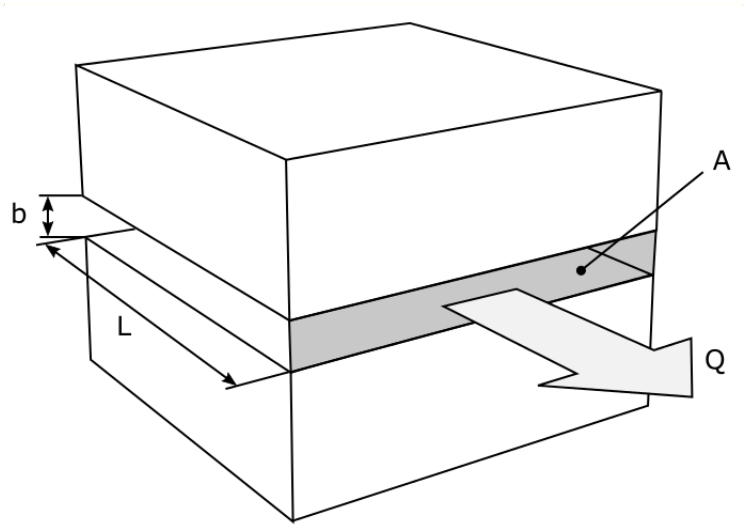

Figure 2: Air gap through a building envelope.

Power law model

The power law model is another common way of describing the airflow through an air gap. It is expressed as follows:

$$Q = C\Delta P^n \tag{7}$$

where C is the flow coefficient and n is the flow exponent. Values are dependent on the geometries of the air gap and usually found empirically. Typical values for the flow exponent are between 0.5 and 1.0 for fully developed turbulent flow and fully developed laminar flow respectively (Walker et al., 1998). According to CONTAM documentation (Walton and Dols, 2005) the value $n = 0.65$ can be used for small crack-like openings.

Airflow in porous materials

When porous materials are subjected to a pressure difference, air will flow from the side with higher pressure to the side with lower pressure. The airflow for such a case can according to *Darcy's Law* be described with the following equation (Hagentoft, 2001):

$$R_a = A\frac{k \cdot \Delta P}{\mu \cdot d} \tag{8}$$

where

R_a is the airflow rate [m^3/s]
A is the area perpendicular to the airflow [m^2]
k is the permeability [m^2]
μ is the dynamic viscosity of air [Ns/m^2]
ΔP is the pressure difference over the material [Pa]
d is the thickness of the material [m]

2.2 Pressure difference

Since pressure difference over an air gap is the driving force for the airflow the pressure on both sides of the thermal envelope must be found in order to calculate the airflows. In turn, the pressure difference is caused by the following driving forces; *Stack Effect*, *Mechanical Ventilation* and *Wind*. The sum of the pressure differences caused by these driving forces gives the total pressure difference.

$$\Delta P_{Total} = \Delta P_{StackEffect} + \Delta P_{MechanicalVentilation} + \Delta P_{Wind} \tag{9}$$

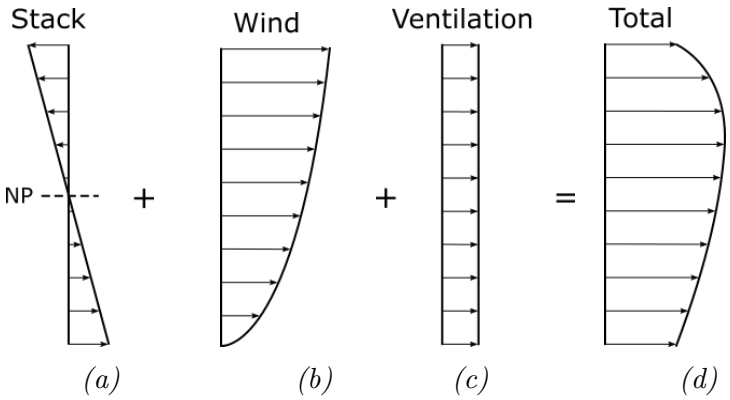

Figure 3: Illustration of the summation of pressure profiles.

Stack pressure

When indoor air is warmer than outdoor air a pressure difference will occur over the thermal envelope. This, since warm air has higher buoyancy than cool air causing the warm air to rise and create a pressure difference. The pressure difference is typically negative at the bottom of the building and positive at the top if the interior is warmer than the exterior and if there are no other driving forces involved. However, the pressure difference increases with increasing distance from the neutral plane and with increasing temperature difference between the interior and the exterior. The phenomenon is called *Stack effect* and the resulting pressure difference can be calculated with the following expression (Hagentoft, 2001):

$$\Delta P = z \cdot (\rho_e - \rho_i) \cdot g \tag{10}$$

where

ρ_e is the density of the exterior air [kg/m^3]
ρ_i density of interior air [kg/m^3]
ΔP is the pressure difference over the thermal envelope [Pa]
z is the distance from the *neutral plane* positive downward direction [m]
g is the constant of gravitational acceleration [m/s^2]

At some specific height there will be no pressure difference over the thermal envelope this height is commonly referred to as the *Neutral Plane*, NP, see Figure 3a. The height of the neutral plane can be found by applying the *Law of Conservation of Mass*, see Section 2.3.

Mechanical ventilation

Mechanical ventilation is a way of increasing and to some extent controlling the air exchange rate of a building. Usually there are three ways of organizing the mechanical ventilation; *Supply Ventilation*, by blowing air into the building creating a positive pressure, *Exhaust Ventilation*, by blowing air out from the building creating a negative pressure, or a combination of both where the flow into the building usually is smaller than the air blown out from the building resulting in a negative pressure. This kind of ventilation is referred to as *Balanced Ventilation* (Hagentoft, 2001).

The relation between increased pressure and airflow for different fans is described using a *Performance Curve*. The performance curve is specific for each type of fan and for a specific fan rotation speed. The *System Curve* describes the relation between pressure and airflow over the ventilation system and is dependent on a number of factors such as leakages, wind and stack effect. The intersection between the two curves; Performance curve and System Curve gives the *Performance Point*, see Figure 4, which is the actual airflow in the system (Warfvinge and Dahlblom, 2010).

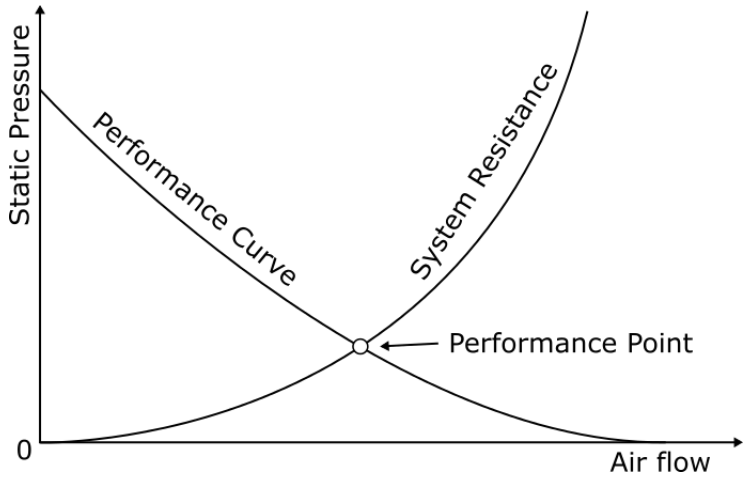

Figure 4: Illustration of the interaction between the performance curve for a fan and the system resistance of a ventilation system.

Wind

Wind is, in terms of physics, air molecules moving with a speed. When the molecules hit a steady surface the speed is reduced and energy transformed to the surface as pressure. In a similar manner when wind moves away from a surface it will give adjacent molecules air speed which in turn causes a negative pressure at the surface. The magnitude of the wind pressure is dependent on the speed of the wind, the direction of the wind and the shape of the surface. For calculations, wind speeds are typically taken

as statistically determined values dependent on geographical location and scope of calculation. The effect from wind direction and shape of the surface is described with a wind pressure coefficient, C_p, where a negative pressure coefficient means suction.

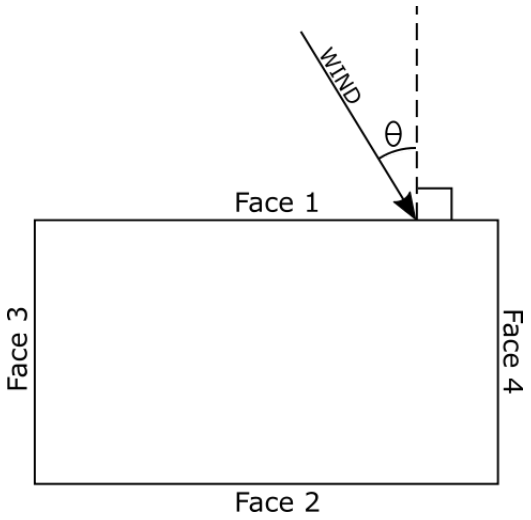

Figure 5: Illustration of wind angle and face enumeration.

The following table gives the pressure coefficients at different wind angles, see Figure 5, for an exposed low rise building (up to 3 storeys). By exposed means that there are no obstacles in the vicinity of the building.

Table 1: Pressure coefficients for a low rise building.

	Wind Angle θ		
Location	0°	45°	90°
Face 1	0.7	0.35	-0.5
Face 2	-0.2	-0.4	-0.5
Face 3	-0.5	0.35	0.7
Face 4	-0.5	-0.4	-0.2

Usually, statistical wind speeds are given for a height of 10 m. Since wind speed is dependent on terrain roughness and height above the ground, these effects must be taken into account. The wind speed may be adjusted with the following equation:

$$U_z = U_m \cdot \kappa \cdot z^a \tag{11}$$

where

U_z is the wind speed at the building height z [m/s]
U_m is the wind speed at the height of 10 m [m/s]
k and a are terrain coefficients (see Table 2) [-]

Table 2: Table showing terrain coefficients for different terrains used for correction of wind speeds from a weather station (see Equation 11).

Terrain Coefficient	k	a
Open flat country	0.68	0.17
Country with scattered wind break	0.52	0.20
Urban	0.35	0.25
City	0.21	0.33

To find the pressure for a certain wind speed at a specific façade, the following equation can be used:

$$P_w = (C_p - C_{pi})\frac{\rho_a U_z^2}{2} \tag{12}$$

where

P_w is the pressure caused by the wind [Pa]
C_p is the wind pressure coefficient [-]
C_{pi} is the wind pressure coefficient for the inside of the building [-]
ρ_a is the density of air [kg/m^3]
U_z is the wind velocity at the specified height [m/s]

The pressure coefficient for the inside of the building, C_{pi} can be found by applying the *The Law of Conservation of Mass*, 2.3.

2.3 Calculating airflow in a building

The total airflow through a building can be quite complicated to calculate, especially if there are many airflow paths and pressures to take into account. This section describes how such complex problems can be dealt with and the necessary principles involved.

Network analysis

When dealing with multiple airflows caused by different driving forces in the same building it is handy to apply *Network Analysis* as a mean of structuring, communicating and analysing the calculations. The pressure at a point in the system is represented as a *node* and is graphically denoted •. Nodes are connected with *Airflow Resistances*, S, graphically denoted:

Here the flow of air between two nodes over an airflow resistance can be calculated with the following:

$$R_a = \frac{P_2 - P_1}{S} \tag{13}$$

R_a	is the airflow [m^3/s]
P_1 and P_2	pressure at each corresponding node [Pa]
S	is airflow resistance [$Pa \cdot m^3/s$]

The following drawing shows the graphical representation of resistances in parallel connection with two nodes and resistances in serial connection with two nodes.

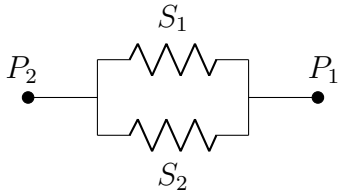

(a) Parallel

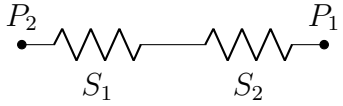

(b) Serial

Figure 6: Drawing showing the graphical representation of two nodes connected with either two parallel resistances or with two serial resistances.

The total airflow resistance for a group of parallel resistances can be calculated as:

$$\frac{1}{S_{total}} = \frac{1}{S_1} + \frac{1}{S_2} + ... + \frac{1}{S_n} \tag{14}$$

and for serial airflow resistances:

$$S_{total} = S_1 + S_2 + S_n \tag{15}$$

A system of airflows, pressures and resistances can in this way be graphically displayed. The network will then represent a number of equations which can be used to find unknown variables such as pressure at specific nodes or the airflow through the system.

Mass balance

The mass of air going in to the building must be equal to the mass going out from the building. This is called *The Law of Conservation of Mass* and can be expressed as follows (Hens, 2012):

$$\sum_i M_{a.in} = \sum_j M_{a.out} \tag{16}$$

where

$M_a = \rho_a \cdot R_a$	is the mass flow rate [kg/s]
ρ_a	is density of air [kg/m^3]
R_a	is the airflow [m^3/s]

2.4 Air speed determination

Air speed measurements are often conducted using an anemometer. The measuring technique gives the air speed at a specific point at some distance from the air gap. Unfortunately, it can not be used to find the airflow through the gap even though the geometries of the gap is known. The reason for this is that the airflow is not following a perfectly linear path at the orifice and the air speed will therefore vary within the airflow path and thus experience different air speeds at the measuring point compared to for instance the sides of the orifice, see Figure 7.

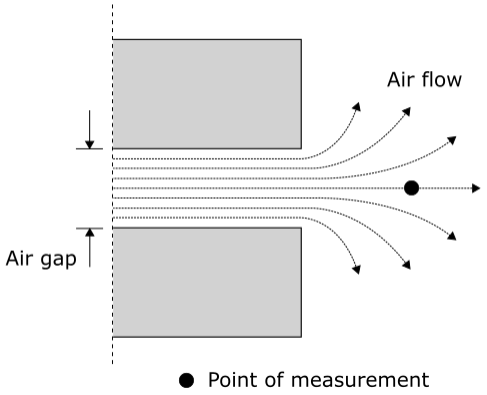

Figure 7: Airflow through gap.

2.5 Radon

For calculations of radon concentrations the *Decay Rate* of radon must be found. Decay rate describes the exponential decay of a contaminant species. Usually radioactive decay, such as for radon, is given as *Half-Life* which is the time it takes for half of the contaminant to decay. The relation between *Decay Rate* and *Half-Life* is given by the following equation (Walton and Dols, 2005):

$$\lambda = \frac{ln(2)}{\tau_{1/2}} \tag{17}$$

where

λ	is the decay rate [s^{-1}]
$\tau_{1/2}$	is the half-life [s]

2.6 Moisture

Water exists in three different phases *Liquid*, *Solid* and *Gas*. All three phases exist within buildings where its phase and amount effects for example deterioration of building materials, energy performance of the building and shrinkage and swelling of timber components.

Moisture in air

Atmospheric air contains a number of gases where water vapour is one of the gases usually present. The amount of water vapour in the air is expressed by either its *Partial Pressure*, p_v [Pa] of the total air pressure or as *Humidity by Volume*, υ [kg/m^3].

Moist air consists ideally of two phases; dry air and water vapour where the amount of water vapour ranges from zero to fully saturated. Saturation is the point where the air can not contain more water vapour and *Condensation* occurs. The point is referred to as *Humidity by Volume at Saturation*, denoted υ_s and is dependent on temperature and air pressure.

The following formula can be used to estimate the humidity by volume at saturation (Hagentoft, 2001).

$$\upsilon_s = \frac{a \cdot \left(b + \frac{T}{100}\right)^n}{461.4 \cdot (T + 273.15)} \tag{18}$$

where

$$\begin{array}{llll} 0 \leq T \leq 30 & a = 288.68Pa & b = 1.098 & n = 8.02 \\ -20 \leq T \leq 0 & a = 4.689Pa & b = 1.486 & n = 12.3 \end{array}$$

It is often convenient to express the humidity in air as the relation between *Humidity by Volume* and *Humidity by Volume at Saturation*. The relation is called *Relative Humidity*, RH, and is expressed as follows:

$$RH = \frac{\upsilon}{\upsilon_s} \tag{19}$$

Hygroscopic moisture

One condition for condensation to occur is that there is a surface on which the air can condensate. Water molecules most often starts to condensate on solid surfaces, this since there is an energy surplus at the solid surface which is reduced if a water molecule attaches to it, the phenomenon is called *Adsorption*. Adsorption also occurs at low relative humidities where layers of water molecules with only a few molecules in thickness builds up. The thickness of the layer increases with increasing relative humidity. This effect, together with the fact that most building materials are porous, is of great importance for the moisture content of a material (Burström, 2007).

Most building materials are to some extent porous, meaning that they consist of a solid phase and a system of pores. Since the total area of the pore-system per volume of

material can be quite large, the adsorption of water molecules significantly affects the moisture content of the material. This leads to a relation between relative humidity in the air and the moisture content of a material. The relationship is usually described with *Sorption Isotherms*, giving the moisture content of a material for different relative humidities and for a specific temperature. Furthermore, the moisture content for some materials is dependent on whether the material is increasing its moisture content *Absorption* or if the moisture content in the material is decreasing, *Desorption*. The discrepancy in moisture content, dependent on its previous state is commonly referred to as *Hysteresis* (Burström, 2007).

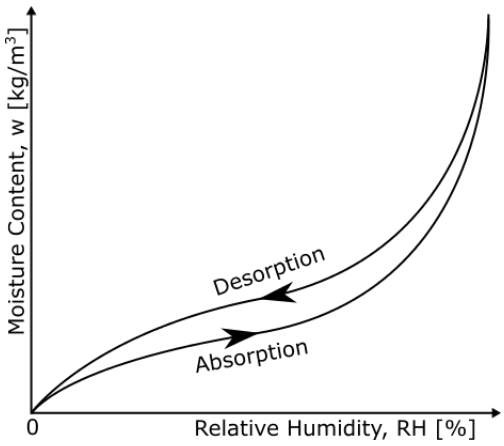

Figure 8: Example of a sorption isotherm showing both desorption and absorption.

However, according to Krus et al. (1998) it has been shown that for building materials in general, sufficient accuracy is achieved by taking a mean value between absorption and desorption.

Moisture transport

Two important moisture transport mechanisms in air is *Diffusion* and *Convection*. Diffusion is the movement of vapour caused by differences in vapour concentration.

Convection occurs when air with a certain vapour concentration, v_{out}, mixes with another volume of air with a different vapour concentration, v_{in}, at an airflow rate R_a [m^3/s]. The net moisture rate G [kg/s] is then expressed as:

$$G = R_a \cdot (v_{in} - v_{out}) \tag{20}$$

where

R_a is the airflow rate [m^3/s]
$\upsilon_{in},\ \upsilon_{out}$ is the humidities by volume [kg/m^3]

For a stagnant layer of air the *Diffusive Flux*, g [kg/m^2s], at steady state can according to Fick's empirical law be expressed as:

$$g = D\frac{\upsilon_1 - \upsilon_2}{d} \tag{21}$$

where

D is the diffusivity of water vapour in air ($25 \cdot 10^{-6} m^2/s$)
$\upsilon_1,\ \upsilon_2$ is the humidities by volume [kg/m^3] on either side of the air layer
d is the thickness of the layer of air [m]

In a similar manner, diffusion through a layer of a porous material can be calculated as:

$$g = \delta_v\frac{\upsilon_1 - \upsilon_2}{d} \tag{22}$$

where

δ_v is the vapour permeability of the material [m^2/s]
$\upsilon_1,\ \upsilon_2$ is the humidities by volume [kg/m^3] on either side of the layer
d is the thickness of the layer of air [m]

Example - Comparison between diffusive and convective moisture transport

Important to notice is the difference in moisture rate, G, when comparing diffusion through a wall with convective moisture transport caused by for instance a leakage. As a comparison consider a particle board of 2 m^2 and a thickness of 0.02 m with a small air gap running across the middle with a rectangular cross section of $1 \cdot 0.001$ m^2. Assume that the pressure difference over the air gap is $\Delta P = 10$ Pa. The vapour permeability of the particle board is assumed to be $\delta_v = 0.55 \cdot 10^{-6}$ [m^2/s] and assume that the difference in humidity by volume between the two sides is $\Delta\upsilon$=5 g/s. Following

the equations presented above, the moisture rate caused by the leakage becomes:

$$R_a = \frac{\Delta P}{S_g + S_e \cdot R_a}$$

$$S_g = A = \frac{12 \cdot \mu \cdot L}{b^2 \cdot A} = \frac{12 \cdot 1.85 \cdot 10^{-5} \cdot 0.02}{0.001^2 \cdot 1 \cdot 0.001} = 4.44 \cdot 10^3 \ \frac{Pa \cdot s}{m^3}$$

$$S_e = B^{-1} = \frac{1.8 \cdot \rho}{2 \cdot A^2} = \frac{1.8 \cdot 1.2041}{2 \cdot (1 \cdot 0.001)^2} = 1.084 \cdot 10^6 \ \frac{Pa}{(m^3/s)^2}$$

$$\implies R_a = 1.615 \cdot 10^{-3} \ \frac{m^3}{s}$$

$$G_{leakage} = R_a \cdot \Delta v = 1.615 \cdot 10^{-3} \cdot 5 = 8.1 \cdot 10^{-3} \ \frac{g}{s}$$

And for the moisture rate caused by diffusion through the particle board:

$$g = \frac{\Delta v}{Z_{vi} + \frac{d}{\delta_v} + Z_{ve}} = \frac{5}{360 + \frac{0.02}{0.55 \cdot 10^{-6}} + 60} = 1.359 \cdot 10^{-4} \ \frac{g}{m^2 s}$$

$$G_{diffusion} = A \cdot g = 2 \cdot 1.375 \cdot 10^{-4} \approx 2.7 \cdot 10^{-4} \ \frac{g}{s}$$

Even with a relatively small air gap for a quite small pressure difference (pressure difference over the thermal envelope subjected to wind can be many times larger) the moisture rate is about 30 times larger. Note: In the example the surface vapour resistances, $Z_{vi} = 360 \ s/m$ and $Z_{ve} = 60 \ s/m$ are added to each side of the particle board.

2.7 Shrinkage in timber

Timber is a porous material consisting of different kinds of cells often referred to as fibres. Most of the fibres are hollow and oriented in the direction of the stem. Timber is an anisotropic material meaning that its properties depends on the orientation along the stem. Therefore, properties are described in respect to the following three orientations: *Axial (grain) direction*, *Tangential direction* and *Radial direction.*

Since timber is a natural material, its properties varies not only with orientation but also with type of species, location of growth and environmental circumstances during growth.

Moisture content

Timber is a hygroscopic material meaning that it absorbs moisture from surrounding air if the timber is dry and releases moisture if the timber is wet (Domone and Illston, 2010).

The moisture stored in the timber is commonly expressed as *Moisture Content* and defined as:

$$u = \frac{m - m_{od}}{m_{od}} \tag{23}$$

where

m is the mass of the timber [kg]
m_{od} is the oven-dry mass of the timber (no free water) [kg]

Moisture in timber is stored both as free water in the cell cavities and in the cell walls. When all the free water in the cell cavities are dried out whilst the cell walls are still saturated the timber is said to have reached *Fibre Saturation Point*, (Burström, 2007).

Shrinkage and swelling in timber is dependent on the moisture absorbed by the cell walls and cell cavities. Increased moisture content results in swelling and decreased moisture content results in shrinkage. The swelling and shrinkage is also dependent on the orientation along the stem. For approximative calculations a linear relation between moisture content and shrinkage can be assumed. To calculate swelling and shrinkage as a function of moisture content, the following equation can be used (Burström, 2007):

$$\Delta\alpha = \frac{u_2 - u_1}{u_f} \cdot \alpha_f \tag{24}$$

where

$\Delta\alpha$ is the shrinkage in respect to the change in moisture content [-]
u_2 is the initial moisture content [kg/kg]
u_1 is the new moisture content [kg/kg]
α_f is the shrinkage factor for the specific type of wood in the shrinkage direction of interest [-]
u_f moisture content at fibre saturation point [kg/kg]

The absolute value of the shrinkage can the be calculated as:

$$\Delta\text{Ł} = \Delta\alpha \cdot \text{Ł} \tag{25}$$

where

ΔL is the change in length [m]
L is the total length [m]

Thermal expansion

As for other materials, timber undergoes thermal expansion when there is an increase in temperature. For estimation of the change in length the *Coefficient of Linear Thermal Expansion* is used. Values for the coefficient for common timber species such as Norway Spruce *(Picea Abies)* is $34.1 \cdot 10^{-6}$ $[K^{-1}]$. However, when compared with dimensional changes caused by moisture the changes are small and in cases with moisture content higher than 3 % the influence from thermal expansion can be neglected according to Domone and Illston (2010).

2.8 CONTAM

Airflow calculations in this project are mainly performed using the simulation software CONTAM 3.2 provided by NIST *(National Institute of Standards and Technology)*. The software calculates contamination concentrations and airflow between user-defined zones dependent on pressures and airflow resistances. Zones are considered well-mixed meaning that temperature and contaminant concentration is homogeneous in the entire zone. The only exception is that the pressure difference caused by wind and stack-effect is allowed to vary with height. In this project CONTAM is used to calculate airflows through leakages and radon concentrations.

Typical working procedure:

1. Draw zones and define their corresponding volumes.
2. Add airflow paths between zones and ambient.
3. Add driving forces such as wind, mechanical ventilation and stack-effect.
4. Run simulation.
5. Interpret results.

Airflow paths Airflow paths can be added between zones and between zones and the ambient environment. The airflow resistance for the airflow paths is then chosen either according to *Power law Model* or *Quadratic Model*, see Section 2.1. NIST also provides a database of leakages typically found in a building which can be used if leakage data can not be found elsewhere. There is also a possibility to add control elements to the model which can be used to automatically modify airflow paths when certain parameters changes.

Ducts There is a possibility to add duct systems with filters and fans and to calculate airflows through the duct system dependent on pressure drops in the system when it interacts with the rest of the building.

Driving forces It is possible to add three kinds of driving forces for airflows in the building; *Wind*, *Stack Effect* and *Mechanical Ventilation*. Wind can in the simplest way be added as an additional pressure to the leakages defined. Stack effect is simply added by giving the zones different temperature compared to the ambient temperature. Mechanical ventilation can be added both as constant airflow as well as a fan following a user-defined performance curve.

Simulation CONTAM can be used to calculate both *Steady State* conditions and *Transient* conditions. However, in this project mainly steady-state simulations are performed. Results are received as text-files with pressures, airflows and contaminant concentrations for each zone as well as for each airflow path.

2.9 COMSOL Multiphysics

COMSOL Multiphysics is a software for numerically simulating and solving physics-based problems. The software uses *Finite Element Method* to solve systems of differential equations defined by the user in the software interface. The software comes with a number of modules customised with the equations and functions necessary to solve the problem of interest. The module used in this project is the CFD-module *(Computational Fluid Dynamics)*, specifically the *Laminar Flow Interface* found within the module. Computations made in the project uses the following Navier-Stokes equation (Comsol, 2005):

$$\rho(\mathbf{u} \cdot \nabla)\mathbf{u} = \nabla \cdot \left[-p\mathbf{l} + \mu(\nabla\mathbf{u} + (\nabla\mathbf{u})^{\mathbf{T}})\right] + \mathbf{F} \tag{26}$$

Where:

$\mathbf{u}$ is velocity vector
$\mathbf{F}$ is the external force applied to the gas
p is the pressure
ρ is the density the gas

3 Leakage variation

There has been indications that the variations of airtightness is correlated to the indoor relative humidity in detached timber houses (Wahlgren et al., 2015). The correlation is likely due to swelling and shrinkage of timber when the relative humidity of surrounding air changes. Therefore, in this chapter three timber joints, commonly regarded as critical when it comes to leakage associated hazards, will be analysed in respect to change in leakage as a function of relative humidity.

3.1 Method

The variation in gap widths for a selection of leakages are evaluated. Swelling and shrinkage in timber components are calculated according to Equation 25. As a starting point the corresponding leakages in the *Reference Model*, see Chapter 5, is used. Since the overall leakage in the reference model is based on the detached timber house outside Landvetter in the report by Wahlgren et al. (2015), the initial gap widths are estimated from the corresponding leakages in the reference model, see Chapter 5. This is done by finding a gap width that corresponds to the air flow for a leakage at 4 Pa pressure difference. The pressure difference of 4 Pa is chosen since it is the reference condition for the leakage data used to define the reference model.

According to Wahlgren et al. (2015) the highest correspondence between change of relative humidity and change in air leakage was seen for the daily mean values of relative humidity. The overall leakage used in the reference model is taken from the blower door measurement conducted at 2013-07-03 which had a daily mean relative humidity at 55 %. This value is therefore used as initial condition for the shrinkage and swelling calculations.

Corresponding relative humidities are then calculated using the equations presented in Section 2.7 with a change of air gap width of 0.2 mm for each calculated step. This is done both in terms of increasing the gap width as well as decreasing the gap width. The equilibrium moisture content varies with temperature. Since the gaps analysed is situated inside the walls and since the shrinkage and swelling is caused by moisture from the indoor air, it is assumed that also the temperature in the gaps are close to the temperature of the indoor air, namely 20 °C. The *Equilibrium Moisture Content* assumed can be seen in Figure 9.

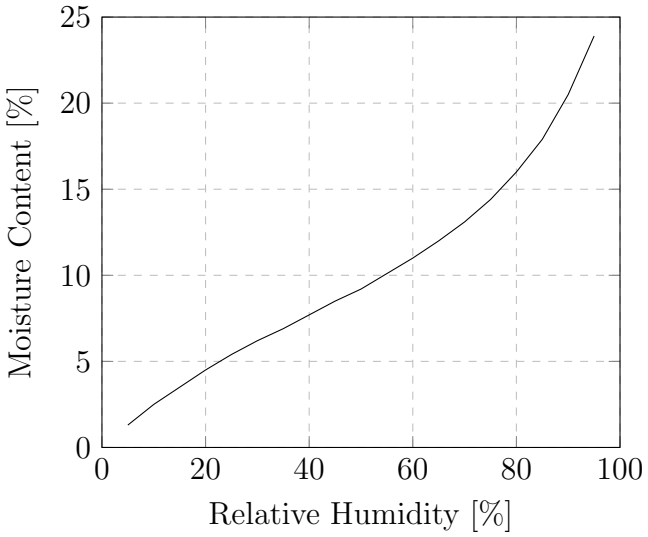

Figure 9: Equilbrium Moisture Content for timber (Simpson, 1998).

The air gaps are assumed to have a rectangular cross section and the pressure losses at inlet and outlet boundaries are therefore calculated according to Equation 5 where the air flow is the total flow over the entire cross section.

Results are presented as change in gap width compared to a decrease in relative humidity as well as decrease in gap width compared to an increase in relative humidity. Flow characteristic for each gap width is calculated and described in form of the *Powerlaw Model*, see Equation 7. To find the air flow as a function of the pressure difference for each gap width the CFD-module in *COMSOL* is used. The constants n and C for each leakage is then determined using the *Power regression method* which finds the value of the constants based on plotted pressure differences and air flows.

Calculations have been made with exfiltration in mind since this is the flow direction most critical regarding moisture problems. The temperature of the air has therefore been assumed to be 20 °C and its density chosen accordingly.

Table 3: Properties used for calculations in the CFD-module in COMSOL

Property	**Setting**
ϱ_{air}	1.2041 [kg/m^3]
μ_{air}	1.85·10^{-5} [Pa·s]
Wall boundary	*No Slip*
Inlet boundary	*Normal Flow*
Outlet boundary	*Suppress Backflow*
Mesh	*Mapped*
Maximum element size	4.5·10^{-5} [m]

Polyethylene-foils are often used to create a layer which prevents both air leakage and moisture diffusion through the wall. The ends of the foils in timber constructions are often fastened by squeezing them between construction joints. If this this is not done properly air leakages are likely to occur in these joints.

For the calculations of shrinkage and swelling all timber parts are considered to be of type Scots pine *Pinu silvestris*. Properties used in Equation 24 are $\alpha_f = 7.7$ % and $\mu_f = 30$ % according to Burström (2007).

3.2 Floor to wall connection

The joist connected to the concrete ground slab is fastened with either screw or nail. The leakage path is assumed to be between the joist and the concrete and the initial gap width is 1.00 mm. The upper part of the joist, meaning where the head of the nail meets the joist, is assumed to be fixed. This means that all the swelling and shrinkage in the joist is affecting the gap width. In other words: $L = (joist\ height)$ in Equation 25. The cross sectional dimension of the joist is 45 x 90 mm.

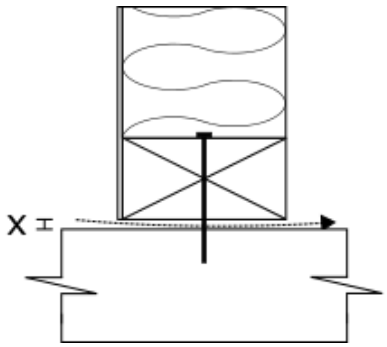

Figure 10: Leakage path in connection between floor joist and concrete ground slab.

Table 4 shows the results of the analysis. Constants C and n are shown for each gap width and with its corresponding moisture content and relative humidity. Higher humidities results in smaller air gaps and the relationship between air flow and pressure difference is linear. However, when the relative humidity decreases the air gap increases and the relationship between air flow and pressure difference becomes exponential.

Table 4: Gap widths in connection between floor slab and wall for different moisture contents and corresponding relative humidity.

x [mm]	**MC [%]**	**RH [%]**	**C [l/smPa^n]**	**n [-]**
0.20	16.9	82	0.00	1.00
0.40	15.2	78	0.00	1.00
0.60	13.5	72	0.01	0.99
0.80	11.8	64	0.03	0.97
1.00	10.1	55	0.06	0.94
1.20	8.4	44	0.10	0.90
1.40	6.7	33	0.17	0.86
1.60	5.0	23	0.27	0.82
1.80	3.3	14	0.39	0.77
2.00	1.6	6	0.54	0.74

3.3 Attic hatch

The frame for the attic hatch is connected to the attic floor joist with either screws or nails. The leakage path is assumed to be between the frame and the attic floor joist, see Figure 11 and 12. The batten covering the gap is assumed to be fastened without the intention to increase the airtightness of the gap. Therefore it is assumed that there is no additional airflow resistance caused by the batten. The initial air gap width is 2.17 mm. It is assumed that the frame in which the attic hatch is fastened is swelling or shrinking in a manner as if the inner part of the frame is fixed. The attic floor joist on the other hand is assumed to shrink and swell as if it was fixed on the side opposite from the attic hatch. In other words: $L = (joist\ width\ +\ frame\ width)$ in Equation 25. The cross sectional dimension of the floor joist is 195 x 45 mm and the cross sectional dimension of the frame joist is 195 x 45 mm.

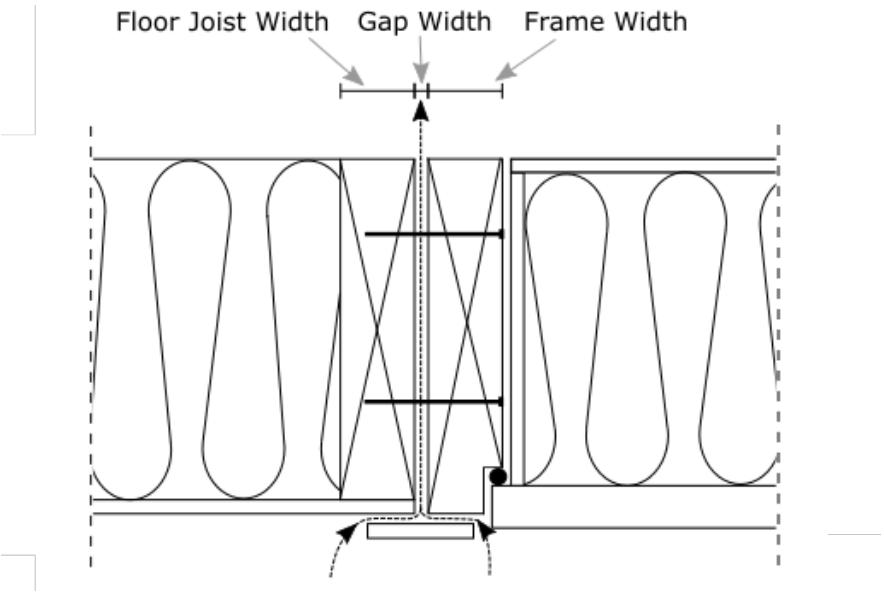

Figure 11: Figure showing leakage path in connection between attic hatch and attic floor joist.

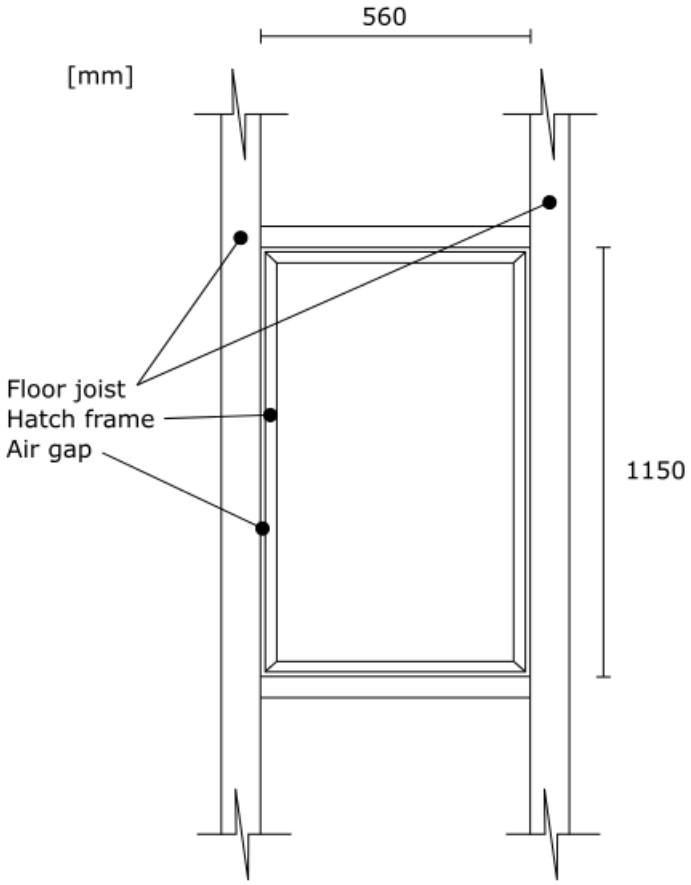

Figure 12: Figure showing principle construction of the attic hatch.

Table 5 shows the results of the analysis. Constants C and n are shown for each gap width with its corresponding moisture content and relative humidity. Since the timber parts are relatively thick, compared to for example the wall to floor connection, the change in air gap width in relation to relative humidity is greater.

Table 5: Gap widths in connection of attic hatch for different moisture contents and corresponding relative humidity.

x [mm]	**MC [%]**	**RH [%]**	**C [l/smPa^n]**	**n [-]**
0.17	18.6	86	0.00	1.00
0.37	17.8	85	0.00	1.00
0.57	16.9	82	0.00	1.00
0.77	16.1	80	0.01	0.99
0.97	15.2	78	0.02	0.99
1.17	14.4	75	0.04	0.97
1.37	13.5	72	0.06	0.96
1.57	12.7	68	0.10	0.93
1.77	11.8	64	0.15	0.91
1.97	11.0	60	0.21	0.88
2.17	10.1	55	0.29	0.85
2.37	9.2	50	0.39	0.82
2.57	8.4	44	0.51	0.79
2.77	7.5	39	0.65	0.77
2.97	6.7	33	0.80	0.74
3.17	5.8	28	0.97	0.72
3.37	5.0	23	1.15	0.70
3.57	4.1	18	1.34	0.68
3.77	3.3	14	1.54	0.66
3.97	2.4	10	1.75	0.65
4.17	1.6	6	1.97	0.64

3.4 Window leakage

For the window construction there are two possible leakage paths. One between the window frame and the wall joists and one between the window and the window frame, see Figure 13.

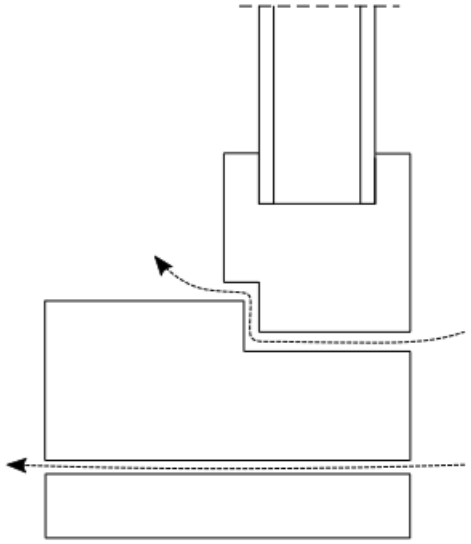

Figure 13: Figure showing leakage paths in the window construction.

Window and window frame

The window itself is hung on hinges and for shrinkage calculations it is assumed to be fixed at the point where the window sash meets the glass. The window frame is assumed to be fixed at its vertical center plane. So that half of its total shrinkage is affecting the air gap. The initial gap width is 0.55 mm. Shrinkage is calculated according to Equation 25 where $L = (sash\ height + 0.5 \cdot (frame\ height))$ and $sash\ height = 40\ mm$ and $frame\ height = 34\ mm$.

Table 6 shows the results of the analysis. Constants C and n are shown for each gap width with its corresponding moisture content and relative humidity. Results show a less significant change in gap width in relation to humidity compared to for example the attic hatch.

Table 6: Gap widths in connection between window and window frame for different moisture contents and corresponding relative humidity.

x [mm]	**MC [%]**	**RH [%]**	**C [l/smPa^n]**	**n [-]**
0.19	0.19	69	0.00	1.00
0.39	0.39	62	0.00	1.00
0.59	0.59	55	0.01	0.99
0.79	0.79	47	0.03	0.96
0.99	0.99	38	0.07	0.91
1.19	1.19	29	0.13	0.85
1.39	1.39	21	0.23	0.78
1.59	1.59	14	0.36	0.71
1.79	1.79	8	0.52	0.64

Window frame and wall joist

The window frame is fixed as described in the previous section meaning that half of its total shrinkage is affecting the air gap. The wall joist is assumed to be fixed at its bottom side so that the total shrinkage of the joist is affecting the gap width. This means that $L = (joist\ height\ +\ 0.5 \cdot (frame\ height))$ in Equation 25 and $joist\ height = 20\ mm$ and $frame\ height = 34\ mm$.

Table 7 shows the results of the analysis. Constants C and n are shown for each gap width with its corresponding moisture content and relative humidity. Results show also for this leakage a less significant change in gap width in relation to humidity compared to for example the attic hatch.

Table 7: Gap widths in connection between window frame and wall joist for different moisture contents and corresponding relative humidity.

x [mm]	**MC [%]**	**RH [%]**	**C [l/smPa^n]**	**n [-]**
0.15	14.3	74	0.00	1.00
0.35	12.2	66	0.00	1.00
0.55	10.1	55	0.01	0.99
0.75	8.0	42	0.02	0.98
0.95	5.9	28	0.04	0.97
1.15	3.9	17	0.07	0.94
1.35	1.8	7	0.11	0.91

Verification of shrinkage calculations

In order to verify the results, a comparison is made between calculated shrinkage and empirical measurements. In Domone and Illston (2010) results from such an empirical study shows that, when dried from 90 % to 60 % relative humidity, Norway spruce *(Picea abies)* had a shrinkage of 1.5 % in the tangential direction and Scots pine *(Pinus sylvestris)* had a shrinkage of 2.2 % in the tangential direction. Using Equation 24 to calculate shrinkage when dried from 90 % to 60 % relative humidity in Norway spruce and Scots pine gives the shrinkage 2.4 % and 2.6 % respectively. Results from calculations can be seen as being within an acceptable order of magnitude.

Verification of COMSOL results

In order to ensure the accuracy of the simulations performed in COMSOL, a mesh convergence analysis is performed as well as comparisons with analytic solutions.

Mesh size A more coarse mesh size reduces the computation speed but decreases the accuracy. Therefore in order to find the largest mesh size allowed without adventuring result accuracy a mesh convergence analysis is performed. This is done for the air leakage in the wall to floor connection. A number of simulations are performed where the element size is decreased by 10 % in each step. Results are compared regarding the constants C and n and the element size is considered acceptable if the variation of C and n between two steps is less than 0.5 %.

Analytic comparison For each specific air leakage at least one of the results are compared with its analytic solution using the *Quadratic Model* described by the Equations 3, 4 and 5.

3.5 Impact of leakage variation

Results from shrinkage and swelling calculations show that relative humidity can have a quite substantial effect on the width of the air gap. For air gaps smaller than 1 mm when also the relative humidity is in the higher end, the air flow has an almost linear relation to the relative humidity. If the gap width is larger, which normally occurs at lower relative humidities, the relation between air flow and relative humidity is exponential where exponent n is smaller than 1.

Results also show that the way a connection is designed can influence how much the gap width varies. If the timber parts surrounding a leakage are thick the shrinkage and swelling movements will be bigger and thus also the air flows. With the addition

that the air flow increases exponentially (as described above) with decreased relative humidity this effect is enhanced even further.

This makes the connection of the attic hatch even more interesting. Since there have been reports suggesting that leaky attic hatches could be the primary cause of mould growth in cold attics (Harderup and Arfvidsson, 2013). The connection as simulated has quite large variations in air flows dependent on moisture content of the connection. The risk of mould growth is even worsened since it is likely that the highest air leakage occurs during winter when the temperature at the attic is at its lowest and thus brings up the relative humidity.

It is important to notice that the change in gap width is assumed to be uniform over the entire leakage paths. This is obviously a simplification, in reality timber fibres will shrink or swell differently in different parts of the joist and cause warping and twisting. It is likely that this will result in larger leakages in some areas along the joist whilst other areas will be more airtight. However, such accuracy is hard to achieve without more thorough investigation of how shrinkage and swelling affects particular leakages.

4 Laboratory Testing of Guesthouse

Since relatively few studies have been performed looking solely at how airtightness correlates to relative humidity in the indoor environment such measurements are conducted on a small guesthouse. The idea is to increase the relative humidity in the indoor environment for a longer period and measure the airtightness repeatedly throughout the period. The procedure is then reversed so that the relative humidity in the indoor environment is decreased and the airtightness measured repeatedly until it is back to its initial value.

Figure 14: Guesthouse during Blower door measurements.

4.1 Building description

The guesthouse used in the experiment is a timber construction with a living space of about 13 m^2. Its main functional purpose is to work as a guesthouse. It will therefore only have temporary visitors and moisture loads and heating demand will vary dependent on whether the building is occupied or not. The foundation consists of plinths on which the house rests. There is no moisture tight layer in the thermal envelope meaning that vapour is allowed to move freely by diffusion in the construction. The floor construction consist of a massive tongue and grove timber floor on top of floor

joists with intermediate insulation. Asphalt boards are fastened on the bottom side of the floor joists. There is no wind barrier in the floor construction and air is therefore allowed to move through gaps inside the floor construction. Walls have an exterior z-panel, air gap and a wind barrier. Behind the wind barrier there are wall joists with intermediate insulation. On the inside there is one layer of asphalt paper and an OSB board. The roof has a roofing paper on top of a layer of tongue and groove board and below there is an air gap, Masonite, insulation, wind barrier and last a tongue and groove board. The guesthouse also has three full height windows and an entrance glass door as well as two smaller windows. Ventilation is natural ventilation with two ventilation ducts situated on each side of the guesthouse right below the ceiling. A floor plan of the building can be seen in Figure 17.

4.2 Blower door test

Blower door test is a standardized test procedure described in the European standard EN 13829:2000 used to measure the airtightness of the building envelope. The equipment consists of a fan placed inside a covered metal frame. The frame itself is then fastened in the door opening of the building that is going to be tested, see Figure 15.

Figure 15: Blower door equipment mounted in the guesthouse.

While in operation the fan blows air through an opening with known cross sectional area and flow resistance. The pressure difference over the opening is measured and the air flow through the opening can then be calculated. According to the law of mass conservation the same mass of air passing through the fan must also pass through leakages in the building envelope, see Chapter 2.3. Also the pressure difference between the interior of the building and its exterior surrounding is measured and the air flow is related to this pressure difference. Since the airtightness of a building is affected by the airflow direction, the blower door is typically run in both direction, taking measurements for both pressurization and de-pressurization.

Equipment used in this project is the *Minneapolis Blower Door*. The equipment is used together with the computer software *Tectite* which automatically adjusts the airflow for a number of different pressure differences and calculates the relation between airflow and pressure difference according to Equation 7.

Since it is only the unintentional leakages that are of interest, openings such as vent ducts must be properly sealed, see Figure 16. It is also important that the frame itself is properly adjusted so that no air is allowed to pass between the door opening and the blower door frame. This is especially important when measuring a smaller building such as the guesthouse. This since a possible leakage area between the blower door frame and the door opening could be a relatively large contribution to the overall leakage area. However, this might be less sensitive if measuring a larger building since the total leakage area is likely to be bigger.

In order to test the influence of possible leakages between the door opening and the blower door frame a sensitivity analysis is performed. The airtightness is measured when the blower door frame is sealed also with the use of adhesive tape and results are compared with the airtightness achieved when no adhesive tape is used. The results show a very small difference in airtightness it is therefore considered to be enough to use the blower door frame without additional sealing.

Figure 16: Ventilation duct sealed by squeezing a plastic sheet behind the ventilation cover.

A typical test procedure is performed as follows:

1. Close all intentional exterior openings.
2. Install the blower door frame and fan in the door opening.
3. Start new test in *Tectite*
4. In *Tectite* set indoor and outdoor temperatures.
5. Run automated multipoint test and use flow rings recommended by the software.
6. Save test results.

4.3 Controlling the indoor environment

During the first phase, the moistening phase, the relative humidity in the indoor environment is increased. This results in increased moisture content in the timber parts which in turn results in swelling. The purpose of this phase is to measure how an increase in relative humidity affects the air tightness of the building. Since the guesthouse only is available for measurements during 15 days and since both moistening and drying is to be tested, it is necessary to increase relative humidity to a quite hight level so that the effects on airtightness can be clearly seen. It is therefore decided to

aim for a relative humidity of 90 % during the moistening phase. The humidity is increased using a small air humidifier normally used for offices and residential spaces where the relative humidity is low. The humidifier evaporates water to vapour using ultrasound and the rate of evaporation can be adjusted manually. Since the indoor relative humidity is dependent on the somewhat unstable relative humidity outdoors it is very difficult to adjust the humidifier so that it maintains an indoor relative humidity of 90 %, a control system is therefore built and connected to the humidifier. The control system consists of a programmable micro controller (Arduino Uno) and a humidity sensor. The controller takes readings every minute from the humidity sensor which is placed inside the guesthouse (close to log number three, see Figure 17). If the relative humidity is higher than 90 %, the controller sends radio frequency signals to a remote switch telling it to turn the humidifier off. Likewise, if the relative humidity is lower than 90 % the humidifier is turned on. Since the humidifier does not have any means of spreading the vapour in the room itself, it only produces vapour, a ventilation fan is placed a couple of metres away from the humidifier and directed towards the humidifier. This way the air in the guesthouse is circulated and forced to pass the vapour stream from the humidifier resulting into a more evenly spread vapour.

During the second phase, the drying phase, the humidifier is turned off and the relative humidity in the guesthouse is lowered using both a radiator and the blower door equipment. During the first time the blower door is run at a low pace during daytime in order to ventilate the the guesthouse and reduce the relative humidity. At night time as well as the last days of the drying phase a radiator is used to increase the temperature difference between the air inside and outside the guesthouse, this results in a stack effect which increases the air exchange rate. This way the relative humidity is lowered both by increasing ventilation with exterior air and by increasing the saturation vapour pressure. The sealing of the ventilation ducts is removed during the drying phase and is only used when blower door tests are performed.

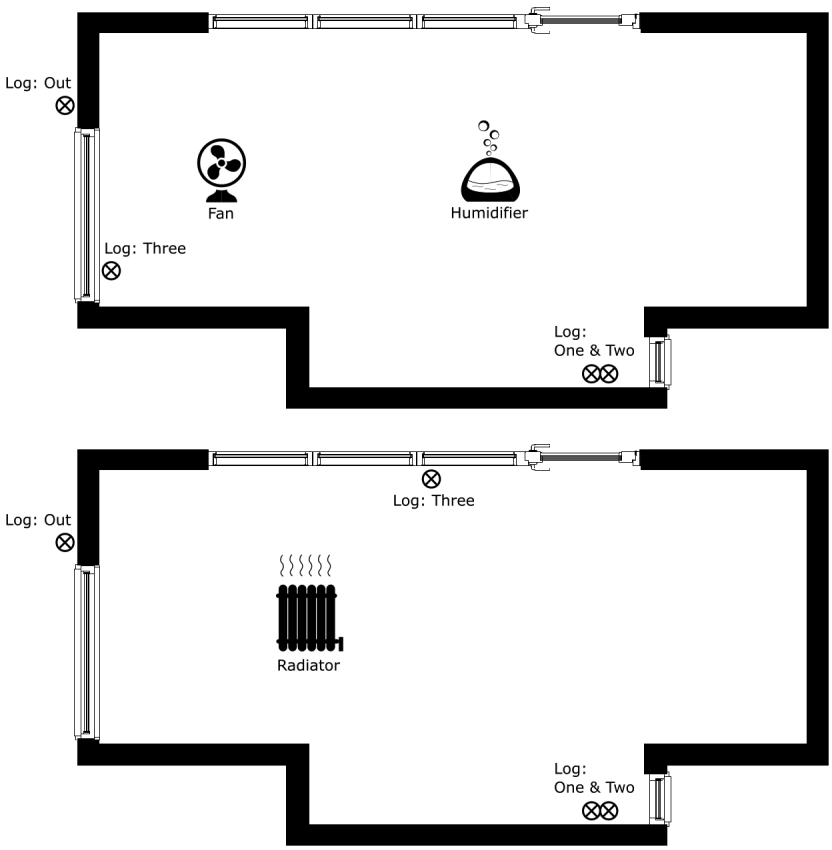

Figure 17: Arrangement of equipment during moistening phase (upper) and drying phase (lower).

4.4 Measurements of temperature, humidity and airtightness

Throughout the entire test period temperatures and humidities are measured each minute at four different locations, outside the guesthouse, right beside the larger window inside the guesthouse and two at different heights right beside the smaller window inside the guesthouse. During the drying phase the log close to the larger window inside the guesthouse is moved to the front of one of the full height windows, see Figure 17. The reason for this is to avoid having the log affected by air flows coming from the window. Unfortunately, during the measurements some error occurred in log number three, the one placed beside the larger window inside the guesthouse and therefore data from this log is missing between day two and day six.

Apart from temperature and moisture measurements, moisture content is always measured right before a blower door test is performed. This is done using a non-destructive moisture meter which utilizes a method based on the dielectric constant- and frequency

principle. Four measurements are taken each time on floor, ceiling and wall respectively and an arithmetic mean value is calculated for each of them. The method used by the instrument is not as accurate as those using destructive methods and results may vary significantly between different positions even though measurements are taken on the same surface. The mean value helps correct this to some extent, but the measurements should still only be regarded as rough estimations rather than absolute values.

The guesthouse is constructed inside a large storage space where the relative humidity is typically between 20 % and 35 %. The moisture content of the construction timber is also measured before the exterior panels are installed and after the construction timber has been stored in the storage space for a number of days. The measurements are however done in a different, more accurate manner than described earlier. Three samples are taken from the construction timber and then weighted and dried in an oven at 105 °C. The weights of the samples are measured a number of times until there is no difference in weight between two measurements. This means that they have reached steady state and the moisture content can be calculated using known oven dried weight of the samples. The moisture content in the construction timber is found to be 9.9 %.

During both phases, moistening and drying phase, blower door tests are performed periodically according to the method described earlier. Tests are performed once a day in the early period of the moistening phase in order to get more detailed results. However, since changes in airtightness happens more slowly after two to three days measurements are instead performed every second day.

In the end of the test period a leakage search is performed using an anemometer. The blower door is then installed in the door opening and the fan is run at a speed causing de-pressurization at a constant pressure difference of 50 Pa. This can easily be done using the option *Cruise* in Tectite. The interior of the guesthouse is then searched for leakages using the anemometer and measured air speeds are noted in a floor plan drawing of the guesthouse, see Figure 23. This way an estimation of where the largest leakages can be found is documented. However, it is important to note that the air speeds measured only works as a rough measurement of how large leakages in the guesthouse are relatively to one and another. It is by no means the way of describing the exact air speed through the leakage.

4.5 Results on humidity and airtightness

Figure 18 shows the results of the moisture content measurements conducted at the beginning of each blower door test. As discussed earlier, measurements should be regarded as rough estimations rather than exact values. Still a trend of increasing moisture content during the moistening phase which occurs during the first 8 days can be seen. After the initiation of the drying phase the moisture content seems to be

dropping, this is especially true for the moisture content in the ceiling. Unfortunately the numbers are too uncertain to be directly coupled with the change in airtightness. A more exact method for measuring moisture content is therefore recommended for any future attempt to replicate the experiment.

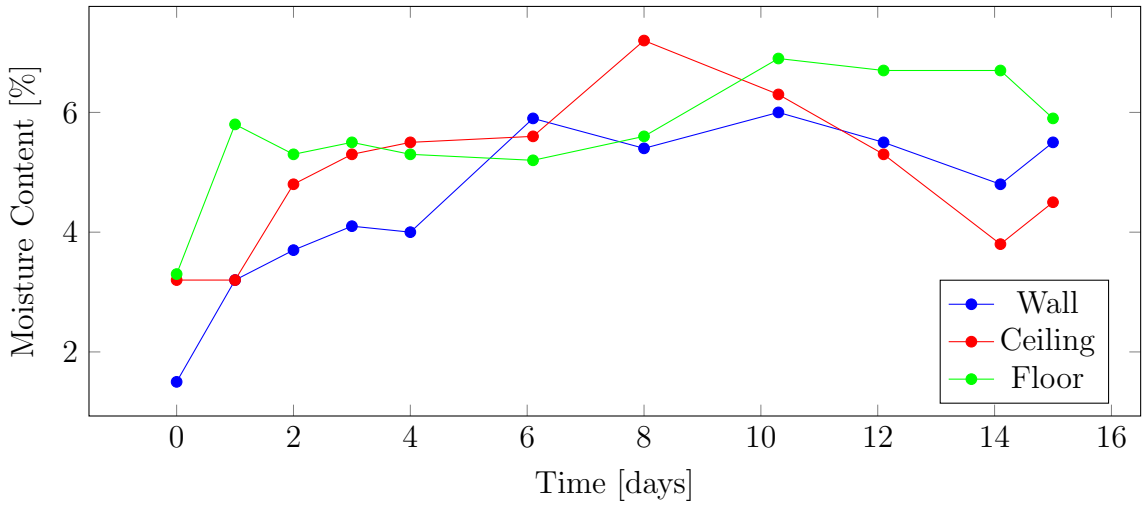

Figure 18: Results from measurements of moisture content in the guesthouse.

During both phases, moistening- and drying phase, temperatures and humidity is measured continuously. The results of these measurements can be seen in the following figures. Temperature is relatively stable during the moistening phase and stabilizes at around one degree higher than the outdoor temperature. The excess heat that increases the temperature is likely to come from the equipment used, namely the fan and the humidifier. When a blower door test is performed or when the guest house is opened to refill the humidifier with water the temperature drops to that of the exterior and increases slowly until the next blower door test. During the first days of the drying phase the temperature is increased during night time by using a radiator. However, since the blower door is used to ventilate during daytime the temperature doesn't reach steady state. The last couple of days, only the radiator is used as a mean of drying and the only interruption of the heating occurs when blower door measurements are performed. The temperature is therefore at times quite stable at around 33 °C.

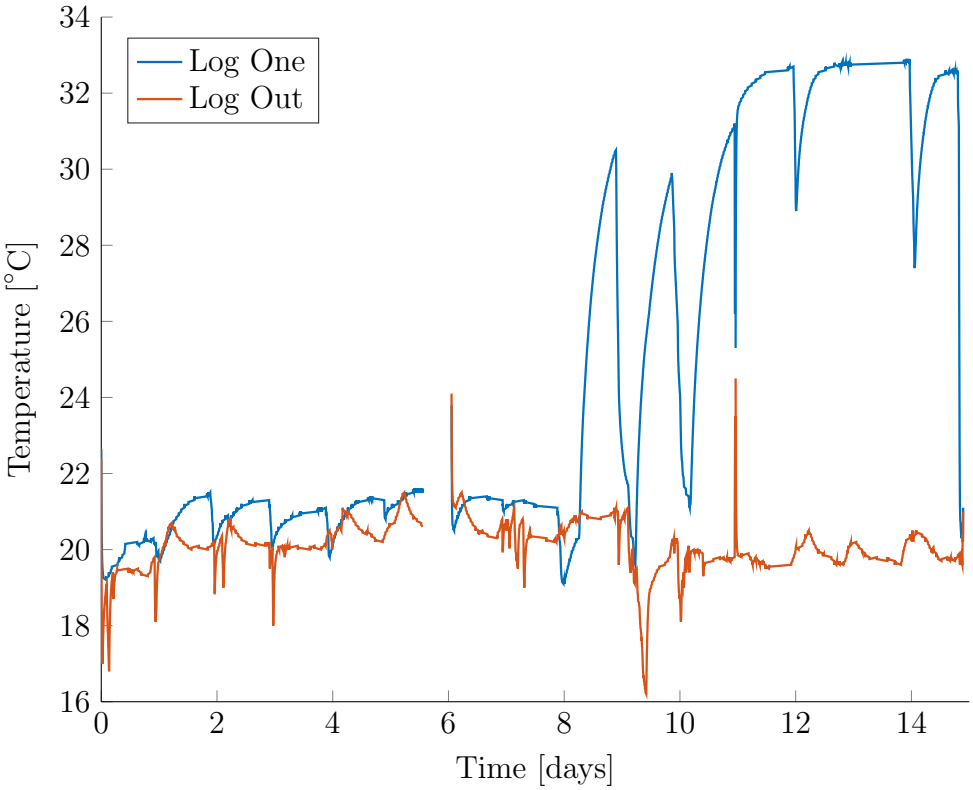

Figure 19: Plot showing temperatures during the entire test period.

During the first day of the moistening phase a fan was not used to help spread the vapour from the humidifier in the room. This resulted in the humidifier using large amounts of water which mostly condensated on the floor around the humidifier. This indicated that the air had very high humidities close to the humidifier while humidity logs shows not very high relative humidities (see Figure 20 and 21). The fan solves this problem which results in the logs showing more similar humidities and also relative humidities around 90 % which is the objective of the control system. Because of the moisture capacity of the timber itself, relative humidities are in general less stable in the beginning of the moistening phase. However, during the last two days the relative humidity is more stable and less influenced by moisture fluctuations in the outdoor air which indicates that the construction is close to a steady state condition. In the beginning of the moistening phase the relative humidity is heavily influenced by the increase in temperature caused by the radiator whilst the effect on the humidity is more long term related.

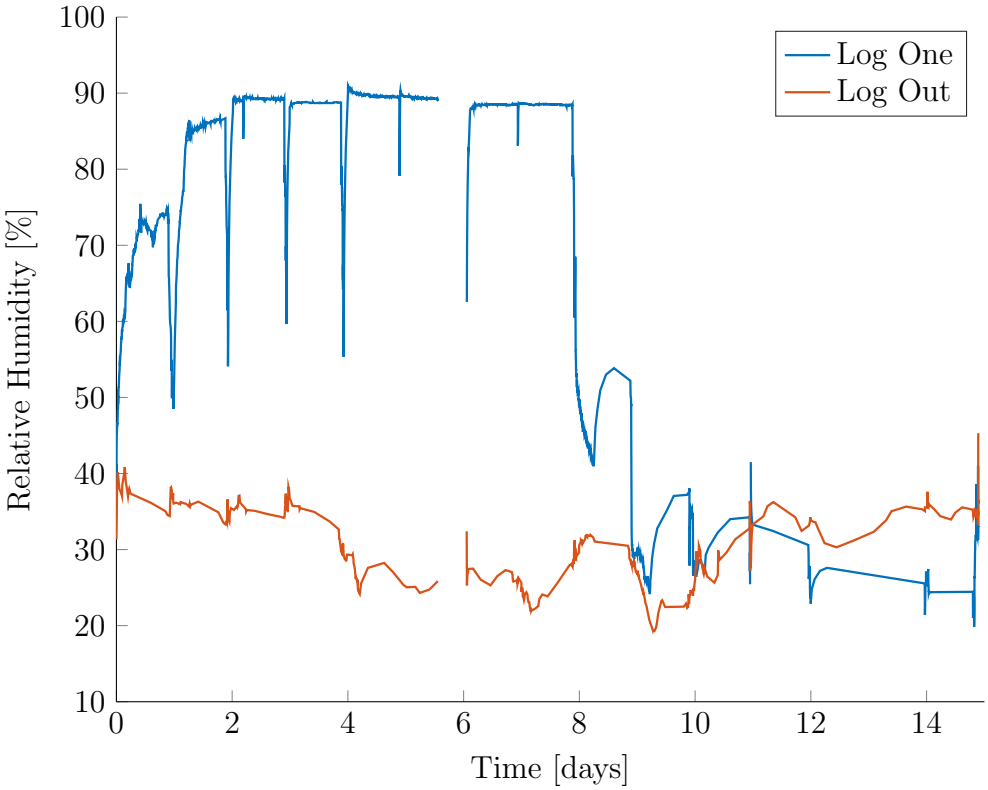

Figure 20: Plot showing relative humidities during the entire test period.

Each sudden drop in humidity is strongly correlated with the time of when blower door tests are performed. However, it is interesting to note that this also affects the humidity- and temperature readings of the outdoor log placed on the exterior beside the larger window. The affect is most evident in the readings of relative humidity and temperature indicating that the blower door test causes a drop in temperature at the location of the exterior log. Since the window itself is closed during the blower test the reason to this behaviour is hard to predict but it might perhaps be related to an air leakage close to the log.

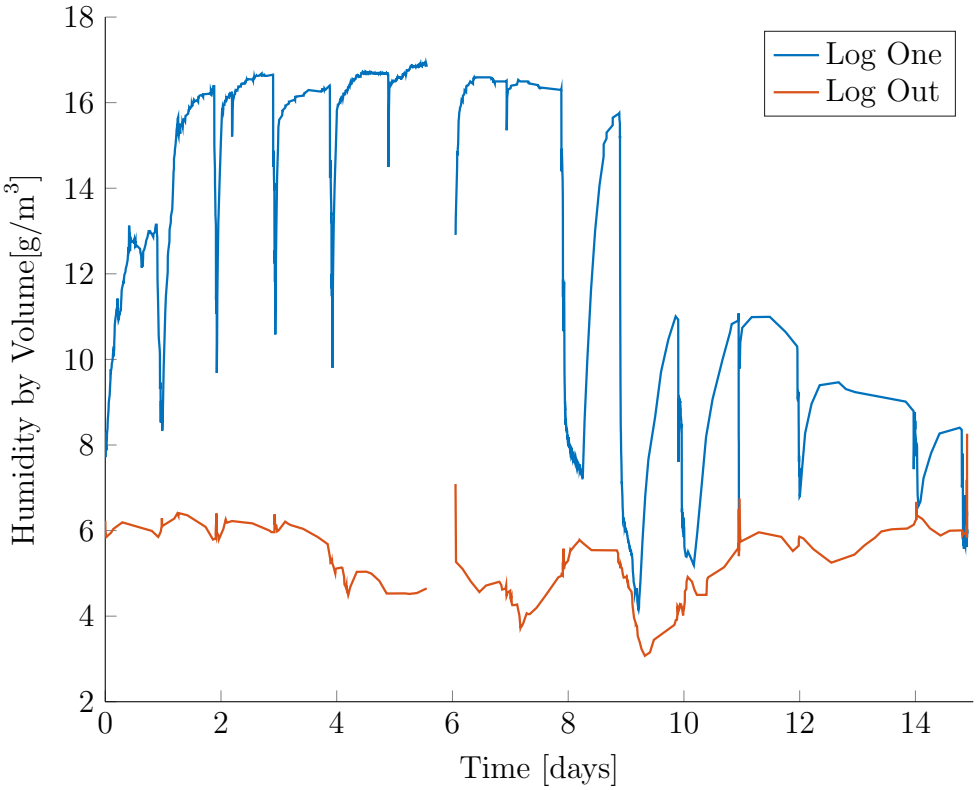

Figure 21: Plot showing humidities during the entire test period.

Figure 22 shows the specific air leakage at a 50 Pa pressure difference plotted together with relative humidities. The two first days of the moistening phase the air leakage drops from 1.17 l/sm^2 to 0.89 l/sm^2, a change of 24 % in relative humidity. During the remaining period of the moistening phase air leakage drops about 3 % per day indicating that even though the relative humidity is somewhat stable in the indoor air, movements in the timber such as swelling are still occurring inside the construction and affecting the air leakage. After initiating the drying phase, results from the first blower door test shows an increase in air leakage from 0.74 l/sm^2 to 0.98 l/sm^2. The remaining days in the drying phase the air leakage continues to increase with about 5 % per day, reaching in the end an air leakage that is slightly higher than it was at the beginning of the moistening phase. The cause of this is likely the radiator which by increasing the temperature also lowers the relative humidity to an extent that is even lower than relative humidity outside the guesthouse.

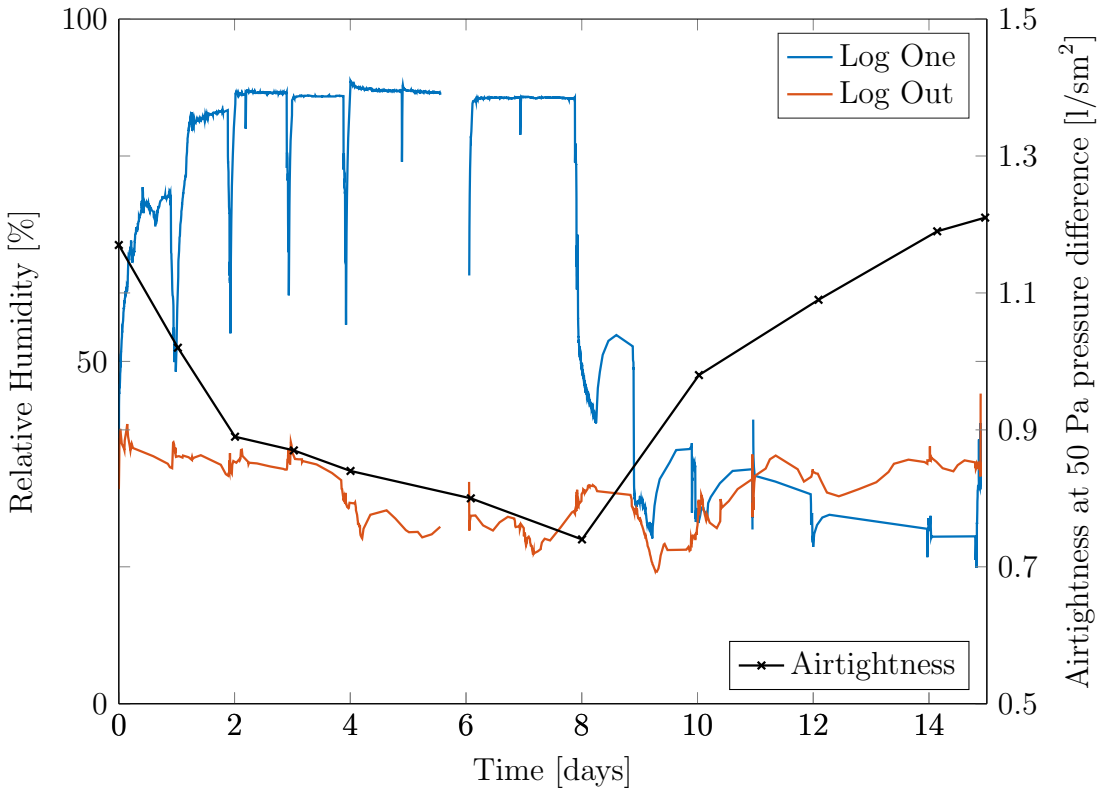

Figure 22: Plot showing relative humidities together with specific air leakage at 50 Pa pressure difference during the entire test period.

At the end of the drying phase a leakage search is performed where leakages and its corresponding air speeds are documented, results can be seen in Figure 23. It is clear from the results that the main leakage source is the connection between the floor and the wall. The reason to this might be the fact that wind barriers are used for walls and roof but not for the floor itself. The tongue and grove connection between the floor planks might be one reason to why the floor itself is airtight despite the lack of a wind barrier.

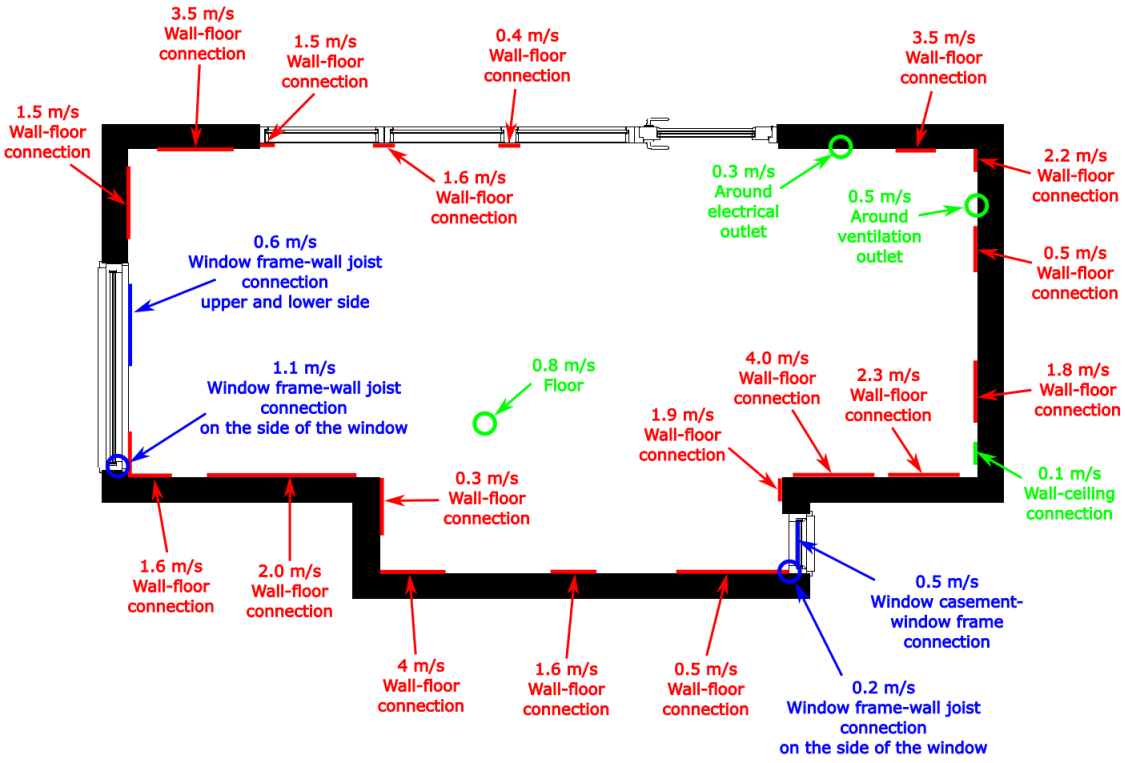

Figure 23: Floor plan with measured leakages 2016-03-28

Results show that the air tightness of a building is affected by the indoor moisture conditions. Under more extreme conditions air leakage may increase by as much as 13 % in only 24 hours. Even though such a rapid change in indoor relative humidity is not likely to occur in reality there are occasions where similar circumstances are present. For example timber in newly built timber constructions should according to recommendations not exceed a moisture content of 16 % Olsson (2014) which, when in equilibrium, corresponds to about 80 % relative humidity at 20 °C. According to (Warfvinge and Dahlblom, 2010), the relative humidity in the indoor environment can drop to 30 % during winter months, similar to the humidity levels measured in the guest house. If such amounts of moisture are built into a construction it is likely that air leakages will increase if the timber construction becomes dryer. It is also likely that tests of airtightness performed during the construction phase are not going to be valid in the long run. It is hard to draw conclusions from the test stating any exact numbers. But the effect might be important to take into account during construction if the goal is to have a building with high airtightness.

5 Numerical Model

In order to evaluate the influence of varying airtightness it is necessary to establish a starting-point which can work as a reference when testing and analysing different leakage scenarios. The starting-point in this study consists of a model with an overall air-leakage corresponding to a chosen reference building and a leakage distribution corresponding to a normal modern building. This chapter describes how the model is defined and the assumptions made in the model.

5.1 Reference building

The reference building is a detached single-family house situated in Landvetter outside Gothenburg. The house was built in 2004, has an insulated concrete ground slab and a cold unfurnished ventilated attic. It is a timber frame house with mineral wool insulation and an air and moisture barrier made of a 0.2 mm thick polyethylene foil. The total floor area is 124 m^2 and the total envelope area is 300 m^2, Wahlgren et al. (2015).

5.1.1 Airtightness

For the reference building there are results available from blower door tests performed at a number of occasions during the period 2013-07-03 to 2014-08-26. Used as a reference leakage value when defining the reference model is the average value from the first measurement, namely 180 liter/s at 50 Pa pressure difference, Wahlgren et al. (2015). There are also air speed measurements available at a number of leakage locations in the building. These measurements were conducted at three occasions during one year. The values are used to give an idea of which of leakages that are the most decisive. The most significant leakages based on the air speed measurements and thermograms are: leakages around window frames and through window casement, leakages at the floor-wall interface and leakages at the connection of the attic door, Wahlgren et al. (2015). It would be convenient to use these measurements as a comparison with respective leakage in the model. However, due to the nature of the method of measurement this is not applicable, see Section 2.4.

5.2 Model in CONTAM

The geometry of the model is simplified to a rectangular box with the dimensions 6×10.3×5.4 meters resulting in a total floor area of 124 m^2 and a total envelope area of 300 m^2. The model has one entrance door with a total area of 2.1 m^2 and a total circumference of 12.4 m. There are 14 windows with a total area of 25.2 m^2 and

a total circumference of 75.5 m. The air flow through the leakages in the building is calculated using CONTAM, where the airflow through each leakage as well as the total airflow through the thermal envelope is calculated for a pressure difference of 50 Pa. Meaning that a *Blower Door* test is simulated according to the European standard EN 13829:2000, the same method used for finding overall leakage in the study Wahlgren et al. (2015). The living space is modelled as a single zone, this is simplification is according to American Society of Heating and Engineers (1997) only valid for buildings with no internal resistance to air-flow. This was confirmed by splitting the living zone into two zones with one larger opening in between where the opening resembled the opening for a staircase. The airflow through the large opening was then calculated in CONTAM and the result showed large airflows with small pressure differences, indicating that the single-zone assumption is valid. However, in order to find the leakages between the attic and the living space the attic itself is modelled as a single zone connected to the living space through leakages. A similar approach is used for cases when airflow from a crawl space is to be studied.

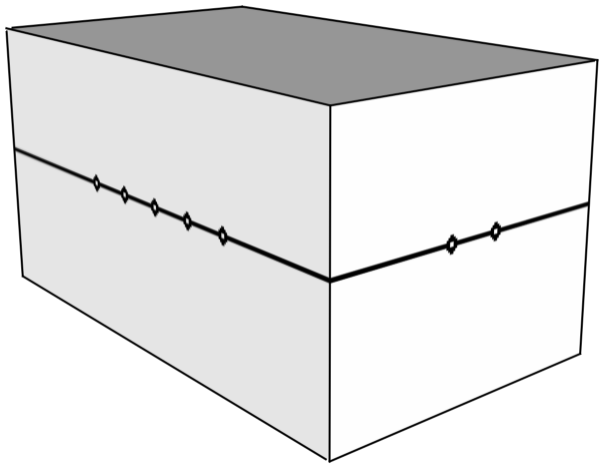

Figure 24: Principal drawing of the model in CONTAM. Every circle represents a leakage path.

5.2.1 Conformity with reference building

The geometry of the reference building is not strictly followed when defining the model. The reason to this is that such level of detail would prolong time for both simulation and the work needed for defining the model. Since leakages are mainly dependent on type of leakages and number of leakages, effort is put into assuring reasonable leakage distribution and similar over-all leakage as for the reference building, disregarding the geometry of the reference building. However, to ensure similar leakage per area of envelope, roughly the same floor area and envelope area is used in the model as for the reference building.

5.2.2 Simulation strategy

The establishment of the reference model is an iterative process. The first step is to choose leakages, leakage sizes and leakage location in the model to use as an input in CONTAM. Next step is to calculate leakage distribution and overall leakage in terms of air mass flow using CONTAM. The results from CONTAM is then compared with the reference object and leakage distribution study respectively. If the correspondence is poor the leakages are adjusted and the procedure repeated once again. The procedure is then repeated until the behaviour of the model resembles the reference object. The workflow is illustrated in the figure below.

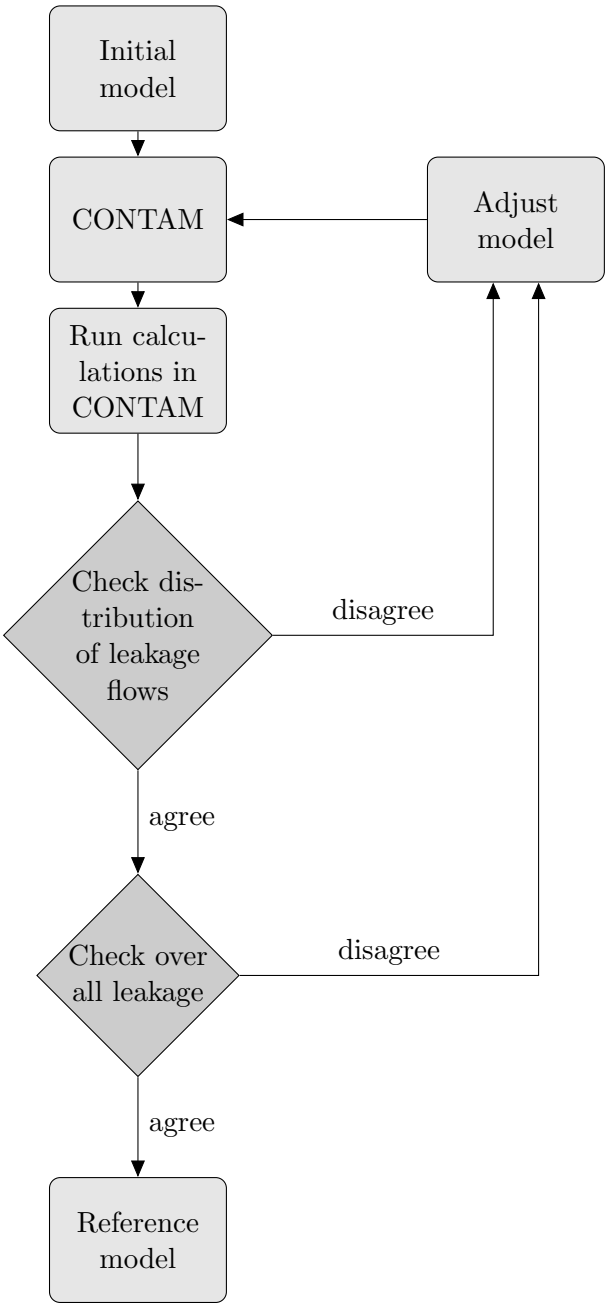

Figure 25: Flowchart describing the process of creating the reference model.

5.3 Individual leakages

Airflow through leakages are simulated in CONTAM using the Power law model, Equation 7 where each type of leakage is described as the cross-sectional area of the orifice perpendicular to the airflow, see Section 2.1. Two databases are used as guidelines

in setting up the leakage model. In accordance with these reference databases, the flow exponent is set to n=0.65 at the reference condition 4 Pa for all leakages. There are three kinds of entry values: "Leakage area per item", "Leakage area per meter" and "Leakage area per area". Leakage data is taken from Emmerich et al. (1996) and American Society of Heating and Engineers (1997) and if necessary adjusted to increase similarity with the reference building as described in Section 5.2.2.

Adding leakage data from the two databases into the model without alteration gives a total leakage greater than for the reference model. A possible explanation for this is the fact that the leakage data in the two databases is from 1996 and 1997 respectively whereas the reference building was built in 2004, newer buildings are in general more airtight than older buildings. Another possible explanation is that American houses, which the databases are based on, are usually less airtight than Swedish houses. In order to compensate for this, some of the leakages from the databases are reduced so that they match better with the overall leakage and leakage distribution of the reference model. In other words the databases are used as guidelines rather than its exact values. Each leakage and how it is adjusted is described below.

All leakages are not found when conducting tests on airtightness. In order to find a leakage distribution, the best assumption is to divide the overall leakage on the leakages that can be found.

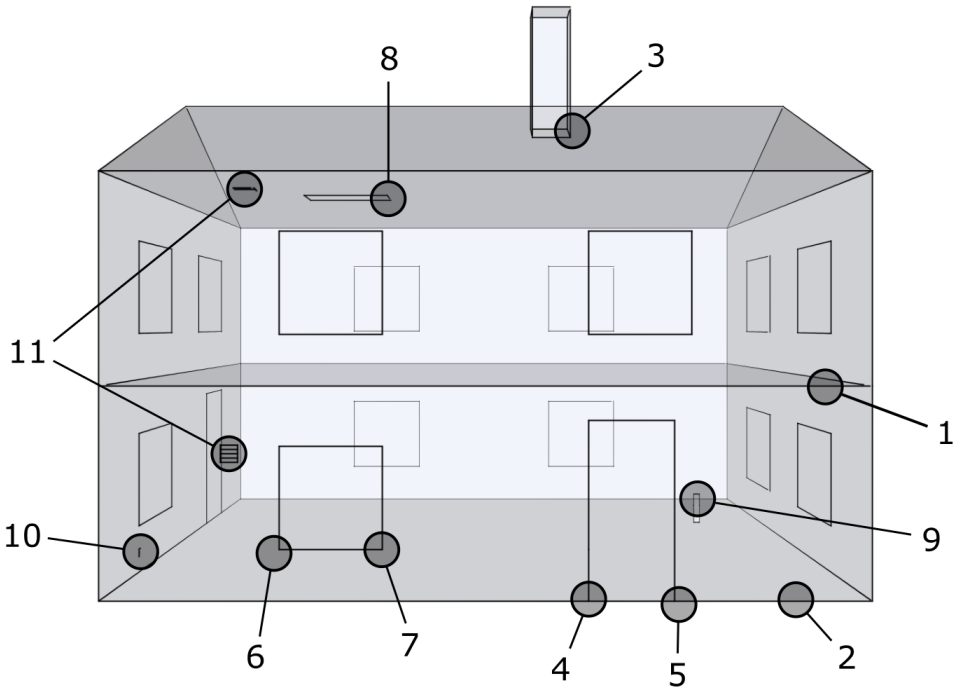

Figure 26: Principal drawing showing leakages taken into account in the model: 1. Ceiling-Wall Joint, 2. Floor-Wall Joint, 3. Chimney, 4. Door, 5. Door frame, 6. Window frame, 7. Window, 8. Attic Hatch, 9. Piping and wiring penetrations, 10. Electric outlet, 11. Ventilation inlet and outlet

Ceiling-Wall Joint The calculated length for this leakage is assumed to be the connection between ceiling and the exterior wall.

Intermediate Floor-Wall Joint The calculated length for this leakage is assumed to be the connection between intermediate floor and exterior wall.

Floor-Wall Joint Includes the connection between exterior wall and the ground slab.

Doors and Windows Leakages occurring in the door and window constructions including frames.

Description	Leakage [cm^2/m]	Length [m]	Height [m]
Ceiling-Wall joint	0.8	33	5.4
Intermediate floor-Wall joint	0.8	33	2.7
Floor-Wall joint	0.8	33	0
Door	0.23	12.4	1.05
Window casement	0.2	75.6	1.5/4.3

Table 8: Table showing leakage areas used in the model.

Doors and Window frames Includes leakages occurring in the connection between the door and window frames to the exterior wall.

Description	Leakage [cm^2/m^2]	Area [m^2]	Height [m]
Door frame	0.3	4.2	1.05
Window frame	0.3	25.2	1.5/4.3

Table 9: Table showing leakage areas used in the model.

Chimney The penetration of the chimney through the thermal envelope is assumed to be similar to the penetration of the ventilation inlet. The leakage for the chimney is therefore given the same value as the leakage of the ventilation inlet.

Attic hatch Leakage caused by the attic door installed in the ceiling between indoor and attic.

Ventilation ducts The number of ventilation ducts is assumed to be two, one for inlet air and one for outlet air.

Electric outlets Leakages caused by the installation of electric outlets.

Penetrations Piping and wiring penetrations are given leakage values per item. It is assumed that a normal building has the following penetrations: drain, water supply, electricity supply and internet/telephone connection.

Description	Leakage [cm^2]	Number	Height [m]
Chimney	2	1	5.4
Attic hatch	12	1	5.4
Penetrations	2	4	0
Electric outlets	0.5	12	0.1/2.9
Ventilation ducts	1	2	2/5.4

Table 10: Table showing leakage areas used in the model.

5.4 Leakage distribution

To ensure that the distribution of the leakages is within reasonable limits a comparison is made with previous research. In a study of Finnish detached houses the following leakage distribution was found: "Penetrations: 9 %", "Joints: 60 %" and "Doors and windows: 31 %" Kalamees et al. (2008). Since building techniques in Sweden and Finland are similar the results can be used to confirm the plausibility of the leakage distribution in the model. Studies recapitulated by American Society of Heating and Engineers (1997) concludes following leakage distribution: "Walls and ceiling (including joints): 53 %" and "Doors and windows: 15 %". This means that the remaining leakages are 32 % and should fit under the category "Penetrations". However, these studies were performed in 1982 on American houses and it is likely that the air tightness in penetrations has improved since then. The numbers can still be used as a comparison.

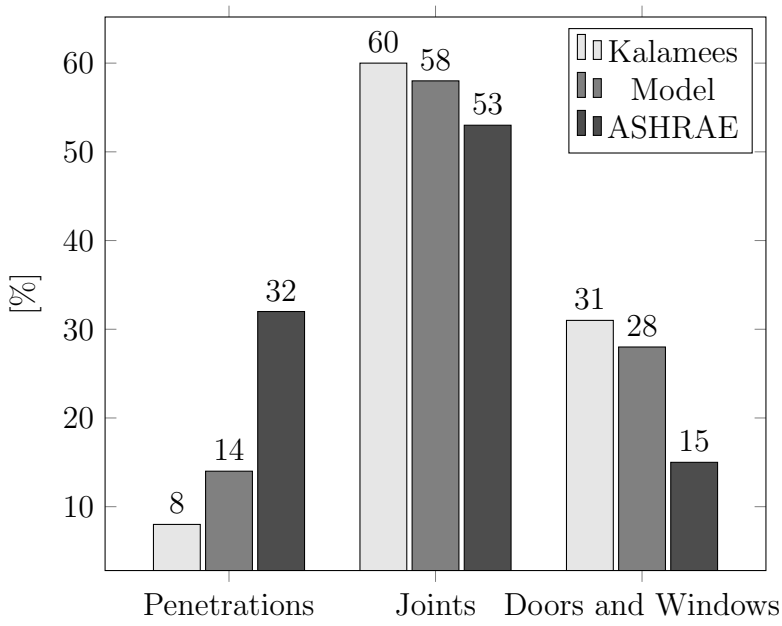

Figure 27: Comparison between leakage distribution in model and leakage distribution in the study performed by Kalamees et al. (2008)and American Society of Heating and Engineers (1997).

The comparison is only used to make sure that the model is not representing any extreme scenario. Since leakage distribution and leakage magnitude is highly dependent on workmanship and knowledge it is likely that even a quite different leakage distribution could be representative for the reference building. Also the fact that the leakages are varying over the year might have an substantial impact on the distribution of the leakages. It might for instance be true that the overall leakage is caused by a variation of leakage only in some of the leakages which if increased in size would indeed change the leakage distribution.

6 Parameter Study

This chapter describes the cases investigated in order to find possible effects of varying airtightness.

6.1 Problems associated with poor airtightness

In this section known consequences of having a poor airtightness is presented. These consequences works as a base for formulating cases where the effects of varying airtightness can be investigated.

Energy Airtightness affects the energy performance of a building in different ways. If the building has a heat exchanger connected to the ventilation system, a less airtight building means that less heat can be recovered. The airtightness may also affect the performance of the insulation. Air leakages through the thermal envelope may result in air movements inside the insulation which in turn reduces the thermal performance of the insulation. Another consequence occurs during windy circumstances. Higher wind speeds means higher pressure differences over the thermal envelope which in turn results in higher air exchange rate. Also high temperature difference over the thermal envelope causes higher pressure difference because of stack effect. The more leaky the building the higher the air exchange rate becomes.

Comfort Infiltration through air leakages causes draught which in turn reduces the operative temperature and causes discomfort. The reaction from the user is often to turn up the heating system which increases the energy demand of the building.

Radon Radon is a radioactive gas produced when radium decays. Radon continues to decay and emits radiation that causes health problems such as increased risk of lung cancer. Radon has its source in the ground and travels with air through air leakages in the ground construction into the building.

Noise and air quality A key aspect in reducing the contamination of the indoor air is to ventilate with cleaner outdoor air. But in some cases the outdoor air must be filtered before it is mixed with the indoor air in order to create satisfactory indoor air quality. A leaky building allows outdoor air to enter the building without passing the filter which in turn results in poor indoor air quality. Another consequence of air leaks is that they allow noise to enter the building from the outside.

Moisture Indoor air is often more moist than outdoor air. Air moving from the interior towards the cooler exterior of the thermal envelope might condensate inside the construction and cause moisture related problems such as mould growth or rot. Another similar problem may occur in houses with cold attics. If there is a leakage between the indoor space and the attic, for example around the attic hatch, air driven by stack effect may flow up into the attic. If the attic is cooler than the indoor air the relative humidity will increase and in worse case condensation may occur at the inside of the roof. If high relative humidities have a long duration mould may start to grow and in the long run affect the living spaces and cause health issues.

6.2 Cases

In this section, the combined effects from wind, stack effect and change in airtightness is investigated with focus on exfiltration and infiltration as well as radon concentration.

6.2.1 Exfiltration and Infiltration

Since infiltration and exfiltration are directly coupled to the airtightness of the building the change of magnitude of these airflows are investigated when the airtightness is changed. The apportionment between infiltration and exfiltration is dependent on two factors; distribution of leakages and distribution of pressure difference over the thermal envelope. This is tested for two main cases wind and stack effect. Here are the total exfiltration and infiltration as well as individual airflows calculated.

The pressure difference over the thermal envelope is dependent on three factors; wind, stack effect and ventilation. The combined effect of these factors together with the leakage distribution determines the location of the neutral plane which in turn determines the apportionment between infiltration and exfiltration. For the case with only stack effect an increase in leakages in the upper part of the building results in heightening the neutral pressure plane. On the other hand, if the building becomes more leaky the negative pressure difference caused by the ventilation system will decrease and cause a lowering of the neutral pressure plane. The combination of these effects is of interest since the result determines the height of the neutral pressure plane.

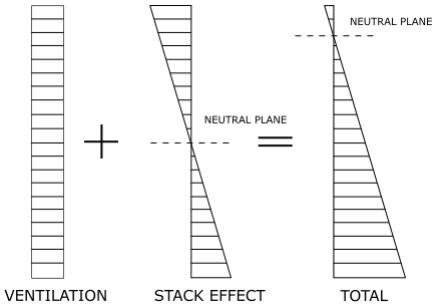

Figure 28: Pressure differences caused by stack effect and ventilation.

6.2.2 Radon from crawl space

It has been suggested that radon concentrations might in general be higher in buildings with crawl space compared to buildings with concrete ground slab or basements. This suggestion is supported by the results from a study by Majborn (1992) where radon concentration has been studied dependent on the sub-structure of the building. The study shows for instance higher geometric mean radon levels in crawl spaces compared to basements. For this reason the reference model, see Figure 26, is altered so that the foundation is a suspended foundation instead of concrete ground slab. However, the total air leakage through the thermal envelope remains unchanged as well as the location and the dimension of the leakages. The initial state of the radon concentration is set to a value inside the crawl space so that the resulting concentration in the living space becomes the maximum indoor value recommended by the Swedish Radiation Safety Authority which is 200 Bq/m^3. The total airtightness of the model is then reduced for different wind scenarios and temperature differences in order to investigate how the radon concentration in the indoor environment is affected.

6.3 Simulation results

Simulations are run for two different climate scenarios, February and July. As input for each scenario monthly mean temperature, wind speed and relative humidity are used. The months February and July are chosen since February has the lowest monthly mean humidity by volume in Gothenburg and July has the highest monthly mean humidity by volume in Gothenburg Petersson (2007). The highest humidity by volume outdoors typically corresponds to the highest relative humidity indoors. This since the interior is ventilated with exterior air with additional moisture coming from indoor activities. In the same way, the lowest humidity by volume outdoors corresponds to the lowest relative humidity indoors. Relative humidity affects shrinkage and swelling, see Section 2.6 and thus also the airtightness. This means that the building should have highest airtightness in February and lowest in July. However, temperatures are chosen

as the lowest daily mean values for each month. This since the lower temperatures represents a case with higher stack effect and possibly also higher leakage airflows. Each month is run with two different wind scenarios, wind direction perpendicular to the long side of the building and wind direction perpendicular to the short side of the building. It is assumed that the roof is completely airtight and that the wind only affects the pressure in the attic by the attic ventilation gap located at the base of the roof. This is the reason to why there are no pressure coefficients for the roof. Wind pressure at the roof base is complicated to estimate since the geometry is more complicated compared to the flat surfaces of the walls and roof. For this reason the wind pressure at the roof base, over the ventilation gap, is assumed to be the same as for a vertical wall at the same height.

Table 11: Monthly mean values for wind speed, relative humidity and temperature.

Month	**Wind Speed [m/s]**	**Relative Humidity [%]**	**Temperature [°C]**
February	5	82	-4
July	5	73	15.5

Since also the direction of the wind influences the pressure difference over the thermal envelope, two different wind directions are taken into account. Wind perpendicular to the long side of the building and wind perpendicular to the short side of the building. Important to notice is the location of the ventilation gap in the attic, see Figure 29 and 30. Since the attic ventilation gap is only located along the long sides of the building the pressure difference between the attic and the exterior is highly affected by the direction of the wind.

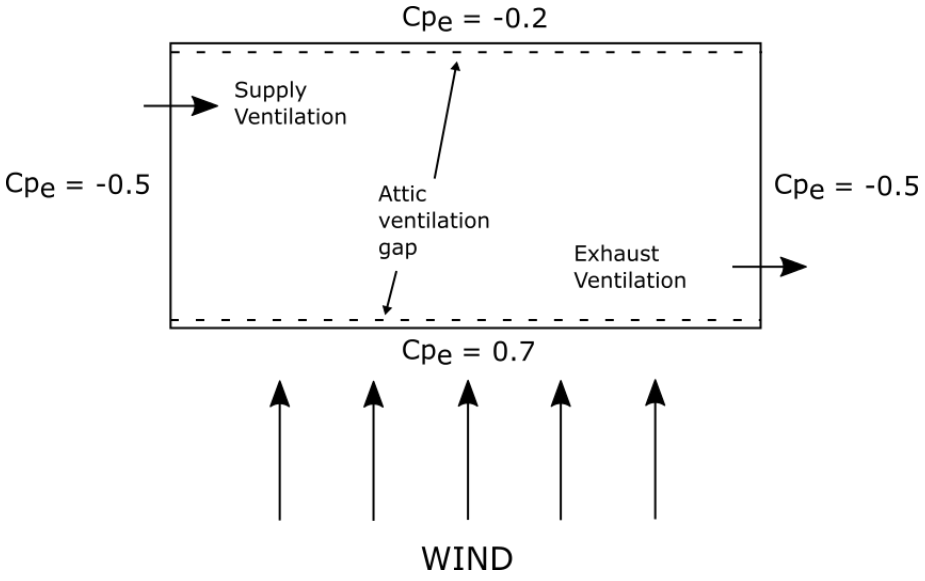

Figure 29: Principle drawing of the scenario with wind perpendicular to the long side of the building with its corresponding wind pressure coefficients.

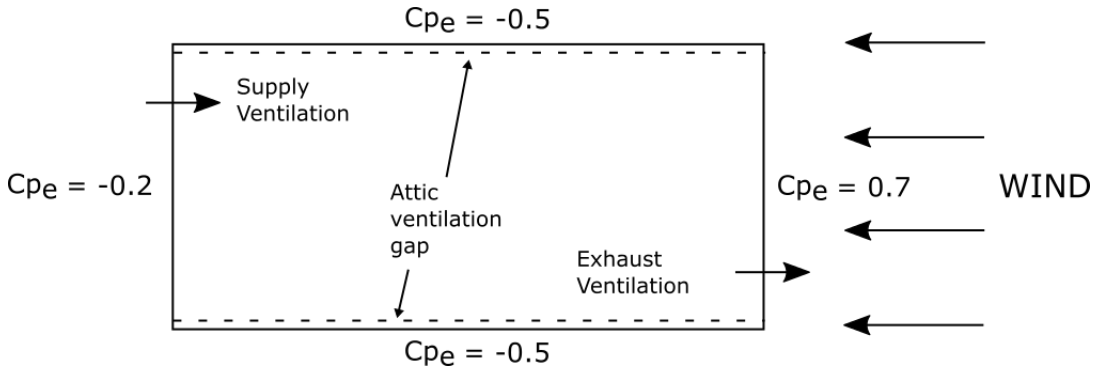

Figure 30: Principle drawing of the scenario with wind perpendicular to the short side of the building with its corresponding wind pressure coefficients.

The type of ventilation system affects the pressure difference over the thermal envelope. In this study two kinds of ventilation systems are used, one which gives a constant air flow no matter the surrounding pressures and one system which regulates the airflow dependent on the pressure drop in the duct system using a performance curve, see Section 2.2. In reality, a ventilation system that gives a constant airflow is a bit more complicated since it needs pressure sensors to adjust the fan speed so that the desired airflow is achieved. However, a system where fan speed is adjusted once and the air flow dependent on the pressure drop in the duct system is somewhat more simple. It is therefore assumed that the latter is more common and results presented are mainly from simulations using this particular set-up. Results from simulations using constant air flow can be found in Appendix A. The system with a performance curve has one exhaust fan and one supply fan driving the air in a simple air duct system. The duct system on the supply side has an inlet with a fan and a duct junction leading the inlet air through ducts to two different heights in the building, 2.7 m and 5.4 m respectively. On the exhaust side, air is exhausted from two levels in the building, 2.7 m and 5.4 m using two ducts connected to an exhaust fan.

In detached houses exterior air going through the supply ventilation is usually passing over a filter causing an additional pressure drop which must be handled by the ventilation fans. In order to take the effect from such a filter into account an additional pressure drop is added to the supply ventilation. The pressure drop can be expressed using the *Powerlaw Model*, Equation 7 where $n = 0.56$ and $C = 0.0043$, see Appendix D.

The performance curves for the exhaust fan and the supply fan are adjusted so that they give supply and exhaust air flows close to 44 l/s and 22 l/s respectively for a scenario without stack effect, (20 °C in all zones) and with an airtightness of $q_{50} = 0.6$ l/m^{2}s. The adjustment of the curves is similar to what is done in reality, when ventilation fans are installed the rotation speed is adjusted to give the desired airflow which in turn alters the performance curve. The imbalance between exhaust and supply air causes a

negative pressure difference between interior and exterior side of the thermal envelope. The purpose of this is to avoid air moving from the interior through leakages towards the exterior (*Exfiltration*) which can lead to decreasing the dew point of the air and in worst case cause condensation.

Figures below show the performance curves for exhaust and supply fans used in the simulations, original performance curves can be found in Appendix D.

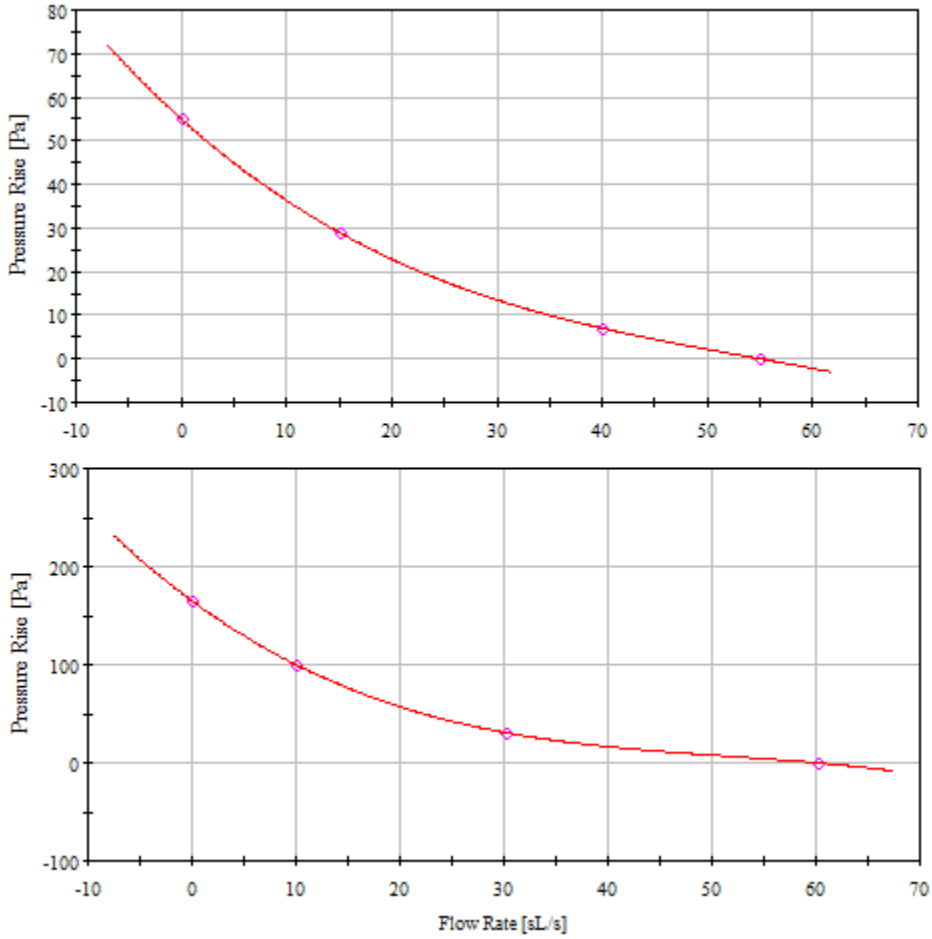

Figure 31: Performance curve for supply ventilation (upper curve) and performance curve for exhaust ventilation (lower curve).

6.3.1 Normal leakage distribution

In this scenario the supply and exhaust airflow follows the performance curves described above. Leakage distribution is the same as described in Chapter 5. Results are plotted with airflow of interest on the vertical axis and airtightness (q_{50}) on the horizontal axis.

The stack effect is higher in February than in July. Since wind speeds are the same for both months it is possible to compare how much this stack effect contributes to the exfiltration and infiltration. Wind direction affects the pressure in the attic. If the wind is perpendicular to the long side, wind causes a positive pressure over the ventilation gap in the attic on the front side and consequently a negative pressure over the ventilation gap on the back side. However, if wind is perpendicular to the short side of the building both ventilation gaps are exposed to a negative pressure. This is one of the reasons to why there is a difference in exfiltration between the two wind directions. This is particularly obvious when looking at how much air is going up to the attic, highest airflows is happening when wind is hitting the building at the short side. The fact that exfiltration is higher with wind on short side in July than both cases in February suggest that when looking at exfiltration the effect from the wind is stronger than the stack effect in July.

The flow direction from the attic is important to notice. If the building is situated in a place which has different wind directions during the year, air entering the attic from the interior may increase the relative humidity in the attic and allow for mould to start to grow. If the wind direction changes mould spores could follow the air back down into the living space and cause bad smell for inhabitants.

Interesting to notice is that even though there is an imbalance between exhaust and supply ventilation exfiltration is hard to avoid. It seems that as soon as either stack effect in February or wind in any direction is present exfiltration will to some extent occur. This is also true when the building is more airtight.

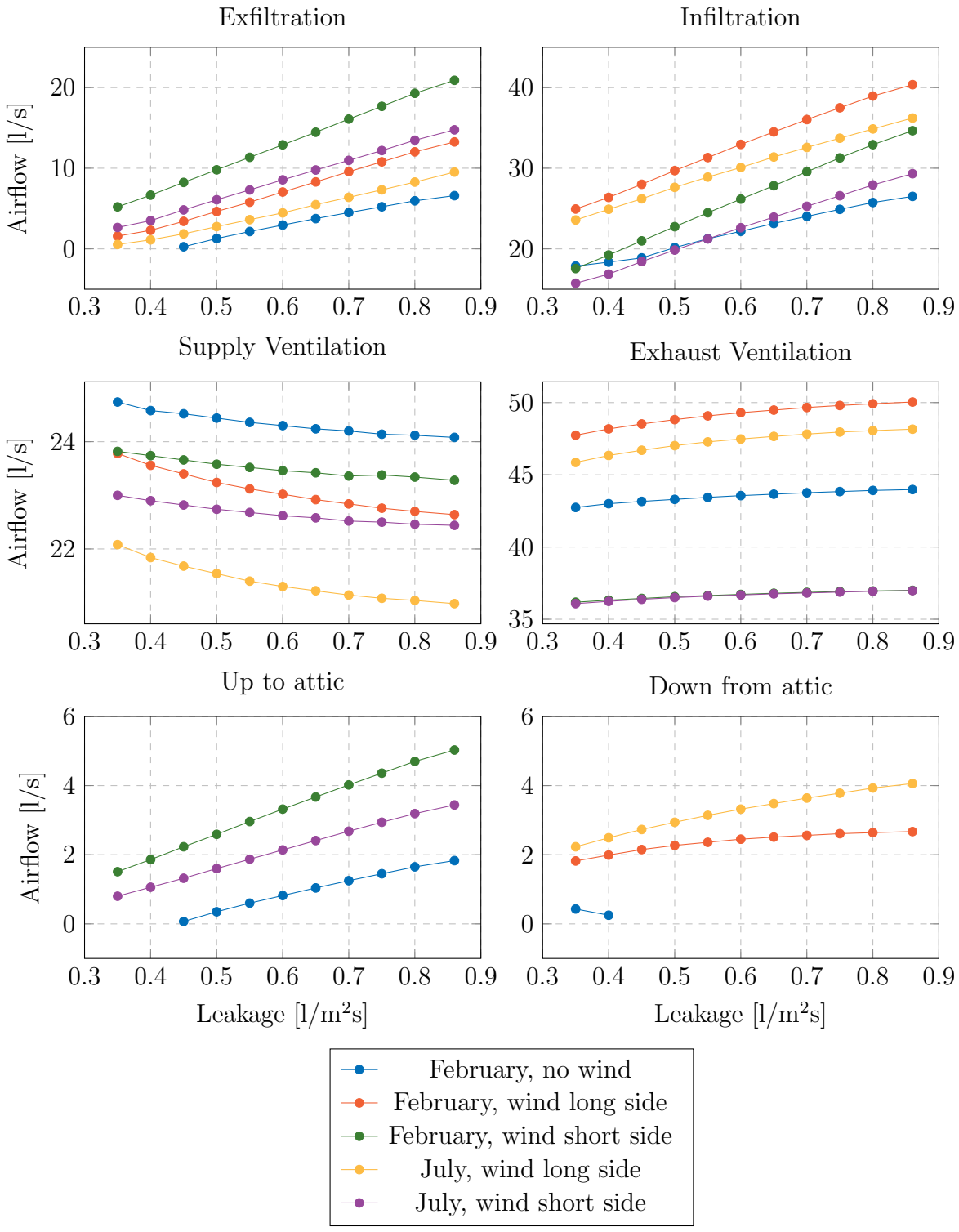

Figure 32: Results from simulation with leakage distribution according to reference model.

The figure below shows the distance from the bottom of the building to the neutral pressure plane for different airtightness. The scenario shown is for February without wind and with ventilation controlled by the performance curves.

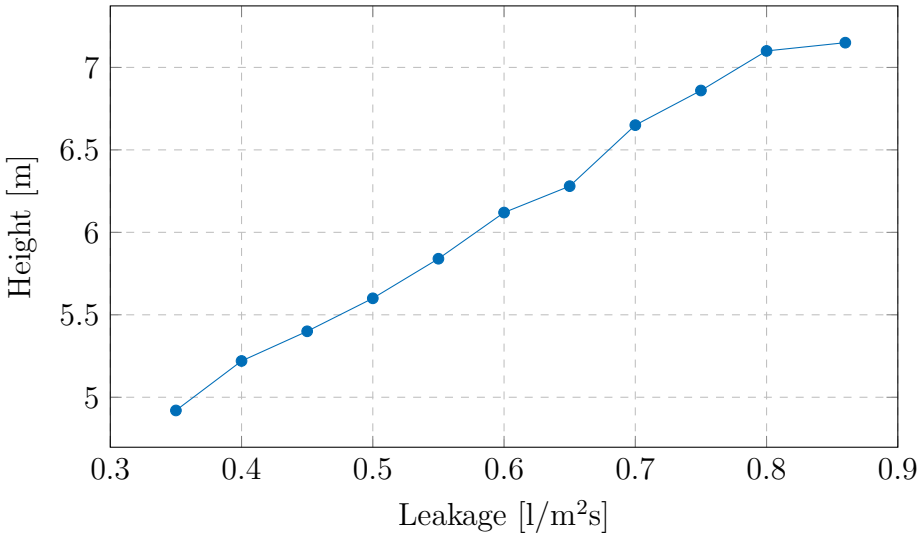

Figure 33: Diagram showing the height of the neutral pressure plane for a leakage distribution according to the reference model with no wind and temperature as in February.

The height of the neutral pressure plane decreases with increased airtightness, the reason for this is that the more airtight the building is the higher is the negative pressure caused by the imbalance between exhaust fan and supply fan. The trend is linear although there is some irregularities because of the way the leakages are simulated. Each leakage is simulated so that all air in one leakage type flows at the same height. This means that if the neutral pressure plane is right above the leakage, air will flow in one direction and if the neutral pressure plane is right below the leakage, air will flow in the opposite direction. Also numerical inaccuracies might cause some of the irregularities.

6.3.2 Leakages mainly on first floor

Since the distribution of the leakages in the first case is quite even it is interesting to see what happens if the leakage distribution changes. The worst case, if looking at exfiltration of air up to the attic, is when leakages are distributed mainly in the lower parts of the building. This since it would decrease the height of the neutral plane and hence increase the pressure difference over the attic hatch. All leakages on the second floor, except leakages caused by the attic hatch and chimney penetration, are therefore removed and consequently the leakages on the first floor are increased in size. Simulations are then run for the two wind scenarios for both February and July.

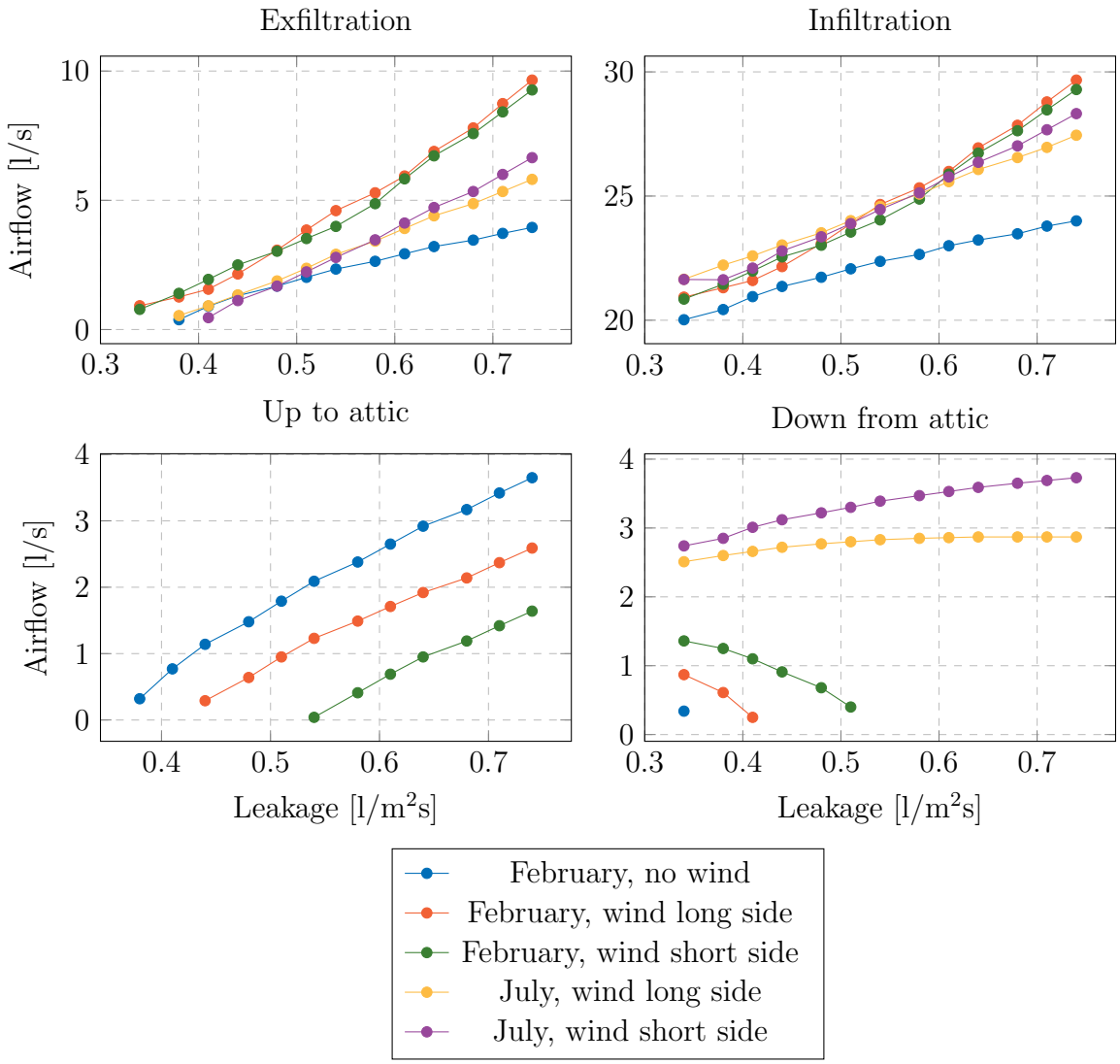

Figure 34: Results from simulations with leakages mainly on the first floor.

6.3.3 Radon source and crawl space

Radon commonly found in residential buildings is of the isotope Radon-222. According to WHO (*World Health Organization*) radon is, after smoking, the most important cause of lung cancer. WHO claims that the risk increases by 16 % with an increase of 100 Bq/m^3 and that the relation is linear, meaning that if the radon concentration is doubled than the risk is also doubled.

For this reason the radon levels indoors are simulated for changes in airtightness. Since the problem is greater for buildings with a crawl space, a crawl space is added to the

reference building and the radon source is simulated inside the crawl space. According to Sherman and Dickerhoff (1998), crawl spaces are less airtight than buildings without crawlspaces and in a study on US detached houses by Chan et al. (2013) it was shown that vented crawl spaces had a *Normalize Leakage Area* 24 % higher than houses with slab. For this reason an additional leakage area per m^2 floor area is added to the bottom floor in the reference building. This gives a new airtightness of 0.69 l/m^2s compared to the value of 0.60 l/m^2s for the reference building without a crawl space. This means a decrease in airtightness of 15 %, which is considered to be in the same order of magnitude as the decrease in airtightness suggested by Chan et al. (2013). The leakage value used for the floor is 0.4 cm^2/m^2 from Persily and Ivy (2001).

The radon levels are not only dependent on the radon generation rate in the crawl space but also the *Decay Rate*, λ which can be calculated according to Equation 17 in Theory chapter if the half-life is known. The half life of Radon-222 is 3.8235 days according to Picolo (1996) which yields the decay rate, λ=5.04 s^{-1} according to Equation 17.

Simple model for estimating radon source

In order to estimate how radon levels in the indoor environment changes with airtightness it is necessary to establish a model for predicting the radon generation rate in the crawl space. Since the ground itself is the source of radon generation, the radon at ground level is dependent on the airflow coming up from the ground carrying radon. The airflow itself is dependent on the pressure difference between the surface and the pressure deep down in the ground. The mechanisms involved in creating this pressure difference is the stack effect inside the building which causes a negative pressure in the crawl space and air buoyancy effects in the ground caused by temperature differences between warmer and colder areas. The latter comes as a result of the thermal pillow that is formed underneath the crawl space when the building is heated.

The buoyancy difference between the air in the ground inside the thermal pillow and the air in the ground further away from the building causes a pressure difference which drives air upwards into the crawl space, bringing radon gas. It is assumed that the temperature difference causing this affect is constant over the year, resulting in constant radon source. However, the amount of radon entering the building is also dependent on the pressure in the crawlspace, the greater the negative pressure is the more radon enters the crawl space. These two effects are simulated separately using a constant radon source in combination with a pressure driven source, see Figure 35. Since the airflow is directly proportional to the radon coming up from the ground and since all constants in Equation 8 are assumed to be constant; the radon generation in the crawl space is directly proportional to the pressure difference in the crawl space. The following expression in CONTAM can then be used to simulate radon generation rate

in the crawl space as a function of the pressure difference:

$$S = G \cdot \Delta P^n \tag{27}$$

where

S is the contaminant source strength [kg/s]
G is the generation rate coefficient [kg/Pa^{n}s]
ΔP is the pressure difference (atmospheric pressure - zone pressure) [Pa]
n is the pressure exponent [-]

Since the relation between radon generation and pressure difference is assumed to be linear the coefficient n is set to 1.

The total radon generation in the crawl space can then be expressed as a combination of the two effects with the following expression:

$$S = G \cdot \Delta P_{buoyancy} + G \cdot \Delta P_{ground} \tag{28}$$

where $\Delta P_{buoyancy}$ is the pressure difference caused by the buoyancy effect in the ground and ΔP_{ground} the pressure difference in the crawlspace.

However, it is a simplification which assumes that the temperature difference between the interior of the thermal pillow and the surrounding ground is constant over the year. The last term in Equation 28 can then be expressed as a constant radon source.

In a simple simulation performed in *COMSOL*, the height of the thermal pillow was approximated to 8 m and temperature difference between approximated to 6 °C. Using Equation 10, the pressure difference, $\Delta P_{buoyancy}$, is found to be 2 Pa.

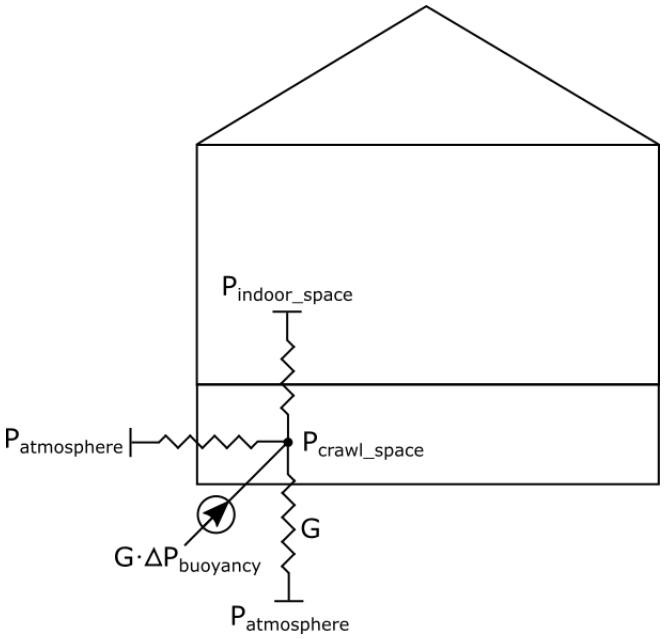

Figure 35: Principle drawing of the model for estimating radon generation rate in the crawl space.

However, since it is of interest to see the changes in radon levels indoors dependent on changes in airtightness, the generation rate G in Equation 27 is adjusted so that the maximum radon level of 200 Bq/m^3 allowed by *Swedish Radiation Safety Authority* is reached indoors. This is done for the climate scenario February, for the wind direction that gives the highest radon levels, in this case wind on the short side of the building. This set-up fits well with the recommendations for measurements recommended by *Swedish Radiation Safety Authority* saying that radon measurements should be performed continuously for a longer period, at least one month, between 1 of October and 30 of April since this is the period which usually gives the highest radon levels indoors. Something which is also confirmed in the simulation results below.

In order to verify the assumptions made in the model, results are compared with measurements and simulations performed in other studies. Since it is the radon generation rate that is modelled, comparisons are made in terms of how great the difference is between winter and summer.

Levels of radon in the indoor space is dependent on the pressure difference between the crawl space and the indoor space. When the air tightness increases, the negative pressure caused by the exhaust ventilation increases, see Figure 37, and thus also the pressure difference between crawl space and the indoor space. This results in higher concentrations of radon in the crawl space and thus also in the indoor space. However, the main reason to why radon levels are higher indoors when the building is more airtight is that the less airtight building has a higher air exchange rate which reduces

the radon concentrations.

Leakages that are altered in order to change the airtightness of the building are joints between construction parts and the leakage in the attic hatch. However, leakages caused by duct penetrations and electrical outlets are not altered, nor the additional leakage per floor area added between indoor space and crawl space. This means that when the pressure difference between indoor space and crawl space increases because the building is getting more airtight, the air gaps between indoor space and crawl space are not increasing leading to an additional increase in airflow when the airtightness is increased. This is the reason to why the radon levels indoors increases faster when airtightness is decreased in the more airtight building compared to the less airtight building.

For the results below, simulations have been run with a radon generation rate coefficient G in the crawl space of 8.3 [kg/Pas]. Which corresponds to radon concentrations of 200 Bq/m^3 in February with wind perpendicular to the short side.

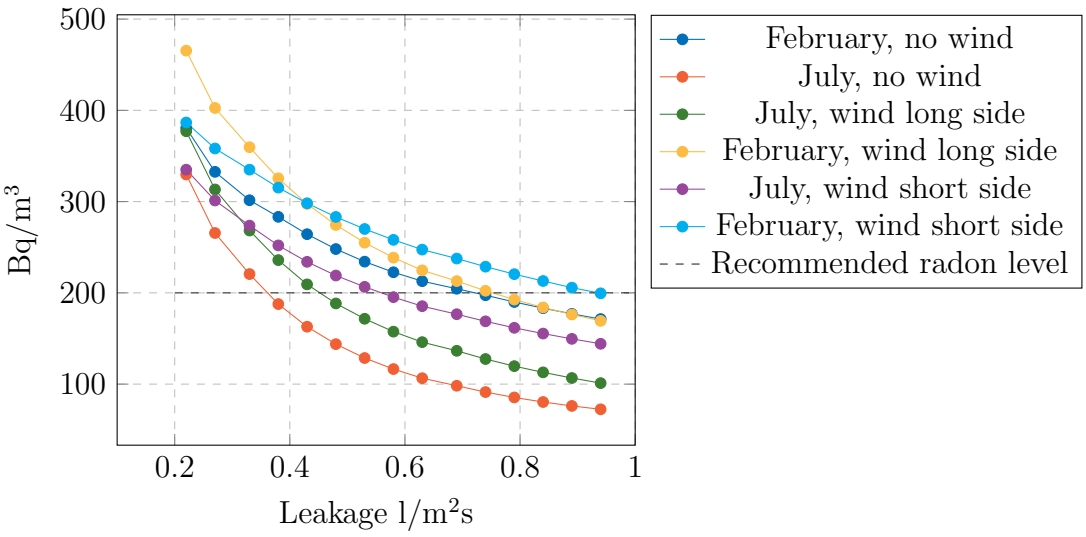

Figure 36: Radon levels in indoor environment for different climate scenarios.

Interesting to notice is that for the more airtight building winds perpendicular to the long side results in higher radon levels while in the less airtight building winds perpendicular to the short side results in higher radon levels. By a closer look at the airflows from the ventilation fans it becomes evident that the negative pressure caused by the imbalance between supply- and exhaust fans are affected by the direction of the wind. In the less airtight building the negative pressure inside is to a greater extent created by the winds themselves. However, when the building gets more airtight a larger part of the negative pressure is caused by the imbalance in the ventilation system. If looking at Figure 29 and 30 one can see that the airflow from the exhaust fan is helped

by winds perpendicular to the long side while it is antagonised by winds perpendicular to the short side. This shows that it is important to be aware of prevailing wind directions and its effects on the pressure differences between foundation and indoor space, especially if the building is located in an environment where wind directions vary greatly throughout the year. It is interesting to relate the results to other pollutants that can be found in crawl spaces. For instance, mould or bad smell coming from the soil. Results show that the wind direction has a significant effect on the magnitude of the airflow coming up from the crawl space carrying these unwanted pollutants.

6.3.4 Pressure difference

In this section the pressure difference over the thermal envelope is simulated for different levels of airtightness. The purpose is to illustrate how the pressure difference over the thermal envelope is affected by choice of ventilation. At an airtightness of 0.6 l/m^{2}s the supply ventilation is adjusted to 22 l/s and the exhaust ventilation is adjusted to 44 l/s causing an negative indoor pressure. Two cases are run, one where ventilation fans are regulated according to the performance curves and one where the air flows are constant.

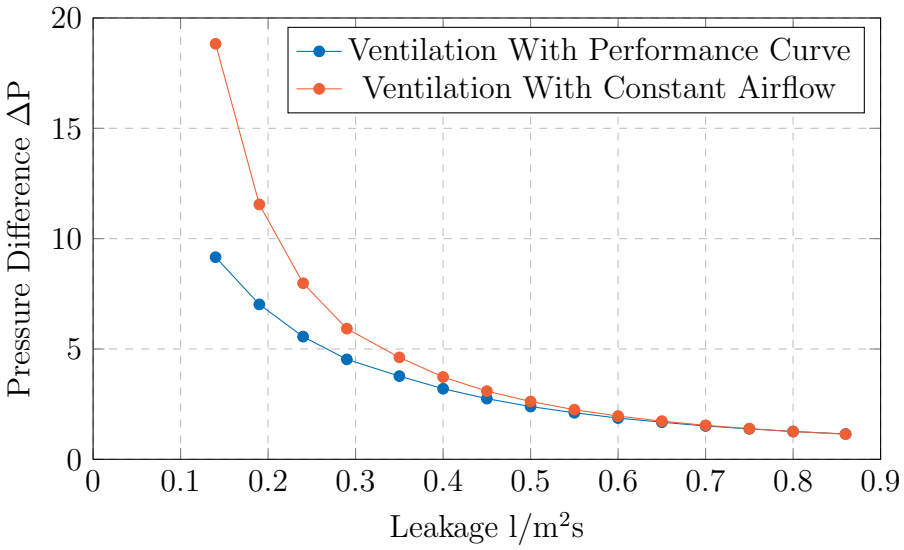

Figure 37: Pressure difference over the thermal envelope when there is no wind and no stack effect.

An increased airtightness means that a larger pressure difference is needed to pull the same airflow through the thermal envelope compared with a less airtight building. The fans with a fixed airflow are unaffected by this effect and thus are able to create a higher pressure difference. On the other hand, the fans following a performance curve have a decreased airflow for an increased airtightness.

In above mentioned scenarios, varying airtightness has only been tested for cases where all leakages that are likely to change are changed in an equal proportion. In future work, it would be useful to investigate, perhaps in full-scale laboratory tests, how individual leakages are affected by changes in humidity.

7 Consequences of air leakages

In this chapter, results from previously performed simulations are put into a context regarding problems often associated with airtightness. Calculations should be regarded as approximative estimations where the purpose is to give an idea of the magnitudes of the problem and to work as a ground for discussion.

7.1 Mold growth in cold attic

According to Hagentoft and Sasic Kalagasidis (2014) problems with mould growth in cold attics have been increasing during the last years. For this reason the possible addition to mould growth as a consequence of varying airtightness is estimated.

The actual mould growth is estimated as a function of temperature and relative humidity in the attic using *Mould Growth Index Model* suggested by Hukka and Viitanen (1999). Airflow to and from the attic is calculated for different airtightness and the values are then used to find the relative humidity and temperature in the attic for a fixed indoor temperature and a fixed moisture supply from the indoor zone. Calculations for finding temperatures and humidities, from the airflows provided by CONTAM-simulations, see Section 6.3, are performed using the graphical programming environment *Simulink*, (Toolbox, 2010).

Airflows to and from the attic are simulated in CONTAM for one-year period where changes in airflows are dependent on variations in outdoor climate. This means that the effects from variations in wind angle and wind speed are not taken into account. For each scenario there is one calculation without any change in airtightness and one simulation where the airtightness is increased during January to Mars. The resulting temperatures and relative humidities from one year are then run repeatedly in the mould growth model until the mould growth cycles between two following years are similar.

The attic is ventilated through two horizontal gaps at the roof base along the long side of the building, see see Figure 29. However, since the effect from wind is not taken into account in the calculations, the air exchange rate of the attic is less than it would be if winds where included. This results in quite hight relative humidities in the attic, especially for less airtight buildings. However, more airtight buildings show lower relative humidities in the attic and since their air exchange rate is less dependent on winds results presented are only from buildings that are relatively airtight.

Table 12: Description of mould index.

Mould Index	Explanation
0	No gowth
1 - 2	Visible by microscope
3 - 5	Visible by eye
6	Very much

Figure 38 shows the mould growth for two scenarios without wind and with different airtightness. One scenario is simulated with a constant airtightness of 0.050 l/sm^2 and one scenario is simulated with a step-change in airtightness during the period January to Mars to 0.061 l/sm^2 while the airtightness for the remaining months of the year stays at 0.050 l/sm^2, a change in airtightness of 25 %. The difference in mould index is greatest two to four years after the simulation is initiated, at this point the mould prevalence goes from *visible by microscope* to *visible by eye*. However, it is important to point out that the index-values should be interpreted as relative and not be taken as absolute.

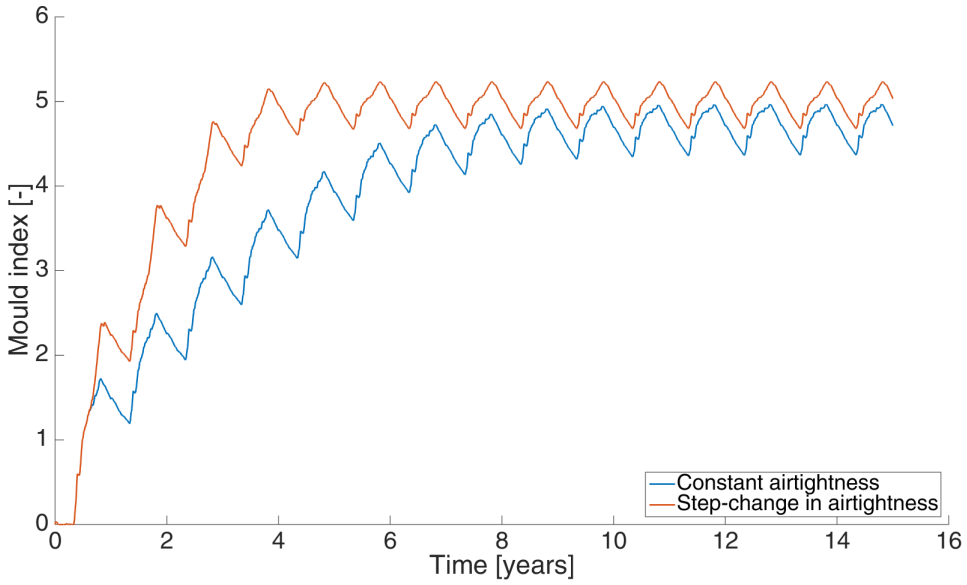

Figure 38: Mould growth with and without a step-change in airtightness.

Figure 39 shows the mould growth for two scenarios without wind and with different airtightness. One scenario is simulated with a constant airtightness of 0.045 l/sm^2 and one scenario is simulated with a step-change in airtightness during the period January to Mars to 0.051 l/sm^2 while the airtightness for the remaining months of the year stays at 0.045 l/sm^2, a change in airtightness of 6.7 %. The small difference in mould

growth is likely due to the fact that the change in airtightness is quite small as well as the fact that there is no wind ventilating the attic.

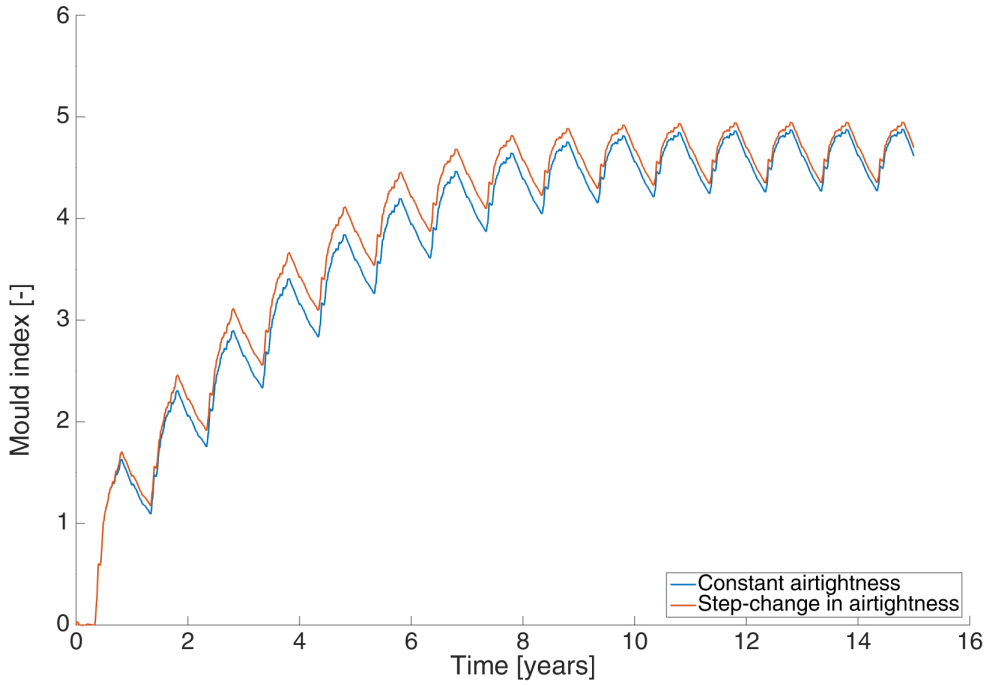

Figure 39: Mould growth with and without a step-change in airtightness.

Figure 40 shows the mould growth for two scenarios without wind and with different airtightness. One scenario is simulated with a constant airtightness of 0.064 l/sm^2 and one scenario is simulated with a step-change in airtightness during the period January to Mars to 0.073 l/sm^2 while the airtightness for the remaining months of the year stays at 0.064 l/sm^2, a change in airtightness of 14 %. Results show no significant difference in mould growth index between the two scenarios. Since the building is rather leaky, relative humidities in the attic are high throughout the year and thus mould growth quickly reaches its final level.

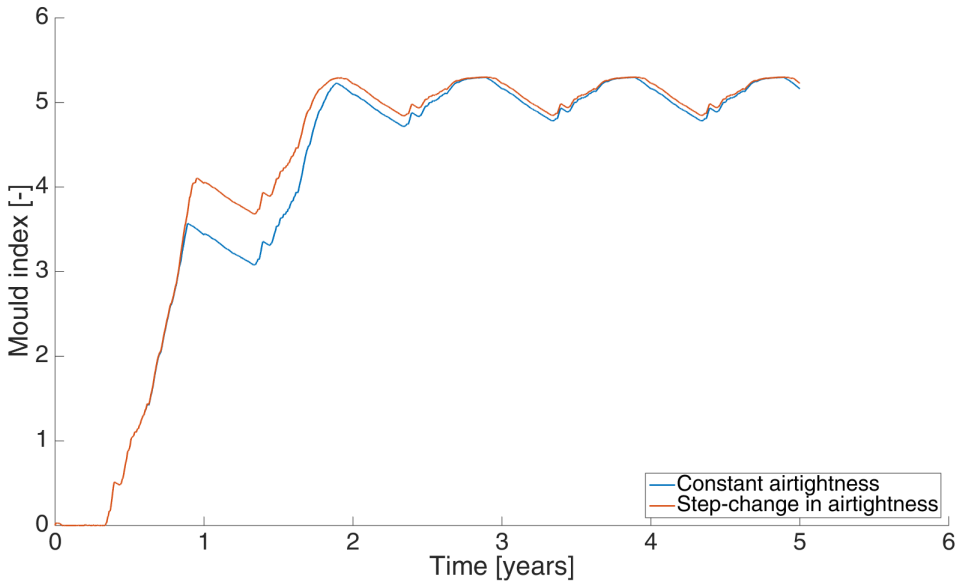

Figure 40: Mould growth with and without a step-change in airtightness.

More leaky buildings have a higher moisture transport rate up to the attic and the relative humidity is above 100 %, meaning condensation, for quite large periods of time during the year. The reason to this is, as mentioned before, that winds are not taken into account in the simulations. Increased ventilation would likely reduce the moisture in the attic at times during the year, which in turn would give an opportunity for the moisture content in the timber to dry out and be able to buffer moisture again when circumstances changes. Such a reduction in moisture would also slow down the growth process of mould. The fact that the direction of the wind greatly affects ventilation of the attic and the flow direction between living space and attic space can bee seen in Figure 32. However, the graphs show that for the more airtight building, Figure 38, both the rate of mould growth as well as the final *Mould Growth Index* is affected by a change in airtightness. Then again, the change in airtightness is quite large, 25 %, and more effects needs to be taken into account in order to evaluate this more accurately.

7.2 Energy use and power demand

In this example the energy demand and heating power is estimated. Energy use is calculated for different wind scenarios for a period of 24 hours with an outdoor temperature of -4 °C, lowest daily mean value in February. Heating power demand is calculated utilizing an estimated Dimensioning Winter Outdoor Temperature, $DVUT_{20}$, for a lightweight building in Gothenburg. Calculations are made according to the

recommendations outlined by Boverket, Swedish National Board of Housing, Building and Planning, (Boverket, 2011). Calculations are made for a building with a heat exchanger.

Table 13: Input data to energy and power calculations.

	Value	**Unit**
U-value (mean)	0.3	W/m^2K
Envelope area	300	m^2
ρc_{air}	1200	MJ/m^3K
T_{in}	21	$°C$
T_{out}	-4	$°C$
Heat Exchange Efficiency	0.6	-
$DVUT_{20}$	-14.6	$°C$

Figure 41 shows the energy use for a 24 hour period with an outdoor temperature of -4 °C and for the different wind scenarios; no wind, wind perpendicular to long side of the building and wind perpendicular to the short side of the building, for a principle drawing see Figure 29 and Figure 30.

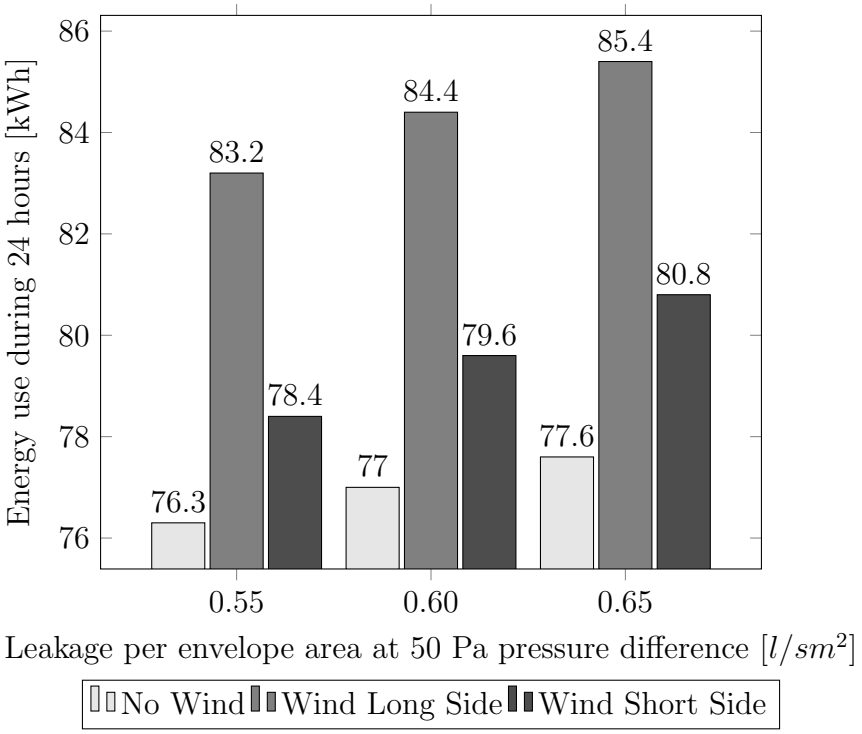

Figure 41: Energy use during 24 hours for three different wind scenarios and three different values of airtightness. The outdoor temperature is -4 °C for all cases.

Figure 42 shows the heating power demand for a scenario without wind and with an outdoor Dimensioning Winter Outdoor Temperature, $DVUT_{20}$, of -14.6 °C.

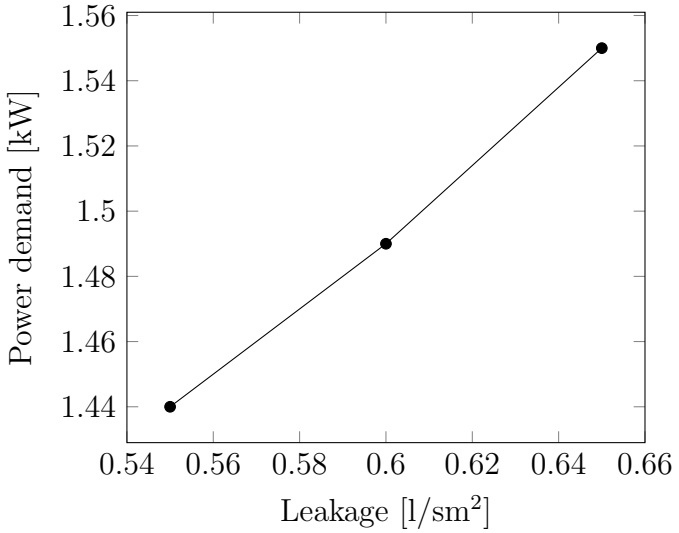

Figure 42: Heating power demand for a scenario without wind and with an outdoor temperature of -14.6 °C.

Table 14: Airflows and energy use for different airtightness and for the scenario without wind and with an outdoor temperature of -4 °C.

Airtightness [l/sm²]	**Infiltration [l/s]**	**Exfiltration [l/s]**	**Exhaust [l/s]**	**Supply [l/s]**	**E24 [kWh]**
0.65	23.15	3.75	43.66	24.24	77.6
0.60	22.18	2.95	43.56	24.30	77.0
0.55	21.25	2.15	43.44	24.36	76.3

Both energy demand and heating power demand is proportional to the total air exchange of the building. Interestingly, when a heat exchanger is used, energy demand and heating power demand also becomes dependent on the amount of air passing the heat exchanger and the amount of air that leaks out from the building. A more leaky building needs a higher difference between supply air and exhaust air and as a result a more leaky building loses more energy through leakages and also, less heat is passed to the incoming air by the heat exchanger. However, for the results presented above, a change in airtightness of ∼1 % means an increase in energy demand of ∼0.1 %.

7.3 Comfort

According to Boverket (2011), airspeeds during winter months should not, for reasons of comfort, exceed 0.15 m/s in the area of occupancy which is defined as the height between 0.1 m and 2.0 m from the floor and at a distance of minimum 0.6 m from the walls. For this reason the air speed from the leakage with the highest airflow into the area of occupancy is estimated.

The graph below shows the resulting airspeeds at a distance of 0.6 m from one of the windows on the wall on the long side of the building. The wind scenario is wind perpendicular to the long side of the building, see Figure 29.

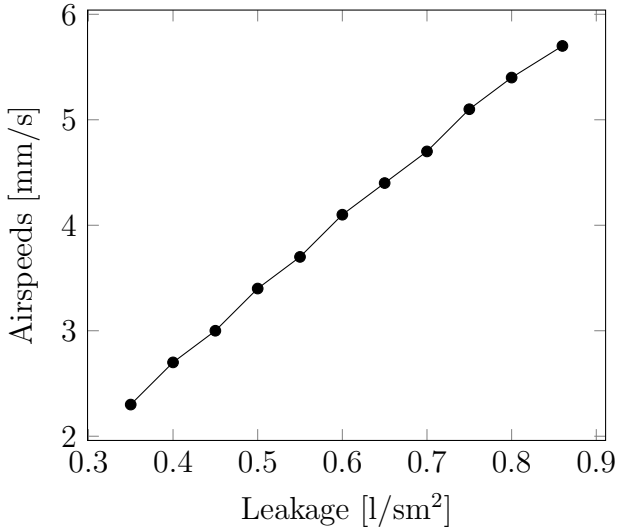

Figure 43: Heating power demand for a scenario without wind.

Airspeeds are well below the highest value stated by Boverket. However, the airspeeds are based on the airflows in the gap which is assumed to be homogeneous throughout the entire gap. In reality this is not the case, the airflow along one leakage varies dependent on variations in gap width, this means that in some areas the airspeed will be greater than in others. Thus, above results should instead be interpreted as the mean airspeed from the air gap in the window. It is also important to note that the variation in airtightness in this scenario is caused by a variation in most of the leakages in the building. However, it is possible that a variation in airtightness is caused by only a few leakages in the building, if the window connection is one of those leakages the airspeed would increase faster with a change in airtightness than it does in the example above.

8 Conclusions

The relation between variation in airtightness and variation in relative humidity indoors has been investigated by full-scale laboratory testing of a guesthouse as well as with simulations of airflows with the software COMSOL. A model has also been built in the software CONTAM which allows for calculations of exfiltration and infiltration as a function of airtightness. Results from the model have been analysed with regards to complications that are typical for air leakages.

The influence of indoor relative humidity on the airtightness was investigated in experiments on a guest house as well as with COMSOL simulations. Results show a strong correlation between increased relative humidity indoors and increased airtightness, as well as a strong correlation between decreased relative humidity and decreased airtightness. In the measurements, relative humidity dropped from 90 % to about 25 % causing the airtightness to change from 0.74 l/sm^2 to 1.21 l/sm^2 at 50 Pa pressure difference. A relative humidity of 80 % corresponds to a moisture content of 16 % which is often found in construction timber. In addition, an indoor relative humidity of 25 % can often be the case during winter months. If, for instance, such levels of moisture is built into the construction, measured airtightness at the completion of a building might not be valid at a later stage when inbuilt moisture has dried out. It is therefore recommended that the timber is dried to a moisture content that is closer to what can be expected when the building is in use and that the building is properly protected against precipitation during the construction phase. If this is not possible, measurements of airtightness in the early stage of the construction might not be valid if the construction damp has not dried out properly.

A number of leakages were numerically analysed to investigate how the airflow through the leakages changes if the timber parts causing the leakages are subjected to swelling or shrinkage. Results show that the variations in leakage is dependent on the geometry of the leakage as well as the thickness of the timber parts involved. The way the shrinkage and swelling affects the airflow is in reality quite complex and the simulations performed does not take phenomenons such as twisting and warping of the timber into account. This results in simulations giving higher changes in airflows than what can be seen in empirical studies on the entire thermal envelope. For example, the airflow in the floor-wall simulation shows a change in airflow from 2.4 l/sm to 6.7 l/sm when the relative humidity changes from 55 % to 23 %, almost 3 times as much. However, the values should be interpreted as extreme but not unlikely to occur in small areas of a leakage. Results show also that there is a large difference between individual leakages in terms of how much the airflow changes when there is a change in moisture content. The differences between individual leakages and results from simulations indicate that even though the total airtightness variation is not more than 10 %, individual leakages may vary much more which in turn may lead to local problems such as moisture related issues or comfort issues.

It is common practise to adjust the balanced ventilation system in the building so that the exhaust airflow is greater than the supply airflow and in this way create a negative pressure to avoid exfiltration. However, since the pressure difference over the thermal envelope is varying dependent on wind and temperature, it is difficult to maintain a negative pressure for all possible occasions. Results from a number of simulations show that, for the worst case with leakage mainly in the lower parts of the building, exfiltration may increase with up to 1.9 % per percentage point of decrease in airtightness. However, for a leakage distribution with leakages more evenly spread, the exfiltration increases with 1.6 % per percentage point of decrease in airtightness.

Results show that, for climate scenarios that cause a negative pressure in the attic, the airflow up to the cold attic increases as the building is getting less airtight. The reason is that when gap widths increase more air is allowed to pass through the gaps. It is likely that an increase in airflow to the attic leads to an increase in relative humidity in the attic and in the long run an increase in mould growth. It is also shown that the airflow to the attic is likely to be reversed when there is a change in wind direction, which, if there is mould growth in the attic, would carry mould spores down to the living space. Simulations of mould growth show a tendency towards increased mould growth if the building is getting more leaky during January to Mars. However, calculations on mould growth were quite simplified and need to be done more thoroughly before any definitive conclusions can be drawn.

Simulations on radon levels in the indoor environment show an increase in radon levels due to less ventilation when the building is getting more airtight. Results show also that the increase in radon levels per change in airtightness is greater for a more airtight building compared to a less airtight building. Wind and stack effects have also a great affect on the radon levels in the indoor environment, this means that radon measurements need to be made during a longer period in order to ensure the validity of the results.

The energy use of the building is affected by variation in airtightness proportionally to the variation in total air exchange of the building. However, results show also the importance of having an airtight thermal envelope when a heat exchanger is used. A less airtight building needs a higher imbalance between exhaust- and supply airflow in order to have a negative indoor pressure. During winter, when the building is less airtight, negative pressure decreases as air leakage increases and less amount of air passes through the heat exchanger. Therefore, in a more airtight building, more energy can be exchanged from the exhaust air to the supply air.

9 Recommendations for future research

The overall ambition of the work in this thesis has been to increase the understanding of the causes of varying airtightness and to identify possible consequences. However, conclusions are rather general and in order to fully understand the effects and causes of varying airtightness additional research is needed:

- Laboratory tests on individual construction details to investigate how the leakages in the detail changes with changes in moisture content. Such tests could be used to better understand what happens in a leakage, which leakages have larger variations and how a wooden construction detail can be designed to minimise moisture induced movements.
- More investigations on the secondary effects of varying airtightness would increase the understanding of the severity of the problems that comes with varying airtightness. This could for example include energy calculations, estimations on discomfort, changes in contaminations levels and simulations of mould growth in different construction-parts such as cold attics.
- More full-scale measurements on the relation between humidity and airtightness in detached houses that are being used. Such an investigation could be used to determine if there is a difference between airtightness variation in, for example, different construction methods or construction types. If a difference in airtightness variation is found this could be investigated with regards to airtightness related complications. For example, does buildings with larger variations in airtightness have more problems with mould growth or comfort?
- Variations in airtightness make a good reason to question the validity of airtightness measurements. An increased knowledge of how the variations works is necessary in order to increase the accuracy of airtightness measurements. For example, find the best time of the year to perform measurements or measure multiple times throughout the year. Another approach could be to find a correction factor for adjusting airtightness results dependent on season.

References

Refrigerating American Society of Heating and Air-Conditioning Engineers. *ASHRAE handbook: Fundamentals.1997*. American Society of Heating, Refrigerating and Air-Conditioning Engineers, Atlanta, Ga, si edition, 1997.

PH Baker, S Sharples, and IC Ward. Air flow through cracks. *Building and Environment*, 22(4):293–304, 1987.

BBR Boverket. Regelsamling för byggande, 2011.

Per Gunnar Burström. *Byggnadsmaterial: uppbyggnad, tillverkning och egenskaper (2:a uppl.)*. Studentlitteratur, 2007.

Wanyu R Chan, Jeffrey Joh, and Max H Sherman. Analysis of air leakage measurements of us houses. *Energy and Buildings*, 66:616–625, 2013.

AB Comsol. Comsol documentation. *Comsol Multiphysics Users Guide*, 2005.

Peter Domone and John Illston. *Construction materials: their nature and behaviour*. CRC Press, 2010.

Steven John Emmerich, Andrew K Persily, US Consumer Product Safety Commission, et al. *Multizone modeling of three residential indoor air quality control options*. National Institute of Standards and Technology, Building and Fire Research Laboratory, 1996.

Carl-Eric Hagentoft. *Introduction to building physics*. External organization, 2001.

Carl-Eric Hagentoft and Angela Sasic Kalagasidis. Moisture safe cold attics-assessment based on risk analyses of performance and cost. In *Proceedings of 10th Nordic Symposium on Building Physics*, pages 1366–1373, 2014.

Lars-Erik Harderup and Jesper Arfvidsson. Moisture safety in cold attics with thick thermal insulation. *Journal of Architectural Engineering*, 19(4):265–278, 2013.

H.S.L. Hens. *Building Physics - Heat, Air and Moisture: Fundamentals and Engineering Methods with Examples and Exercises*. Wilhelm Ernst & Sohn Verlag fur Architektur und technische Wissenschaften. Wiley, 2012. ISBN 9783433030271.

LP Hopkins and B Hansford. Air flow through cracks. *Building Services Engineer*, 42: 123–131, 1974.

Antti Hukka and HA Viitanen. A mathematical model of mould growth on wooden material. *Wood Science and Technology*, 33(6):475–485, 1999.

Targo Kalamees, Minna Korpi, Lari Eskola, Jarek Kurnitski, and J Vinha. The distribution of the air leakage places and thermal bridges in finnish detached houses and apartment buildings. In *Proceedings of the 8th Symposium on Building Physics in the Nordic Countries (NSB2008), Copenhagen, Denmark*, pages 16–18, 2008.

Martin Krus, K Kie, et al. Determination of the moisture storage characteristics of porous capillary active materials. *Materials and Structures*, 31(8):522–529, 1998.

B Majborn. Seasonal variations of radon concentrations in single-family houses with different sub-structures. *Radiation Protection Dosimetry*, 45(1-4):443–447, 1992.

Lars Olsson. *Moisture Conditions in Exterior Wooden Walls and Timber During Production and Use*. Lic - Department of Civil and Environmental Engineering, Chalmers University of Technology, no:. Institutionen fr bygg- och miljteknik, Chalmers tekniska hgskola,, 2014. 101.

Persily. Repeatability and accuracy of pressurization testing. In *Conference on Thermal Performance of the Exterior Envelope of Buildings*. ASHRAE/DOE, 1982.

Andrew K Persily and Elizabeth M Ivy. *Input data for multizone airflow and IAQ analysis*. US Department of Commerce, Technology Administration, National Institute of Standards and Technology, 2001.

BA Petersson. Tillämpad byggnadsfysik, 2007.

JL Picolo. Absolute measurement of radon 222 activity. *Nuclear Instruments and Methods in Physics Research Section A: Accelerators, Spectrometers, Detectors and Associated Equipment*, 369(2):452–457, 1996.

Max H Sherman and Darryl J Dickerhoff. Airtightness of us dwellings/discussion. *ASHRAE Transactions*, 104:1359, 1998.

William Turner Simpson. *Equilibrium moisture content of wood in outdoor locations in the United States and worldwide*, volume 268. US Dept. of Agriculture, Forest Service, Forest Products Laboratory, 1998.

Optimization Toolbox. Users guide, the mathworks. *Inc.: Natick, MA, USA*, 2010.

Paula Wahlgren, Magnus Hansn, and Ove Svensson. Lufttäthetens variation över året. (1501), 2015.

Iain S Walker, David J Wilson, and Max H Sherman. A comparison of the power law to quadratic formulations for air infiltration calculations. *Energy and Buildings*, 27 (3):293–299, 1998.

George N Walton and W Stuart Dols. Contam user guide and program documentation. 2005.

Catarina Warfvinge and Mats Dahlblom. *Projektering av VVS-installationer*. Studentlitteratur, Lund, 2010.

A Appendix - Parameter Study Results

Radon simulations performed where the addition to the radon source caused by buoyancy effects in the ground is neglected. Radon production is pressure driven according to Equation 27.

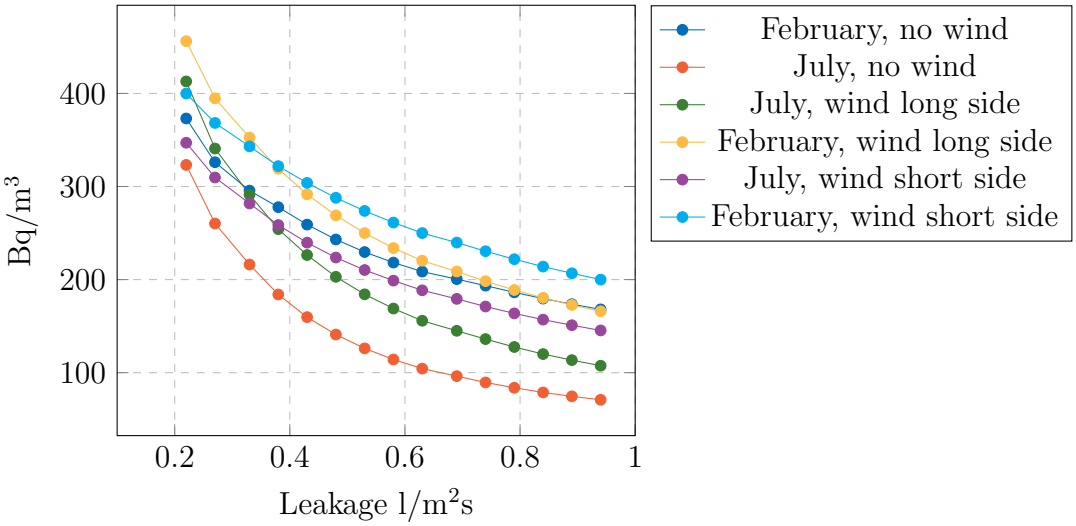

Figure 44: Plot showing radon levels in the indoor environment when the buoyancy effect in the ground is neglected.

Results from simulations where the ventilation has a constant flow; supply ventilation: 22 l/s and exhaust ventilation: 44 l/s. Temperatures in Febraury is -4 ∘C and in July 15.5 ∘C. Wind speeds are 5 m/s and principle drawing of the wind direction can be seen in Figure 29 and 30. Leakage distribution is the same as in the reference model described in Chapter 5.

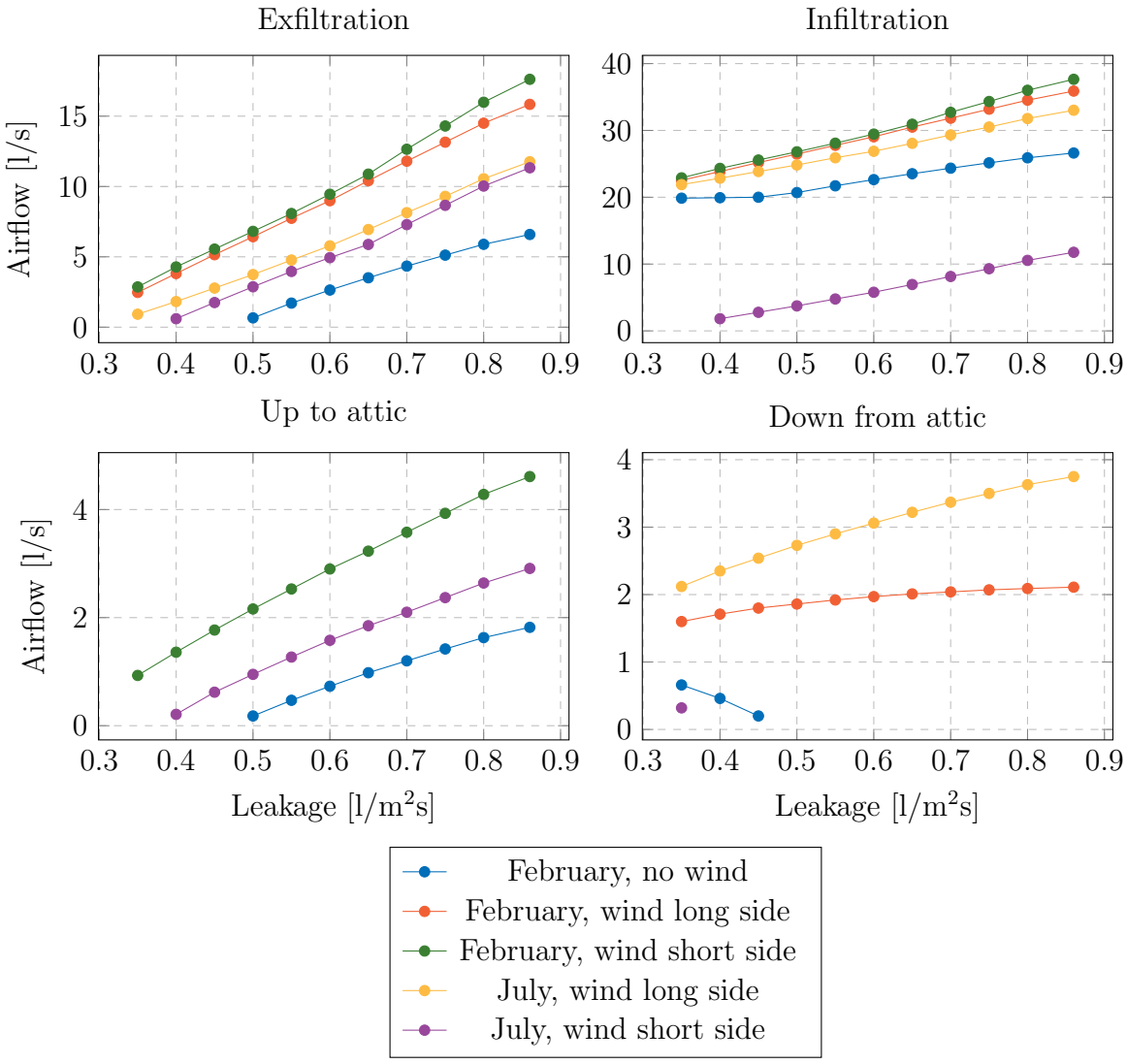

Figure 45: Results from simulations with leakage distribution according to reference model.

Results from simulations where the ventilation has a constant flow; supply ventilation: 22 l/s and exhaust ventilation: 44 l/s. Temperatures in Febraury is -4 ∘C and in July 15.5 ∘C. Wind speeds are 5 m/s and principle drawing of the wind direction can be seen in Figure 29 and 30. Leakage distribution is the same as in the reference model described in Section 6.3.2 (leakages mainly on first floor).

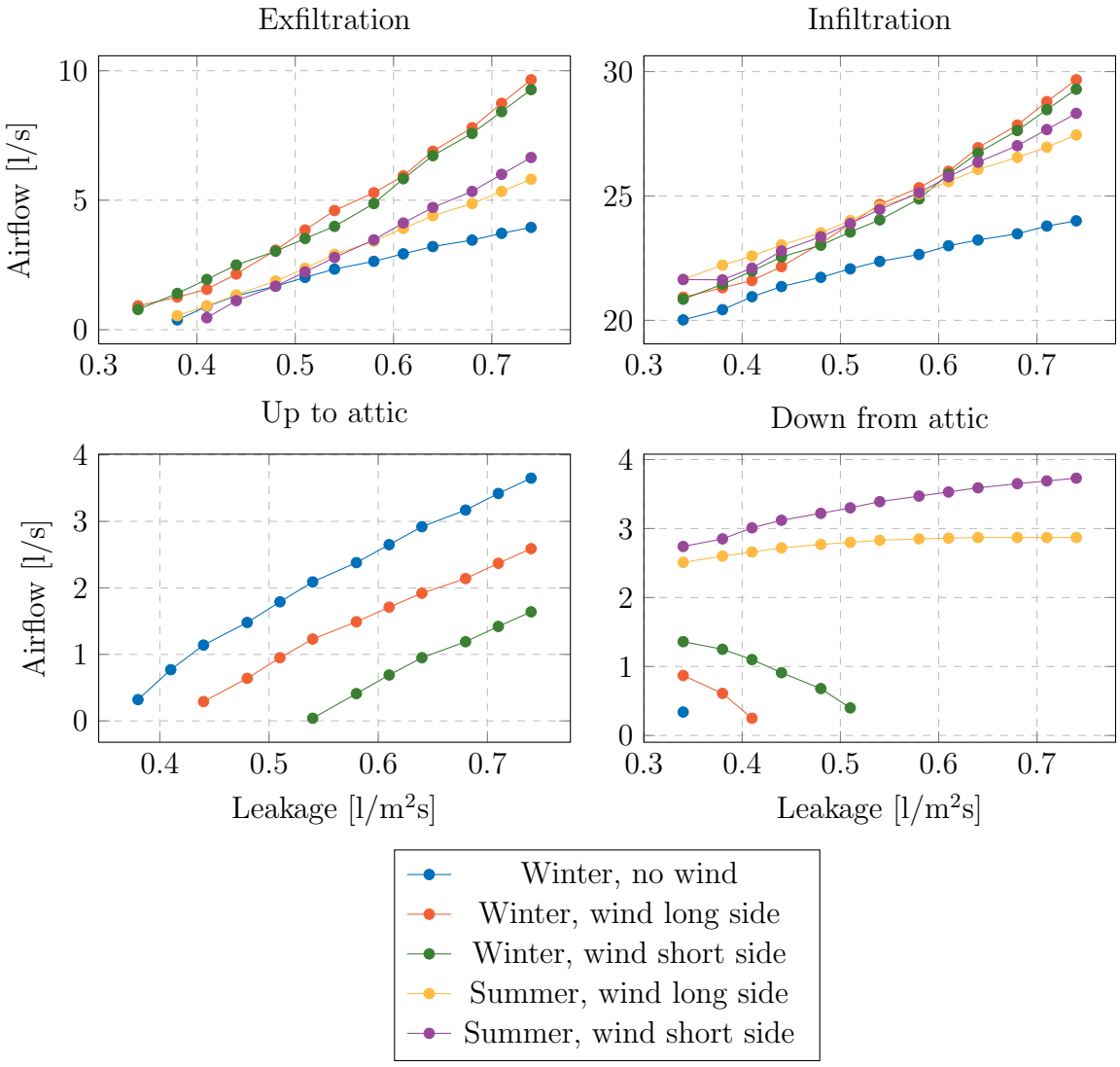

Figure 46: Results from simulations with leakages mainly on first floor.

Results from simulations where the ventilation follows a performance curve but are unaffected by the pressure from the wind. Temperatures in Febraury is -4 ∘C and in July 15.5 ∘C. Wind speeds are 5 m/s and principle drawing of the wind direction can be seen in Figure 29 and 30. Leakage distribution is the same as in the reference model described in Chapter 5.

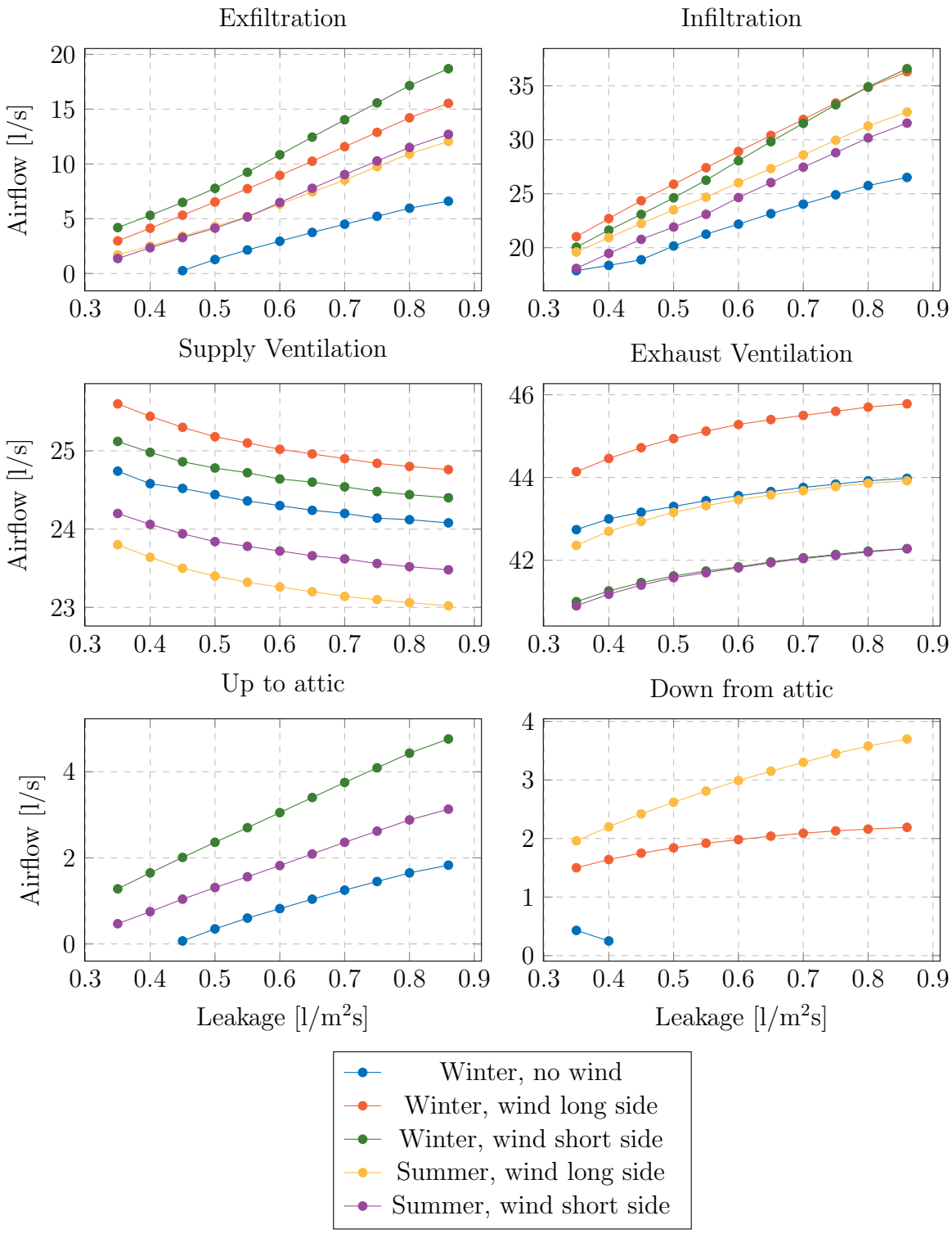

Figure 47: Results from simulations with leakage distribution according to reference model.

B Appendix - Results from Guest House

Temperature measurements from all four logs in the guesthouse. For log placement see Figure 17.

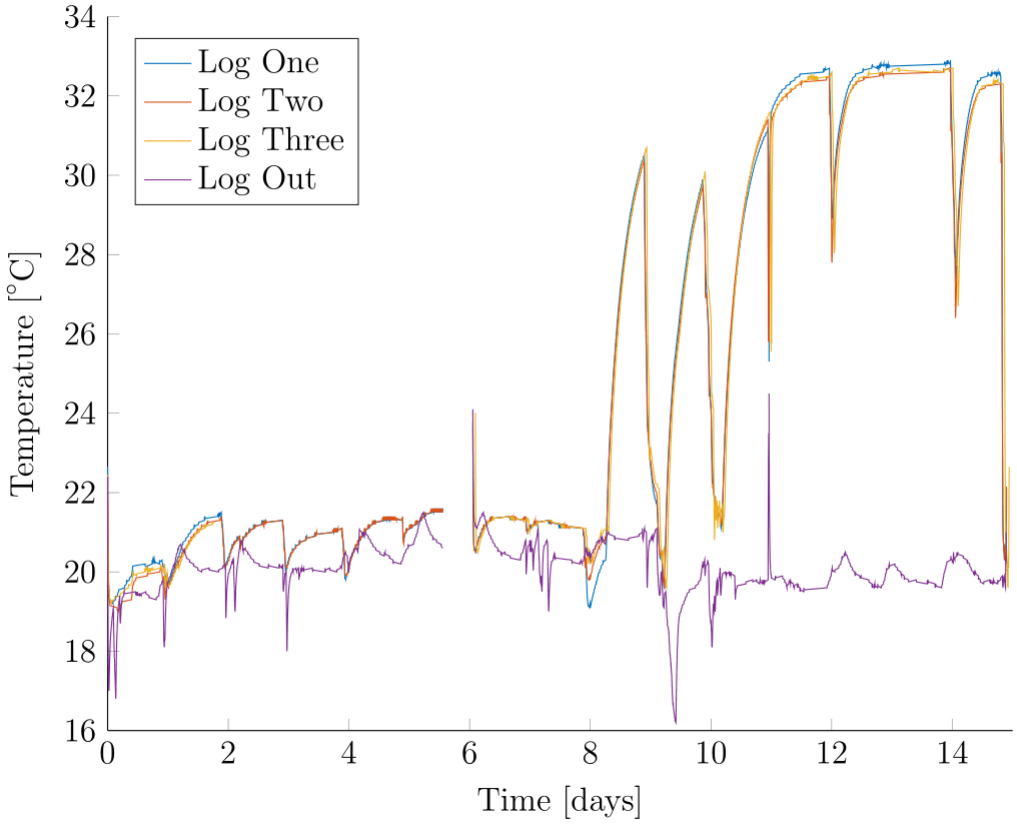

Figure 48: Plot showing temperatures during the entire test period.

Relative humidity measurements from all four logs in the guesthouse. For log placement see Figure 17.

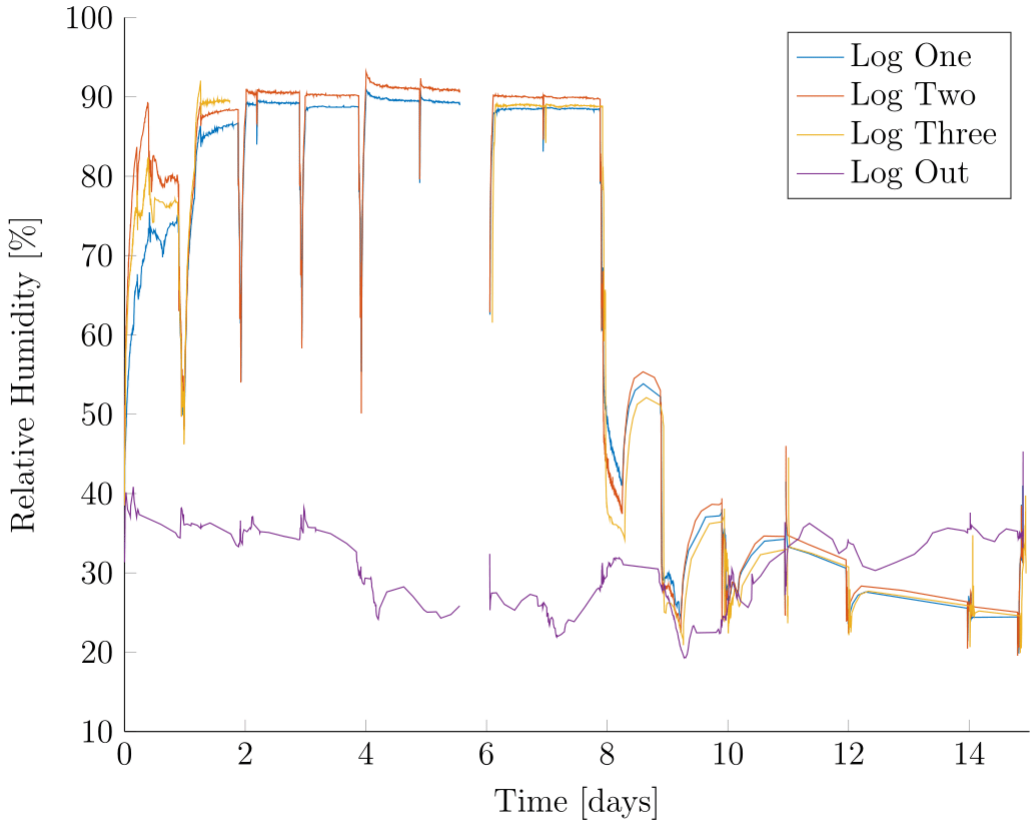

Figure 49: Plot showing relative humidities during the entire test period.

Humidity by volume measurements from all four logs in the guesthouse. For log placement see Figure 17.

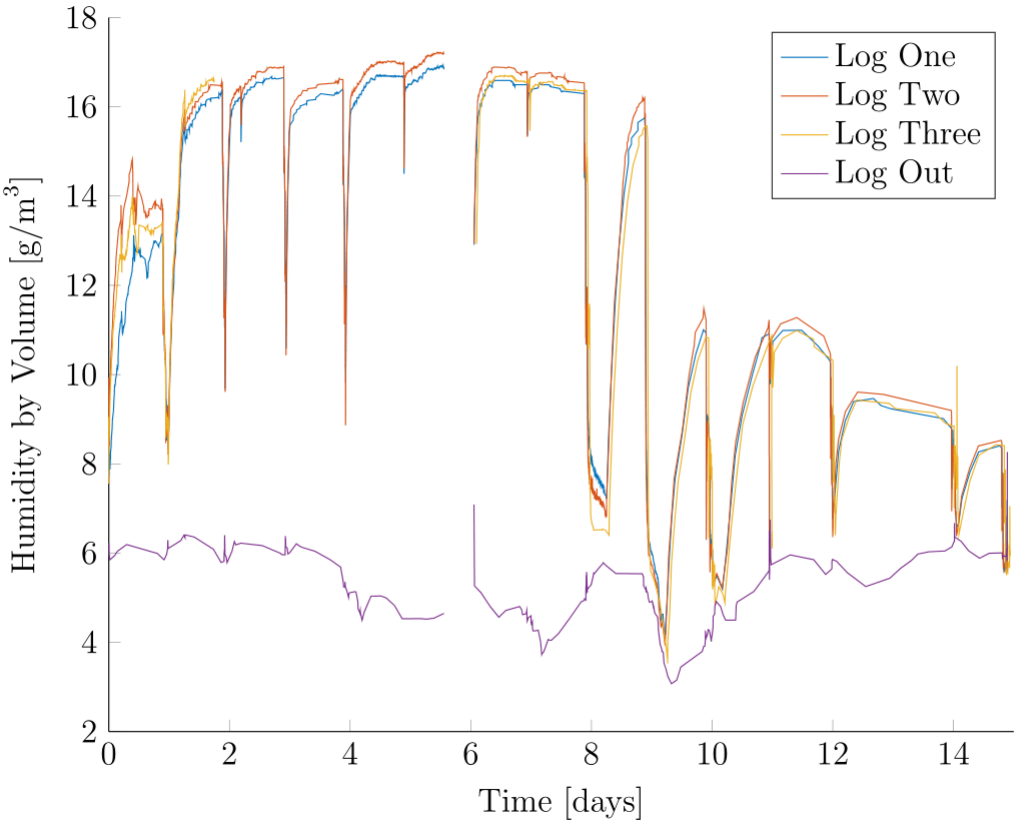

Figure 50: Plot showing humidities during the entire test period.

Relative humidity and measurement from all four logs in the guesthouse and blower door results. For log placement see Figure 17.

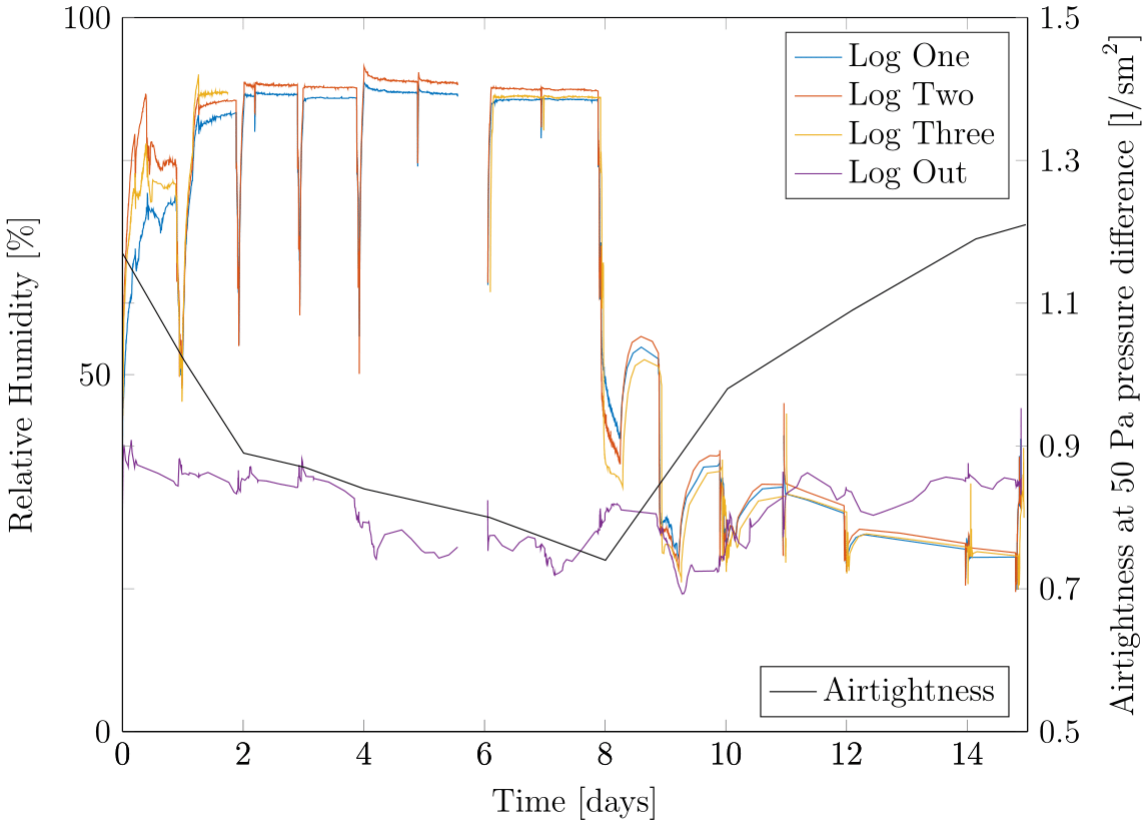

Figure 51: Plot showing relative humidities together with specific air leakage at 50 Pa pressure difference during the entire test period.

C Appendix - Leakage Variation Results

This appendix shows detailed results from simulations of airflows in four leakages performed in COMSOL.

Table 15: Window frame, airflows are given as liters per second and gap length [l/sm].

RH	Gap	5 Pa	10 Pa	30 Pa	40 Pa	50 Pa	60 Pa	70 Pa	n	C
74%	0.15	0.0007	0.0013	0.0040	0.0053	0.0066	0.0079	0.0092	1.40	1.00
66%	0.35	0.0084	0.0169	0.0506	0.0674	0.0842	0.1011	0.1179	1.40	1.00
55%	0.55	0.0328	0.0656	0.1960	0.2607	0.3250	0.3890	0.4527	1.39	0.99
42%	0.75	0.0831	0.1657	0.4905	0.6496	0.8067	0.9617	1.1149	1.38	0.97
28%	0.95	0.1682	0.3339	0.9728	1.2793	1.5780	1.8695	2.1543	1.37	0.95
17%	1.15	0.2960	0.5832	1.6564	2.1552	2.6331	3.0925	3.5354	1.34	0.93
7%	1.35	0.4728	0.9209	2.5270	3.2454	3.9212	4.5611	5.1703	1.32	0.92

Table 16: Window casement, airflows are given as liters per second and gap length [l/sm].

RH	Gap	5 Pa	10 Pa	30 Pa	40 Pa	50 Pa	60 Pa	70 Pa	n	C
69%	0.20	0.0024	0.0048	0.0143	0.0190	0.0237	0.0285	0.0332	1.00	0.00
62%	0.40	0.0191	0.0382	0.1143	0.1522	0.1898	0.2272	0.2643	1.00	0.00
55%	0.60	0.0646	0.1288	0.3791	0.5004	0.6192	0.7355	0.8494	0.98	0.01
47%	0.80	0.1523	0.3005	0.8530	1.1074	1.3493	1.5801	1.8011	0.94	0.03
38%	1.00	0.2927	0.5672	1.5170	1.9258	2.3032	2.6552	2.9861	0.88	0.07
29%	1.20	0.4907	0.9244	2.2983	2.8550	3.3574	3.8179	4.2449	0.82	0.14
21%	1.40	0.7434	1.3512	3.1298	3.8169	4.4264	4.9776	5.4827	0.76	0.23
14%	1.60	1.0400	1.8191	3.9566	4.7516	5.4474	6.0703	6.6374	0.70	0.35
8%	1.80	1.3661	2.3042	4.7519	5.6409	6.4159	7.1042	7.6764	0.65	0.50

Table 17: Wall floor connection, airflows are given as liters per second and gap length [l/sm].

RH	**Gap**	**5 Pa**	**10 Pa**	**30 Pa**	**40 Pa**	**50 Pa**	**60 Pa**	**70 Pa**	**n**	**C**
82%	0.20	0.0020	0.0041	0.0123	0.0164	0.0204	0.0245	0.0286	1.00	0.00
78%	0.40	0.0164	0.0328	0.0983	0.1310	0.1636	0.1961	0.2284	1.00	0.00
72%	0.60	0.0554	0.1106	0.3289	0.4365	0.5431	0.6486	0.7533	0.99	0.01
64%	0.80	0.1309	0.2601	0.7608	1.0023	1.2383	1.4693	1.6955	0.97	0.03
55%	1.00	0.2535	0.4997	1.4215	1.8508	2.2625	2.6585	3.0407	0.94	0.06
44%	1.20	0.4316	0.8395	2.2945	2.9428	3.5514	4.1269	4.6742	0.90	0.10
33%	1.40	0.6697	1.2791	3.3321	4.2068	5.0131	5.7649	6.4718	0.86	0.17
23%	1.60	0.9677	1.8067	4.4745	5.5680	6.5620	7.4793	8.3362	0.82	0.27
14%	1.80	1.3207	2.4043	5.6754	6.9760	8.1467	9.2210	10.2186	0.77	0.39
6%	2.00	1.7202	3.0516	6.9005	8.3970	9.7356	10.9578	12.0896	0.74	0.54

Table 18: Attic, airflows are given as liters per second and gap length [l/sm].

RH	Gap	5 Pa	10 Pa	30 Pa	40 Pa	50 Pa	60 Pa	70 Pa	n	C
86%	0.17	0.0006	0.0011	0.0034	0.0045	0.0056	0.0067	0.0078	1.00	0.00
85%	0.37	0.0058	0.0117	0.0350	0.0467	0.0583	0.0700	0.0816	1.00	0.00
82%	0.57	0.0214	0.0427	0.1279	0.1704	0.2128	0.2550	0.2972	1.00	0.00
80%	0.77	0.0526	0.1052	0.3139	0.4174	0.5202	0.6224	0.7240	0.99	0.01
78%	0.97	0.1051	0.2096	0.6212	0.8233	1.0229	1.2203	1.4154	0.99	0.02
75%	1.17	0.1840	0.3657	1.0717	1.4131	1.7474	2.0750	2.3963	0.97	0.04
72%	1.37	0.2939	0.5817	1.6773	2.1961	2.6980	3.1847	3.6573	0.96	0.06
68%	1.57	0.4392	0.8633	2.4350	3.1596	3.8509	4.5132	5.1499	0.93	0.10
64%	1.77	0.6229	1.2135	3.3312	4.2789	5.1705	6.0150	6.8189	0.91	0.15
60%	1.97	0.8470	1.6314	4.3408	5.5170	6.6092	7.6322	8.6003	0.88	0.21
55%	2.17	1.1120	2.1131	5.4388	6.8418	8.1299	9.3280	10.4525	0.85	0.29
50%	2.37	1.4170	2.6515	6.5979	8.2207	9.6976	11.0618	12.3356	0.82	0.39
44%	2.57	1.7595	3.2384	7.7987	9.6335	11.2920	12.8163	14.2349	0.79	0.51
39%	2.77	2.1359	3.8642	9.0230	11.0612	12.8941	14.5724	16.1300	0.77	0.65
33%	2.97	2.5422	4.5204	10.2600	12.4956	14.4947	16.3235	18.0163	0.74	0.80
28%	3.17	2.9729	5.1975	11.4959	13.9205	16.0835	18.0556	19.8818	0.72	0.97
23%	3.37	3.4250	5.8923	12.7372	15.3475	17.6707	19.7856	21.7398	0.70	1.15
18%	3.57	3.8936	6.5979	13.9738	16.7663	19.2463	21.5014	23.5832	0.68	1.34
14%	3.77	4.3749	7.3103	15.2042	18.1748	20.8101	23.2032	25.4110	0.66	1.54
10%	3.97	4.8646	8.0238	16.4198	19.5669	22.3542	24.8841	27.2165	0.65	1.75
6%	4.17	5.3620	8.7406	17.6354	20.9546	23.8935	26.5590	29.0146	0.64	1.97

D Appendix - Ventilation Fan and Filter

The following pages shows the properties of the ventilation fan and filter used for the simulations in CONTAM.

FLK 100

Beskrivning

Filterbox FLK is made from pre-galvanized steel. They are all delivered with a G4 filter supported by a net. Sizes from 100 mm to 400 mm.

Tekniska data

Storhet	Värde	Enhet
Längd	227	mm
Bredd	205	mm
Höjd	170	mm

Tryckfall

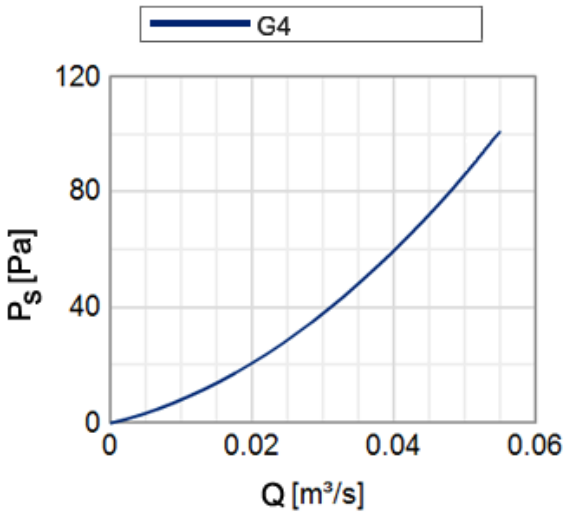

AB C.A. ÖSTBERG • Industrigatan 2 • 774 35 Avesta • Sverige • Telefon +46 226 860 00 • Fax +46 226 860 05 • info@ca-ostberg.se

VKAP 3.0

VKAP 100 MD 3.0

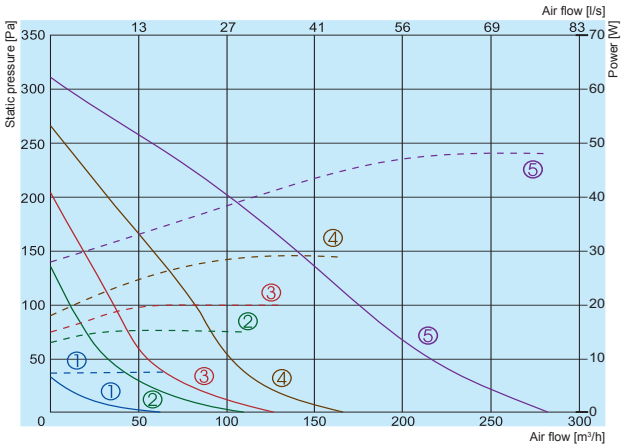

——— Performance
------- Power consumption

① 80V
② 120V
③ 140V
④ 170V
⑤ 230V

100 MD 3.0	LWA total, dB(A)	Lwa, dB(A)						
		125 Hz	250 Hz	500 Hz	1 kHz	2 kHz	4 kHz	8 kHz
Inlet	61	45	57	52	56	51	40	31
Outlet	61	44	58	52	55	50	39	30
Surrounding	46	26	27	36	44	41	30	23

Measured at 200 m³/h, 62 Pa

VKAP 100 LD 3.0

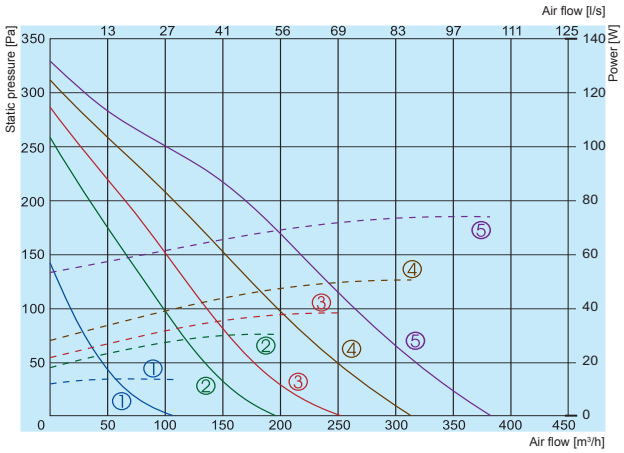

——— Performance
------- Power consumption

① 80V
② 120V
③ 140V
④ 170V
⑤ 230V

100 LD 3.0	LWA total, dB(A)	Lwa, dB(A)						
		125 Hz	250 Hz	500 Hz	1 kHz	2 kHz	4 kHz	8 kHz
Inlet	70	53	58	60	66	65	58	47
Outlet	71	54	60	61	67	66	58	48
Surrounding	61	34	58	44	55	54	47	37

Measured at 257 m³/h, 104 Pa

VKAP 125 MD 3.0

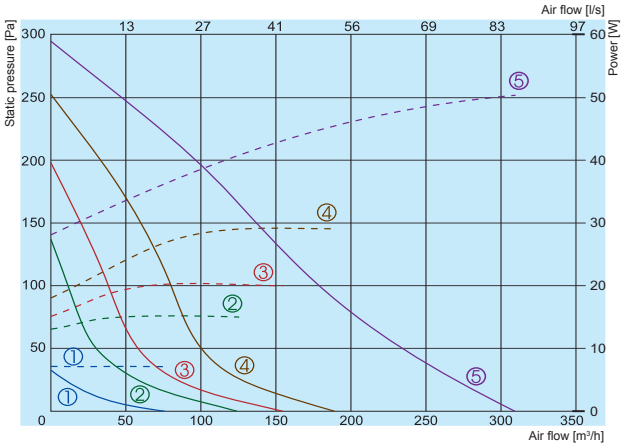

——— Performance
------- Power consumption

① 80V
② 120V
③ 140V
④ 170V
⑤ 230V

125 MD 3.0	LWA total, dB(A)	Lwa, dB(A)						
		125 Hz	250 Hz	500 Hz	1 kHz	2 kHz	4 kHz	8 kHz
Inlet	59	43	52	53	54	51	41	33
Outlet	60	42	53	54	54	52	42	34
Surrounding	45	21	30	36	42	40	29	18

Measured at 191 m³/h, 83 Pa

The fan characteristic curves were determined in accordance with EN ISO 5801. The sound levels were determined in accordance with DIN 45635 resp. ISO 3744 at a distance of 1 m from the fan.

E Appendix - Technical Drawings of the Guest House

The following pages shows a selection of technical drawings of the guest house. All technical drawings were provided by Peter Lindblom who constructed the guest house.

Förklaringar

alla mått i mm

Föreskrifter

Hänvisning

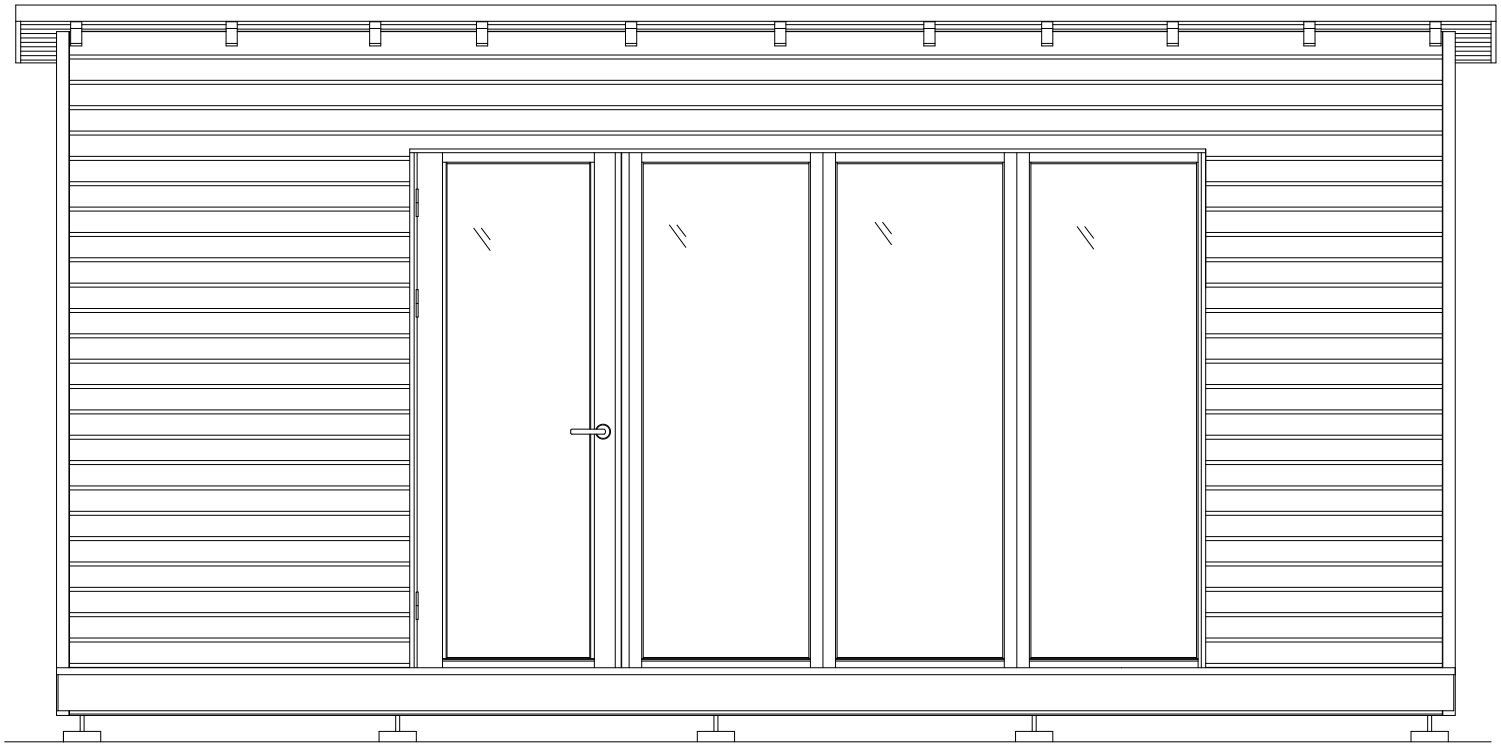

FASAD 1

BET	ANT	ÄNDRINGEN AVSER	SIGN	DATUM

GÄSTSTUGA

UPPDRAG NR	RITAD AV	HANDLÄGGARE
1		P.Lindblom
DATUM	ANSVARIG	

Fasad 1

SKALA	NUMMER	BET
1:10 (A1) 1:20 (A3)	A30-5-01	

REF:

LAGER:

PLO:

Förklaringar

alla mått i mm

Föreskrifter

Hänvisning

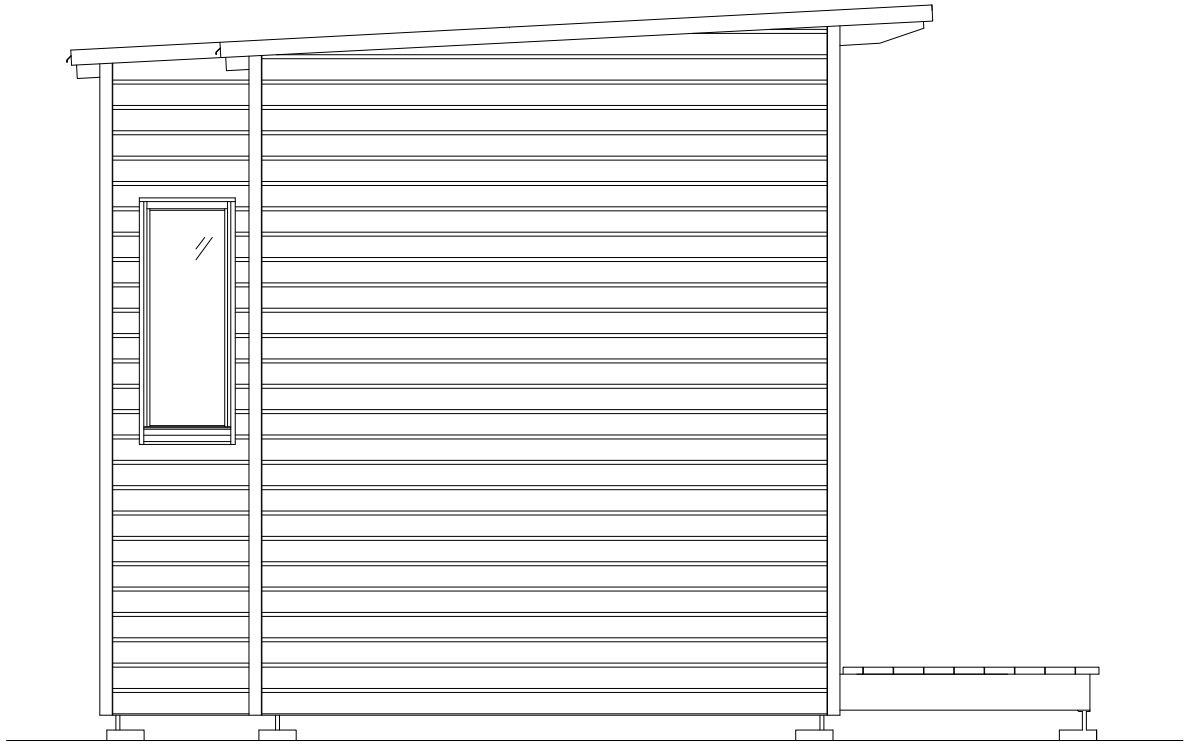

FASAD 2

BET	ANT	ÄNDRINGEN AVSER	SIGN	DATUM

GÄSTSTUGA

UPPDRAG NR	RITAD AV	HANDLÄGGARE
		P.Lindblom
DATUM	ANSVARIG	

Fasad 2

SKALA	NUMMER	BET
1:10 (A1) 1:20 (A3)	A30-5-02	

REF:

LAGER:

PLO:

REF:

LAGER:

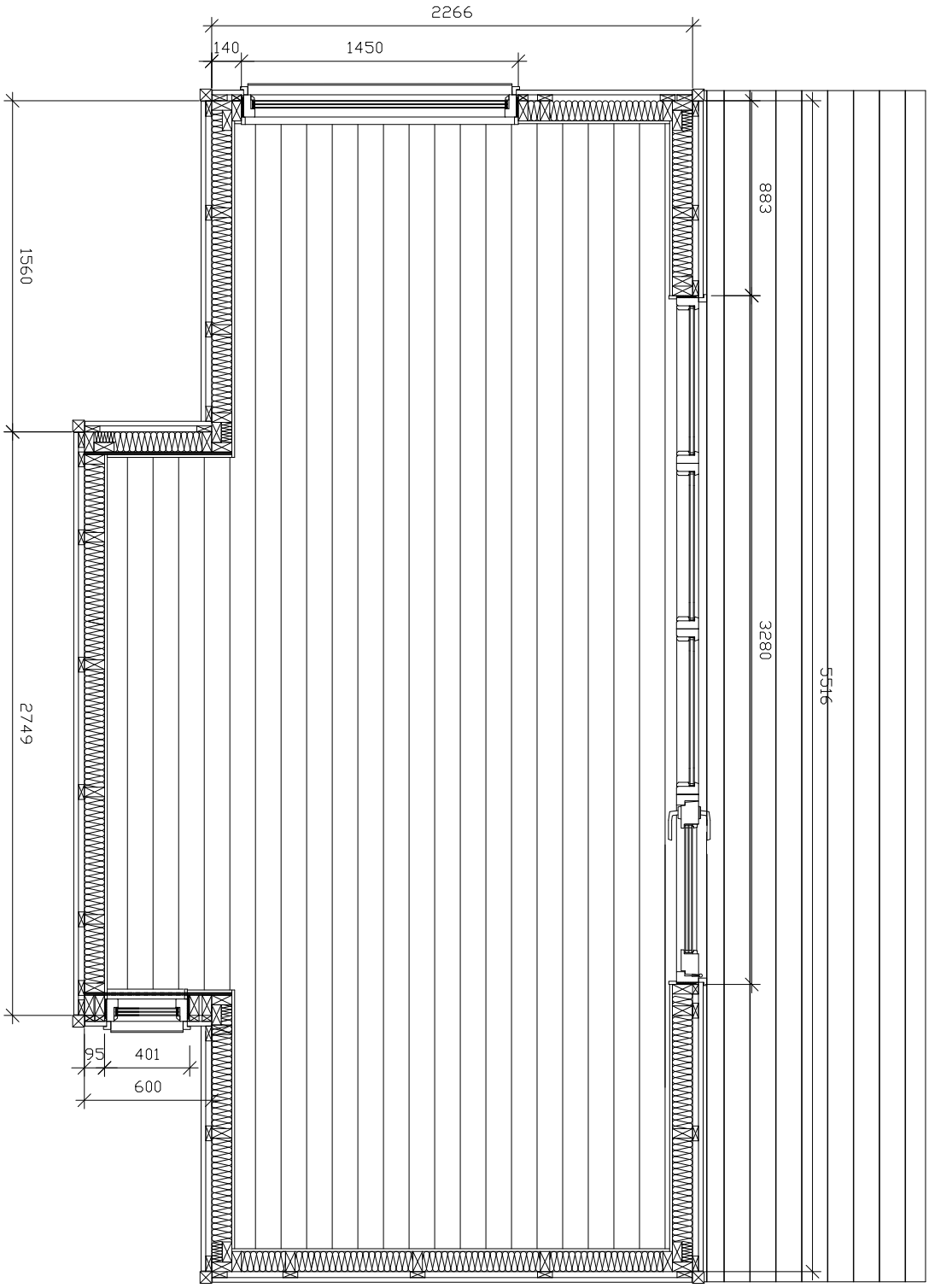

Förklaringar

alla mått i mm

Väggreglar 45x95 s600 om ej annat anges

Föreskrifter

Hänvisning

BET	ANT	ANDRINGEN AVSER	SIGN	DATUM

GÄSTSTUGA

Plan1; stommått

UPPDRAG NR		RITAD AV	HANDLÄGGARE
DATUM		ANSVARIG	P Lindblom

SKALA 1:10 (A1) 1:20 (A3)	RITNINGSNR A30-5-10	BET

PLO: